U. S. DEPARTMENT OF COMMERCE

BUREAU OF STANDARDS JOURNAL OF RESEARCH

Vol. 6 MAY, 1931 No. 5

CONTENTS

RP. No.	TITLE AND AUTHOR	Page
303.	Note on contraction coefficients of jets of gas. Edgar Buckingham	765
304.	The effect of small variations in pitch upon the inductance of a solenoid. Chester Snow	777
305.	Heat content values for aqueous solutions of the chloride, nitrates, and hydroxides of hydrogen, lithium, sodium, and potassium at 18° C. Frederick D. Rossini	791
306.	Accurate measurement of small electric charges by a null method. Lauriston S. Taylor	807
307.	Light sensitivity of rosin paper-sizing materials. Arthur E. Kimberly and J. F. G. Hicks	819
308.	Dimensional changes in the manufacture of electrotypes. N. Bekkedahl and W. Blum	829
309.	The heat of ionization of water. Frederick D. Rossini	847
310.	Factors affecting the strength of masonry hollow units. Douglas E. Parsons	857
311.	Determination of the benzene and the normal hexane content of a midcontinent petroleum. Johannes H. Bruun and Mildred M. Hicks-Bruun	869
312.	Calorimetric determinations of thermal properties of methyl alcohol, ethyl alcohol, and benzene. E. F. Fiock, D. C. Ginnings, and W. B. Holton	881
313.	Characteristics of airplane antennas for radio range-beacon reception. H. Diamond and G. L. Davies	901

BUREAU OF STANDARDS JOURNAL OF RESEARCH

CONTENTS OF RECENT NUMBERS

November, 1930 (Vol. 5, No. 5)

RP243. Mechanism of heat flow in fibrous materials. J. L. Finck. Price 5 cents.

RP244. Compressibility and thermal expansion of petroleum oils in the range 0° to 300° C. R. S. Jessup. Price 15 cents.

RP245. Interference measurements in the first spectra of krypton. C. J. Humphreys. Price 5 cents.

RP246. Kennelly-Heaviside layer height observations for 4,045 and 8,650 kc. T. R. Gilliland. Price 10 cents.

RP247. A study of the method for titrating aldose sugars with standard iodine and alkali. G. M. Kline and S. F. Acree. Price 10 cents.

RP248. Properties of lead-bismuth, lead-tin, type metal, and fusible alloys. J. G. Thompson. Price 10 cents.

RP249. A study of the adsorption of sulphuric acid by leather. John Beck, jr. Price 5 cents.

RP250. A study of the so-called "over-reduced" condition in molten steel. J. V. McCrae, R. L. Dowdell, and Louis Jordan. Price 15 cents.

RP251. The constant occurrence of nonreducing disaccharides in hydrolyzed inulin. Richard F. Jackson and Emma McDonald. Price 5 cents.

RP252. Precision of color temperature measurements under various observing conditions; a new color comparator for incandescent lamps. Deane B. Judd. Price 10 cents.

RP253. The ring structure of mannose. The optical rotation of 4-glucoside-α-mannose. Horace S. Isbell. Price 5 cents.

December, 1930 (Vol. 5, No. 6)

RP254. Further study of paper-coating minerals and adhesives. Merle B. Shaw, George W. Bicking, and Martin J. O'Leary. Price 10 cents.

RP255. The structure of the spectrum of singly ionized zirconium. C. C. Kiess and Harriet K. Kiess. Price 10 cents.

RP256. A redetermination of the constant of gravitation. Paul R. Heyl. Price 15 cents.

RP257. The properties of pure nickel. Louis Jordan and Wm. H. Swanger, with collaboration of members of bureau staff as indicated. Price 10 cents.

RP258. The freezing point of nickel as a fixed point on the International Temperature Scale. H. T. Wensel and Wm. F. Roeser. Price 5 cents.

January, 1931 (Vol. 6, No. 1)

RP259. The heat of formation of water. Frederick D. Rossini. Price 10 cents.

RP260. The heats of combustion of methane and carbon monoxide. Frederick D. Rossini. Price 5 cents.

RP261. A portable instrument for measuring air permeability of fabrics. Herbert F. Schiefer and Alfred S. Best. Price 10 cents.

RP262. Prism size orientation in minimum-deviation refractometry. L. W. Tilton. Price 10 cents.

RP263. Optimum use of material in biological assays. Warren W. Nicholas. Price 5 cents.

RP264. Viscous flow and surface films. Ronald Bulkley. Price 10 cents.

RP265. Determination of magnesium in Portland cement and similar materials by the use of 8-hydroxyquinoline. J. C. Redmond and H. A. Bright. Price 5 cents.

RP266. An improved apparatus and method for the analysis of gas mixtures by combustion and absorption. Martin Shepherd. Price 15 cents.

RP267. Determination of small quantities of volatile organic acids in sulphuric acid solutions. D. N. Craig. Price 5 cents.

Research papers are available as separates for purchase from the Superintendent of Documents United States Government Printing Office, Washington, D. C.

U. S. DEPARTMENT OF COMMERCE
R. P. LAMONT, Secretary
BUREAU OF STANDARDS
GEORGE K. BURGESS, Director

BUREAU OF STANDARDS JOURNAL OF RESEARCH

May, 1931
Vol. 6, No. 5

UNITED STATES
GOVERNMENT PRINTING OFFICE
WASHINGTON : 1931

For sale by the Superintendent of Documents, Washington, D. C. - - - - Price $2.75 Per Year on Subscription

For a partial list of previous research papers appearing in BUREAU OF STANDARDS JOURNAL OF RESEARCH, see pages 2 and 3 of the cover.

NOTE ON CONTRACTION COEFFICIENTS OF JETS OF GAS

By Edgar Buckingham

ABSTRACT

1. A jet of liquid from a sharp-edged orifice contracts more than a jet of gas because the gas expands after leaving the orifice; and theoretical expressions for the ratio of the two contraction coefficients have hitherto been deduced from the assumption that the expansion is the same in all directions. In the present paper this is replaced by the assumption that the force exerted on the upstream face of an orifice plate on the end of a pipe depends only on the static pressure and the momentum of the approaching stream.

2. The resulting expression is compared with the experiments of Witte on water, of Bachmann on air, and recent unpublished experiments on natural gas. The conditions presupposed by the theory are strictly satisfied in Bachmann's experiments but in the others they are satisfied only when the ratio, β, of orifice to pipe diameter is small.

3. The conclusions are as follows:

(*a*) Bachmann's experiments on air at low differentials agree with Witte's on water within 0.5 per cent.

(*b*) The measurements on natural gas agree with Bachmann's on air within 0.5 per cent.

(*c*) As far as the critical pressure ratio, the new formula represents the results on natural gas within 0.5 per cent for $\beta=0.27$; within 0.3 per cent for $\beta=0.38$; and within 0.8 per cent for $\beta=0.5$. For $\beta=0.7$ the departure increases to nearly 4 per cent.

CONTENTS

	Page
I. Introduction	765
II. Development of a new formula	766
1. Conditions	766
2. Notation	766
3. Remarks	767
4. Basis for a new treatment of the problem	767
5. Isentropic flow from (p_1, ρ_1) to p_2	768
6. Flow at constant density from (p_1, ρ_1) to p_3	768
7. Application of the fundamental assumption	769
III. Examination of the experimental data	769
IV. Comparison with the new formula	773
V. Conclusions	774

I. INTRODUCTION

The pressure in a jet of fluid issuing from a square-edged orifice in a thin plate does not fall to equality with the outside pressure until the filaments have become parallel. Between the plane of the orifice and the vena contracta there is a radial pressure gradient outward, and if the fluid is a gas it expands transversely as well as longitudinally, whereas in the case of a liquid there is no expansion. The cross section of the vena contracta is therefore larger with a gas than with a liquid.

The ratio of the two sectional areas would be given by a complete solution of the equations of motion, but until the mathematical

difficulties of the problem have been overcome, any attempt to compute the ratio a priori must rest on simplifying, approximate assumptions. Two such computations have recently been made,[1] [2] both based on the assumption that the gas in the jet expands uniformly in all directions; but while the formulas obtained agree well with the experimental data with which they have been compared, the fundamental assumption has been criticized [3] as very improbable under the conditions of acceleration and distortion prevailing in the jet. I have therefore thought it worth while to start from a different initial hypothesis and to compare the result obtained with certain additional experimental data which have not yet been published and so have not been available to previous writers.

II. DEVELOPMENT OF A NEW FORMULA

1. CONDITIONS

The orifice is to be a cylindrical hole in the center of a thin, flat diaphragm across the end of a straight pipe. The outside space into which the discharge takes place is to be so large that the static pressure in it is sensibly uniform everywhere outside the jet from the orifice; and the jet will be regarded as having a definite boundary, as far as the vena contracta, the frictional drag at the boundary being negligible. We consider only steady states of flow.

The fluid shall be some gas, such as air, which may be treated as subject to the ordinary ideal gas equations over the short range of pressure and density involved in flow through an orifice at jet speeds below the speed of sound in the jet.

The Reynolds number shall be high enough that the motion is no longer appreciably affected by viscosity, and that the velocity and static pressure are sensibly uniform all over the section at the vena contracta, the pressure there being the same in the jet as in the surrounding space.

2. NOTATION

The following notation will be adopted, all values being expressed in terms of a set of normal units, such as the cgs or the "British absolute" system.

A = the area of cross section of the pipe;

mA = the area of the orifice, m being the area ratio and $\sqrt{m}=\beta$ the diameter ratio;

p_1 = the static pressure in the pipe ahead of the orifice;

ρ_1 = the density of the gas at that place;

S_1 = the linear speed of flow along the pipe;

p_2 = the pressure in the outside space;

ρ_2 = the density of the gas after isentropic expansion from (p_1,ρ_1) to p_2;

S_2 = the speed at the vena contracta;

μ_a = the contraction coefficient, so that the area of the vena contracta is $\mu_a mA$;

M = the mass flow; evidently

$$M=\mu_a m A \rho_2 S_2 \tag{1}$$

[1] R. Witte, Techn. Mech. u. Thermodyn., **1**, p. 118; March, 1930.
[2] G. Ruppel, Techn. Mech. u. Thermodyn., **1**, p. 151; April, 1930.
[3] A. Busemann, Techn. Mech. u. Thermodyn., **1**, p. 338; September, 1930.

p_3 = the outside pressure that would be required to produce this same mass flow, from the same initial pressure and density, if the density were kept constant at the value ρ_1, which could, in principle, be accomplished by withdrawing heat at a suitable rate instead of allowing the flow to be adiabatic;

S_3 = the speed at the vena contracta in this case; and

μ = the contraction coefficient. By the definition of S_3 and by (1) we have

$$\mu m A \rho_1 S_3 = M = \mu_a m A \rho_2 S_2 \tag{2}$$

$\gamma = C_p/C_v$ = the specific heat ratio of the gas;

F_0 = the force exerted by the gas inside the pipe tending to push the orifice plate downstream off the end of the pipe. To simplify the appearance of the equations the following abbreviations will also be employed

$$\left.\begin{aligned} \frac{p_2}{p_1} &= y & \frac{p_3}{p_1} &= w \\ \frac{\gamma}{\gamma-1} y^{\frac{1}{\gamma}} \left(1 - y^{\frac{\gamma-1}{\gamma}}\right) &= \phi \end{aligned}\right\} \tag{3}$$

3. REMARKS

If the density does not change during a fall of pressure, compressibility does not come into play, so that its value is immaterial and the shape of the jet depends only on the value of the Reynolds number $R = \frac{DS\rho}{\eta}$, in which D is the diameter of the orifice and η the viscosity of the fluid.

Since R depends on ρ as well as η, if its values are all so high that changing from one to another does not affect the shape of the jet, it follows that the shape is unaffected, not only by a change of viscosity caused by substituting one fluid for another, but also by a simultaneous change from one constant density to another. Hence at high values of R the contraction coefficient will be the same in the supposed case of discharge of a gas at the constant density ρ_1 as it would be in the discharge of a liquid of that or of any other constant density; and the value of μ may therefore be determined by experiments on water at high values of R.

4. BASIS FOR A NEW TREATMENT OF THE PROBLEM

We assume that with given initial conditions (p_1, ρ_1), and with a given mass flow M—which implies a particular linear speed S_1 along the pipe—the force F_0 exerted by the gas on the upstream face of the orifice plate is the same when the subsequent discharge through the orifice takes place isentropically, as if it went on with artificial cooling at constant density. This enables us to dispense with the assumption of uniform expansion beyond the plane of the orifice, and with several auxiliary approximations of which the importance is difficult to estimate.

The approximation to reality will be closer for small than for large values of $(p_1 - p_2)/p_1$ and, probably, for small than for large values of m; and it is hardly to be expected that the results obtained from the

assumption will agree well with experiment for large values of m or for pressure ratios near the critical.

In so far as the assumption is valid, it permits of applying the momentum principle, and we proceed as follows:

5. ISENTROPIC FLOW FROM (p_1, ρ_1) TO p_2

The equations of energy and continuity are

$$S_2^2 - S_1^2 = \frac{2\gamma}{\gamma - 1} \cdot \frac{p_1}{\rho_1}\left(1 - y^{\frac{\gamma-1}{\gamma}}\right) = \frac{2p_1\phi}{\rho_1 y^{\frac{1}{\gamma}}} \tag{4}$$

and

$$M = A\rho_1 S_1 = \mu_a m A \rho_2 S_2 = \mu_a m A \rho_1 y^{\frac{1}{\gamma}} S_2 \tag{5}$$

whence

$$S_2 = \sqrt{\frac{2p_1\phi}{\rho_1 y^{\frac{1}{\gamma}}\left(1 - \mu_a^2 m^2 y^{\frac{2}{\gamma}}\right)}} \tag{6}$$

and

$$M = \mu_a m A \rho_1 y^{\frac{1}{\gamma}} \sqrt{\frac{2p_1\phi}{\rho_1 y^{\frac{1}{\gamma}}\left(1 - \mu_a^2 m^2 y^{\frac{2}{\gamma}}\right)}} \tag{7}$$

The time rate of increase of momentum is

$$M(S_2 - S_1) = \frac{2\mu_a m A p_1 \phi}{1 + \mu_a m y^{\frac{1}{\gamma}}} \tag{8}$$

and the force acting is

$$F = A(p_1 - m p_2) - F_0 \tag{9}$$

whence, equating (8) with (9) and dividing by Ap_1, we have

$$1 - my - \frac{F_0}{Ap_1} = \frac{2\mu_a m \phi}{1 + \mu_a m y^{\frac{1}{\gamma}}} \tag{10}$$

6. FLOW AT CONSTANT DENSITY FROM (p_1, ρ_1) TO p_3

The equations of energy and continuity are

$$S_3^2 - S_1^2 = 2\frac{p_1}{\rho_1}(1 - w) \tag{11}$$

and

$$M = A\rho_1 S_1 = \mu m A \rho_1 S_3 \tag{12}$$

whence

$$S_3 = \sqrt{\frac{2p_1(1-w)}{\rho_1(1 - \mu^2 m^2)}} \tag{13}$$

and

$$M = \mu m A \rho_1 \sqrt{\frac{2p_1(1-w)}{\rho_1(1 - \mu^2 m^2)}} \tag{14}$$

The rate of increase of momentum is

$$M(S_3-S_1)=\frac{2\mu m A p_1(1-w)}{1+\mu m} \tag{15}$$

and the force acting is

$$F=A(p_1-mp_3)-F_0 \tag{16}$$

whence by (15)

$$1-mw-\frac{F_0}{Ap_1}=\frac{2\mu m(1-w)}{1+\mu m} \tag{17}$$

7. APPLICATION OF THE FUNDAMENTAL ASSUMPTION

The assumption is that if equations (7) and (14) give the same value of M, the value of F_0 will be the same in (10) as in (17). Accordingly, we may eliminate the unknown force F_0 by subtracting (17) from (10) and after dividing by m we have

$$w-y=\frac{2\mu_a\phi}{1+\mu_a m y^{\frac{1}{\gamma}}}-\frac{2\mu(1-w)}{1+\mu m} \tag{18}$$

Upon equating (7) and (14), removing the common factors, and squaring, we have

$$\frac{\mu^2(1-w)}{1-\mu^2m^2}=\frac{\mu_a{}^2y^{\frac{1}{\gamma}}\phi}{1-\mu_a{}^2m^2y^{\frac{2}{\gamma}}} \tag{19}$$

and after eliminating w between (18) and (19) we have a quadratic equation of which the solution may be expressed in the form

$$\frac{\mu_a}{\mu}=\frac{B}{A}\left(1-\sqrt{1-\frac{AQ}{B^2}}\right) \tag{20}$$

where

$$\left.\begin{aligned} A&=y^{\frac{1}{\gamma}}\left[(2\mu+\mu^2m^2-1)\phi-\mu^2m^2y^{\frac{1}{\gamma}}(1-y)\right]\\ B&=\mu\phi\\ Q&=1-y\\ \phi&=\frac{\gamma}{\gamma-1}y^{\frac{1}{\gamma}}\left(1-y^{\frac{\gamma-1}{\gamma}}\right)\\ y&=\frac{p_2}{p_1}\end{aligned}\right\} \tag{21}$$

The result embodied in equations (20) and (21) is to be compared with experiment and we have next to examine the available data.

III. EXAMINATION OF THE EXPERIMENTAL DATA

In the absence of accurate measurements of the diameter of the vena contracta, we have recourse to the values of discharge coefficients obtained from measurements of mass flow.

The "adiabatic" discharge coefficient C_a for a gas is defined by

$$M=C_aM_{i\cdot a} \tag{22}$$

where M is the observed mass flow and $M_{t\cdot a}$ is the "theoretical" mass flow found from equation (7) by ignoring the phenomena of contraction and setting $\mu_a=1$. Since C_a is not constant, we may write

$$C_a=CY_a \tag{23}$$

where C is the limiting value which C_a approaches as $p_2\doteq p_1$, and the "expansion factor" Y_a is a function of p_2/p_1 which reduces to unity when $p_2=p_1$.

The discharge coefficient C_l for a liquid is defined by

$$M=C_lM_{t\cdot l} \tag{24}$$

in which $M_{t\cdot l}$ is the "theoretical" mass flow found by setting $\mu=1$ in equation (14). But if we set $\mu_a=\mu=1$ and $p_3=p_2$, equation (7) approaches (14) as a limiting form when $p_2=p_1$. Hence C_l and C are identical, and instead of attempting to find the value of C by extrapolating to very small pressure differences from measurements of C_a, we may equally well find it from experiments on a liquid.

The stipulation that the Reynolds number shall be so high that its precise value is no longer important, implies that the dissipative resistances due to viscosity have become insignificant. The contraction coefficients μ_a and μ may therefore be regarded as sensibly identical with the discharge coefficients C_a and C, and for the purpose of comparison with equation (20) we may set

$$\frac{\mu_a}{\mu}=\frac{C_a}{C}=Y_a \tag{25}$$

The experimental data suitable for a direct test of the formula are very few; for it was postulated that the discharge should take place into a space that was large enough for the static pressure in it to be uniform, and the only satisfactory experiments of this sort that have come to my attention are those of Bachmann[4] on the discharge of air into the atmosphere through an orifice on the end of a pipe.

The internal diameter of the pipe was 8.25 cm and the diameter of the orifice was 2.003 cm, so that the diameter ratio was $\beta=0.2428$ and the area ratio was $\beta^2=m=0.0590$. Of the 18 values of C_a obtained at speeds below the critical, the one that was measured at the lowest rate of discharge and is therefore the least reliable is far out of line with the others. The remaining 17 are represented without systematic departures by the equation

$$C_a=0.5989\left(1+0.2431\,\frac{p_1-p_2}{p_2}\right) \tag{26}$$

the greatest departure being less than 0.5 per cent and the mean departure less than 0.2 per cent.

The important thing for our present purposes is the expansion factor

$$Y_a=1+0.2431\,\frac{p_1-p_2}{p_2} \tag{27}$$

[4] H. Bachmann, "Beitrag zur Messung von Luftmengen," Dissertation, Darmstadt; 1911.

but it is interesting to compare the value of C with values obtained from orifices installed in pipes, with p_2 taken as the minimum pressure observed on the downstream side of the orifice.

Witte's [5] experiments on water flowing through perfectly square-edged orifices installed in smooth pipes, with the pressures taken at the face of the plate, gave values of C which, for diameter ratios between $\beta=0.2$ and $\beta=0.75$, or $0.04<m<0.56$, are represented without systematic error by the equation

$$\frac{C}{\sqrt{1-m^2}}=K=0.5983+0.395m^2 \tag{28}$$

The maximum departure is about 0.25 per cent and the mean departure for the 17 orifices tested is less than 0.1 per cent, so that the representation by equation (28) is very good.

For Bachmann's area ratio, (28) gives $C=0.5986$, but this must be corrected to obtain the corresponding value which would have been found if the pressure difference had been measured between the upstream and downstream minima instead of between the two faces of the plate. Experiments on air which will be published in the near future show that this correction factor is about 0.9983, so that we have from Witte's experiments on water $C=0.5976$ as compared with the value 0.5989 from Bachmann's work—an excellent agreement.

The equation adopted for representing the results of the experiments on compressed air, described in Bureau of Standards Research Paper No. 49,[6] namely

$$C=0.5970+0.09\ m^2 \tag{29}$$

gives $C=0.5973$ for Bachmann's value of m.

Next to Bachmann's data, the best at my disposal were obtained from experiments on natural gas, performed at Los Angeles in 1929 under the direction of H. S. Bean of the Bureau of Standards, as part of an investigation being carried on by the Natural Gas Division of the American Gas Association, in cooperation with the Bureau of Standards. The circumstances were more favorable as regards steadiness of flow than in the experiments on compressed air just referred to, so that the precision was higher and the results are preferable.

The orifices were installed in straight pipes, as in Witte's experiments on water, so that the discharge space was restricted and the static pressure in it not entirely uniform. It is to be presumed, however, that if the area ratio m is small, and if the minimum pressure, observed at the wall of the pipe on the discharge side is taken as the value of p_2, the arrangement will correspond fairly closely with that presupposed in developing equation (20); and the agreement noted above between Witte's and Bachmann's results lends support to this presumption.

New commercial steel pipes of 4, 8, and 16 inches nominal diameter were employed, and a honeycomb of smaller pipes was placed in each, from 10 to 15 pipe diameters ahead of the orifice. The orifices (23 in number) had diameter ratios ranging from 0.124 to 0.869, but the

[5] See footnote 1, p. 766.
[6] B. S. Jour. Research, **2**, p. 561; March, 1929.

data to be considered here are only those obtained with the 14 orifices for which the diameter ratios were between 0.3 and 0.75, or $0.09 < m < 0.56$. For, as is the case with Witte's values of C for water, the variations of C can be more accurately represented by simple empirical equations within these limits than for $\beta < 0.2$ or > 0.75.

The results are expressed in the form

$$C_1 = f(x) \tag{30}$$

where $x = (p_1 - p_2)/p_1$ and C_1 is defined by the equation

$$M = C_1 m A \sqrt{\frac{2\rho_1(p_1 - p_2)}{1 - m^2}} \tag{31}$$

M being the actual mass flow. The coefficient C_1 is connected with C_a by the relation

$$C_1 = C_a Z_1 Z_2 \tag{32}$$

where

$$z_1 = \sqrt{\frac{\gamma y^{\frac{2}{\gamma}} \left(1 - y^{\frac{\gamma-1}{\gamma}}\right)}{(\gamma - 1)\ (1 - y)}} \tag{33}$$

and

$$z_2 = \sqrt{\frac{1 - m^2}{1 - m^2 y^{\frac{2}{\gamma}}}}$$

Since $z_1 \doteq z_2 \doteq 1$ when $p_2 \doteq p_1$ or $y \doteq 1$, C_1 and C_a have the same limiting value C and we may write

$$C_1 = CY_1 \tag{34}$$

in which Y_1, like Y_a, is a function of x which reduces to unity when $x = 0$. By equations (32) and (34) we have

$$C_a = CY_a = \frac{C_1}{z_1 z_2} = C\,\frac{Y_1}{z_1 z_2} \tag{35}$$

whence

$$Y_a = \frac{Y_1}{z_1 z_2} \tag{36}$$

and if Y_1 is known, the value of Y_a for use in equation (25) may be found from it.

When the values of C_1 for each of the 14 orifices are plotted against the values of x at which they were measured, the points lie along a straight line, within the experimental errors. The slope of the line varies with m, and the average result for all the orifices is represented by the equation

$$Y_1 = 1 - (0.32 + 0.3m^2)x \tag{37}$$

In order to use this result in connection with Bachmann's values of Y_a for air, an allowance must be made for the difference between

$\gamma = 1.40$ for air and $\gamma = 1.284$, computed from the composition of the Los Angeles gas. For this purpose I have assumed the relation

$$C_1 = f\left(\frac{x}{\gamma}\right)$$

proposed by E. S. Smith,[7] which appears to be accurately true for low values of x, and to be a good approximation even as far as the critical pressure ratio.

On the basis of Smith's relation, equation (37) is to be regarded as a special form of the more general equation

$$Y_1 = 1 - (0.41 + 0.39m^2)\frac{x}{\gamma} \tag{38}$$

and for the case of air, with $\gamma = 1.40$, this reduces to

$$Y_1 = 1 - (0.293 + 0.28m^2)\, x \tag{39}$$

For the purpose of comparison with Bachmann's data on air and with equation (20), equation (39) will be assumed to represent the results that would have been obtained at Los Angeles if the experiments had been made with air instead of natural gas.

IV. COMPARISON WITH THE NEW FORMULA

Since the computations required are tedious, they have been carried out only for a few simple values of m^2 and of p_2/p_1, and the experimental values of Y_a have not been treated individually but taken from the empirical equations which represent them.

Bachmann's results have been taken from equation (27) or

$$Y_a = 1 + 0.2431\frac{p_1 - p_2}{p_2} \tag{40}$$

which represents them within the experimental errors. In accordance with (36) and (39), the equation

$$Y_a = \frac{1 - (0.293 + 0.28m^2)\, x}{z_1 z_2} \tag{41}$$

has been taken to represent the results of the experiments at Los Angeles.

The values of $\mu = C$ required for substitution in equations (20, 21) were computed from equation (28), which represents Witte's experimental results, and then corrected to what they would have been if the pressures had been observed at the upstream and downstream minima, by means of factors determined from the experiments on air already referred to.

[7] The proposal was made in a paper presented to the World Engineering Congress, Tokio, 1929, and subsequently to the Annual Meeting of the American Society of Mechanical Engineers, New York, December, 1929. The introduction of the "expansion factor" Y is also due to Mr. Smith.

In addition to computing values of μ_a/μ from (20), I have also made corresponding computations by means of the equation

$$\frac{\mu_a}{\mu}=\left[\frac{(1-\mu^2)\frac{p_1}{p_2}-\mu^2\ (1-m^2)}{1-m^2\ \mu^2}\right]^{\frac{2}{3\gamma}} \tag{42}$$

deduced by Witte [8] from the assumption of uniform expansion.

The results are summarized in the following table.

m^2	$\sqrt{m}=\beta$	μ	$\frac{p_2}{p_1}$	Y_a Bachmann equation (40)	Y_a Los Angeles equation (41)	$\frac{\mu_a}{\mu}$ equation (20)	$\frac{\mu_a}{\mu}$ equation (42)
1	2	3	4	5	6	7	8
0.005 (.00348)	0.266 (.243)	0.5970	0.9	1.027	1.028	1.030	1.032
			.8	1.061	1.062	1.066	1.068
			.7	1.104	1.107	1.112	1.108
			.6	1.162	1.167	1.170	1.155
			.53	1.216	1.222	1.221	1.190
.02	.376	.5975	.9		1.028	1.030	1.032
			.8		1.064	1.067	1.068
			.7		1.109	1.112	1.109
			.6		1.170	1.170	1.155
			.53		1.225	1.222	1.191
.06	.495	.6003	.9		1.030	1.030	1.033
			.8		1.067	1.067	1.069
			.7		1.115	1.113	1.110
			.6		1.177	1.172	1.155
			.53		1.233	1.223	1.192
.24	.700	.6038	.9		1.042	1.033	
			.8		1.091	1.072	
			.7		1.149	1.121	
			.6		1.220	1.182	
			.53		1.282	1.235	

Columns 1 and 2 give the values of m^2 for which the computations were carried out, and the corresponding values of the diameter ratio β. The figures in parentheses refer to Bachmann's orifice; they do not differ enough from the figures above them to affect the values in columns 6 to 8.

Column 3 gives the values assumed for μ in equation (20) and column 4 shows the values used for the pressure ratio p_2/p_1. The remaining columns of the table are sufficiently explained by their headings.

V. CONCLUSIONS

1. Comparison of columns 5 and 6 of the table shows that the empirical equation adopted for representing the average results of the Los Angeles experiments on natural gas, when reduced by means of Smith's assumption that $C_1=f(x/\gamma)$, agrees with the results of Bachmann's measurements on air within 0.5 per cent, the systematic difference being within the precision of the Los Angeles experiments.

[8] See footnote 1, p. 766.

The assumption proposed by Hodgson,[9] namely

$$C_1 = f\left[\left(\frac{p_2}{p_1}\right)^{\frac{1}{\gamma}}\right]$$

while not so simple as Smith's relation seems better justified. If the reduction of the Los Angeles results from $\gamma = 1.284$ to $\gamma = 1.400$ is made in accordance with this equation, the greatest difference between columns 5 and 6 is decreased from 0.006 to 0.002.

2. Comparison of columns 6 and 7 shows that the new formula agrees with the Los Angeles results to within 0.5 per cent up to $\beta = 0.376$, and to within 0.8 per cent at $\beta = 0.495$. For $\beta = 0.7$ the agreement is poor throughout, as might be expected; for with so large a diameter ratio the condition of discharge into a pipe is extremely different from the free discharge postulated in deducing the formula.

3. Comparison of columns 6 and 8 shows that Witte's formula (42) represents the facts, as far as they are known, nearly as well as the new formula, for pressure ratios down to about 0.7, but that it is inferior for still lower values of p_2/p_1.

WASHINGTON, February 16, 1931.

[9] Discussion of papers on Fluid Flow presented at the annual meeting of the A. S. M. E., New York, December, 1929.

THE EFFECT OF SMALL VARIATIONS IN PITCH UPON THE INDUCTANCE OF A STANDARD SOLENOID

By Chester Snow

ABSTRACT

A method is described by which the variations in pitch of a single-layer solenoid may be compared with those of the precision lathe screw used to wind it. Assuming that the pitch of the latter is constant, but not known with precision, it is shown how the precision measurements of the length of the windings may be combined with the former measurements to obtain the variation in pitch of the windings relative to an ideal helix whose beginning and end points coincide with the actual one. A mathematical formula for computing the correction δL to the inductance due to this variation in pitch is then developed. This formula requires the graphical integration of a certain function times the deformation and practical methods of evaluating it are described. Application is made to observations on two standard solenoids and shows that the correction δL to the inductance L may amount to 4 or 5 parts in 100,000 even on the most carefully constructed solenoids. In absolute measurements the correction is, therefore, by no means to be neglected, although it seems hitherto not to have been taken into account in determinations of the ohm.

CONTENTS

	Page
I. Introduction	777
II. Formula for δL	778
III. Practical method of evaluating the integral for δL	781
1. First method	781
2. Second method	783
IV. Numerical examples	785
1. First example	785
2. Second example	786
V. Summary	788
VI. Appendix	789

I. INTRODUCTION

In computing the inductance of a single-layer solenoid, it is at first assumed that the turns of wire are uniformly spaced. Measurements, however, show that this is never the case, no matter how carefully they are constructed. It has been possible by several different methods to measure the very small distance $\delta(y)$, by which a turn at mean distance y from one end is displaced from its ideal position. The ideal position of the nth turn is the position of the nth turn of a uniform solenoid of the same total number of turns, N, whose initial and final turns are at the mean position of the initial and final turns of the actual solenoid. The constant pitch of the windings which is used in the formula is defined as the quotient of the measured length of the solenoid by the total number of turns. To the value L of the inductance, computed by any formula which assumes a uniform pitch, we must add a small correction δL, which represents the increase that would be made in the inductance of the ideal solenoid when its turns

are displaced by the amounts $\delta(y)$ which deform it into the actual solenoid. These displacements $\delta(y)$ of each circular turn of wire are only in the direction of the axis of the solenoid so far as concerns the present problems. Variations of diameter of the solenoid, as measured over the windings or between turns, which would be due to the elastic deformation of the wires or of the cylindrical form, or of both, have been measured and their influence gives rise to other corrections which do not concern us here. However, for the sake of other possible applications, we formulate the first order correction δL caused by any infinitesmal deformation of a circuit.

II. FORMULA FOR δL

Let L_o be the inductance of any sort of winding and let $L_o+\delta L$ be the inductance when each element of the wire is given a small displacement which is represented by the vector δ, and which varies from point to point on the wire. Let T_o and $T_o+\delta T$ be the electrokinetic energy in the two cases, the current being one electromagnetic unit in each case. Let q_i be the geometric coordinates which determine the configuration of the wire. They are infinite in number and the wire will be treated as a linear circuit. The electromagnetic force (in the generalized Lagrangian sense) tending to increase any such geometric coordinate is $\frac{\partial T}{\partial q_i}$ and the work δW, which is done by all electromagnetic forces during the displacement δ, is therefore $\sum \frac{\partial T}{\partial q_i}\delta q_i = \delta T$ where δq_i is the i^{th} component of the displacement δ in the Lagrangian sense, and where the current is constant during the displacement. Therefore $\delta T = \delta W$ (with constant current unity). The electrokinetic energy is always given by $T=\frac{1}{2}LI^2=\frac{1}{2}L$ (since the current $I=1$) so that $\delta T=\frac{1}{2}\delta L=\delta W$, or

$$\delta L = 2\delta W \tag{1}$$

That is, the increase, δL, in the self-inductance of any circuit which is produced by giving it any infinitesimal deformation is equal to twice the work δW, which is done by its own electromagnetic forces during the deformation with constant current unity. If the vector H is the magnetic field at a point where the element of wire is the vector ds (treating the wire as a linear element), which field is produced by unit current in the wire in its original configuration (omitting the contribution of the element itself), then the electromagnetic force upon ds is the vector product $[ds\times H]$ and the scalar product of this by the vector displacement $([ds\times H]\cdot\delta)=([H\times\delta]\cdot ds)$ is the work done upon the element so that the total work done is

$$\delta W = \int([ds\times H]\cdot\delta) = \int([H\times\delta]\cdot ds) \tag{2}$$

integrated with respect to ds, along the length of the wire in its initial or unvaried configuration. Combining (1) and (2) gives

$$\delta L = 2\int([H\times\delta]\cdot ds) = -2\int([H\times ds]\cdot\delta) \tag{3}$$

The integral last written represents the total lines of force cut by the displacement. The penalty for idealizing the wire as a linear circuit (with zero cross section) is the same as that incurred in the use of point charges. Since the element's own field does not move it, this singular part of the field must be omitted from H. This may be done when the wire is a closely wound coil by taking H as that due to the equivalent uniform distribution of current, such as the equivalent current sheet in the case of a single layer solenoid or helix. In extreme cases, such as that of a very thick wire, the formulation (3) as a line integral would be inadmissible and must be replaced by an analogous volume integral over the volume of the wire.

For the case in hand we replace the single-layer helix by N equal and parallel circular (linear) turns whose centers are on the y-axis with the origin $y=0$ at one end. In the initial configuration the circles are equally spaced and the inductance is L_o. It is then deformed by displacing each turn (center at y) a distance $\delta(y)$ in the positive y-direction where $\delta(y)$ is derived from the observations. It may be positive or negative, and is not only small compared to the distance between two adjacent turns, but also varies slightly from turn to turn. Instead of integrating along the wire, we may then safely take $\frac{N}{l}dy$ (where l=length of windings so that $\frac{N}{l}$=number of turns per centimeter) as the number of turns in the interval dy. Each of these turns is acted upon by a force $-H_r(a, y)\ 2\pi a$ in the $+y$ direction, where a is the radius of the circular turn and $H_r(a, y)$ is the component of magnetic field perpendicular to the axis, which would be produced by the equivalent current sheet around which a current of strength $\frac{N}{l}$ per centimeter along y is circulating right-handedly (each circular turn carries unit current). The equation (3) then gives

$$\delta L=-\frac{2N}{l}\int_0^l H_r(a, y)\ 2\pi a\ \delta(y)dy \tag{4}$$

If r, θ, and y are cylindrical coordinates, the r-component of H is a function of r and y only; that is, $H_r(r, y)$ and $H_r(a, y)$ denotes its value on the sheet where $r=a$. It is continuous at $r=a$. We may compute $H_r(r, y)$ by recalling that H is the curl of a vector potential A, whose cylindrical components A_r and A_y are zero, while the component A_θ is a function of r and y only. H_r is given by

$$H_r(r, y)=-\frac{\partial A_\theta(r, y)}{\partial y} \tag{5}$$

where

$$A_\theta(r, y)=\frac{aN}{l}\int_0^l dy'\int_0^{2\pi}\frac{\cos\theta\, d\,\theta}{\sqrt{r^2-2ar\cos\theta+a^2+(y-y')^2}} \tag{6}$$

so that by (5)

$$H_r(r, y)=-\frac{aN}{l}\int_0^l dy'\frac{\partial}{\partial y}\int_0^{2\pi}\frac{\cos\theta\, d\,\theta}{\sqrt{r^2-2ar\cos\theta+a^2+(y-y')^2}}$$

$$=+\frac{aN}{l}\int_0^l dy'\frac{\partial}{\partial y'}\int_0^{2\pi}\frac{\cos\theta\, d\,\theta}{\sqrt{r^2-2ar\cos\theta+a^2+(y-y')^2}}$$

Integrating with respect to y' gives

$$H_r(r, y)=\frac{aN}{l}\int_0^{2\pi}\cos\theta\, d\,\theta\left\{\frac{1}{\sqrt{r^2-2ar\cos\theta+a^2+(l-y)^2}}\right.$$
$$\left.-\frac{1}{\sqrt{r^2-2ar\cos\theta+a^2+y^2}}\right\} \tag{7}$$

Placing $r=a$ gives

$$-H_r(a, y)=\frac{2\pi N}{l}\left[\varphi_1(\mu)-\varphi_1(\mu')\right] \tag{8}$$

where

$$\mu^2=\frac{1}{1+\left(\frac{y}{2a}\right)^2}\text{ and }\mu'^2=\frac{1}{1+\left(\frac{l-y}{2a}\right)^2} \tag{9}$$

and

$$\pi\varphi_1(\mu)\equiv-\mu\int^{\pi/2}\frac{\cos 2\theta d\theta}{\sqrt{1-\mu^2\sin^2\theta}}=\frac{2}{\mu}\Big[K(\mu)-E(\mu)\Big]-\mu K(\mu) \tag{10}$$

where K and E are the complete elliptic integrals of the first and second kind of modulus μ. The formula (4), therefore, becomes by the use of (8)

$$\delta L=\frac{8\pi^2aN^2}{l^2}\int_0^l\delta(y)[\varphi_1(\mu)-\varphi_1(\mu')]dy \tag{11}$$

where μ and μ' are functions of y given by (9), and of course $\delta(y)$ is the observed function of y. We may replace the latter by a function $f_1(y)$ defined by

$$f_1(y)=\delta(y)-\delta(l-y) \tag{12}$$

The equation (11) then transforms into

$$\delta L=\frac{8\pi^2aN^2}{l^2}\int_0^l f_1(y)\varphi_1(\mu)dy \tag{13}$$

It is next convenient to introduce a new variable of integration by the transformation

$$\lambda\equiv\frac{y}{2a} \tag{14}$$

If we define $f(\lambda)$ as $f_1(2a\lambda)$ and $\psi(\lambda)$ by

$$\psi(\lambda)\equiv\pi\phi_1(\mu)\text{ where }\mu^2=\frac{1}{1+\lambda^2} \tag{15}$$

then (13) finally becomes

$$\delta L=4\pi\left(\frac{N}{\lambda_m}\right)^2\int_0^{\lambda_m}f(\lambda)\psi(\lambda)d\lambda \tag{16}$$

where

$$\lambda_m\equiv\frac{l}{2a}=\text{the maximum value of }\lambda \tag{17}$$

The deformation of the helix is represented in (16) by the small observed function $f(\lambda)$ which may be plotted as a function of λ from $\lambda=0$ to $\lambda=\lambda_m$. The function $\psi(\lambda)$ defined by (10) and (15) has been computed by the use of tables of the elliptic integrals and plotted in Figure 1 from $\lambda=0.07$ to $\lambda=5.0$. Since it becomes logarithmically infinite at $\lambda=0$, the equation (16) needs some reshaping in order to become practicable for the evaluation of δL by graphical integration.

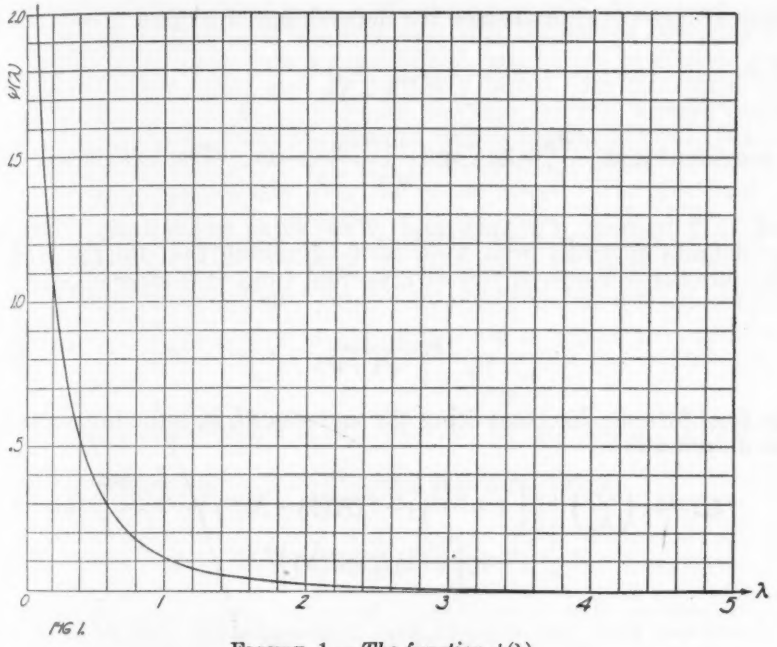

FIGURE 1.—*The function* $\psi(\lambda)$

III. PRACTICAL METHOD OF EVALUATING THE INTEGRAL FOR δL

1. FIRST METHOD

Evidently a positive value ϵ may always be so chosen that the curve of observation $f(\lambda)$ may be represented by

$$f(\lambda)=f(o)+f'(o). \quad \lambda \text{ in the range } o\leqq\lambda\leqq\epsilon \tag{18}$$

so that (16) may be written

$$\delta L=4\pi\left(\frac{N}{\lambda_m}\right)^2\left\{f(o)\int_0^\epsilon\psi(\lambda)d\lambda+f'(o)\int_0^\epsilon\lambda\psi(\lambda)d\lambda)+\int_\epsilon^{\lambda_m}f(\lambda)\psi(\lambda)d\lambda\right\} \tag{19}$$

For the last integral the integrand is easily plotted and is finite, and may be evaluated by graphical integration. The first two integrals are finite although the integrand becomes infinite in the first, but both may be evaluated analytically by means of two integral formulas

which are given in Bureau of Standards Scientific Paper No. 537 on page 449, which are

$$-\pi\int\frac{\phi_1(\mu)d\mu}{\mu^2\sqrt{1-\mu^2}}=\frac{\sqrt{1-\mu^2}}{\mu^2}\{K(\mu)-E(\mu)\} \tag{20}$$

$$-\pi\int\frac{\phi_1(\mu)d\mu}{\mu^3}=\frac{1}{3\mu}\left\{\frac{2(1-\mu^2)}{\mu^2}[K(\mu)-E(\mu)]-E(\mu)\right\} \tag{21}$$

Since $\pi\phi_1(\mu)=\psi(\lambda)$, and since the dependence of μ upon λ becomes

$$\mu^2=\frac{1}{1+\lambda^2} \tag{22}$$

it is evident that $-\frac{d\mu}{\mu^3}=\lambda d\lambda$ and $\frac{-d\mu}{\mu^2\sqrt{1-\mu^2}}=d\lambda$. The left sides of (20) and (21) become $\int\psi(\lambda)d\lambda$ and $\int\lambda\psi(\lambda)d\lambda$, respectively. Taking the definite integrals from $\lambda=0$ to $\lambda=\epsilon$ (noting that for the particular function considered $f(o)=0$), we find from (19) after placing

$$k\equiv\frac{1}{\sqrt{1+\epsilon^2}} \tag{23}$$

the final formula for computing the increase δL in inductance due to the deformation.

$$\delta L=4\pi\left(\frac{N}{\lambda_m}\right)^2\left\{\frac{1}{3}\left[1+\frac{2(1-k^2)}{k^3}\left(K(k)-E(k)\right)-\frac{E(k)}{k}\right]f'(o)+\int_\epsilon^{\lambda_m}\psi(\lambda)f(\lambda)d(\lambda)\right\} \tag{24}$$

Assuming that the straight line representation (18) of $f(\lambda)$ will generally be possible for the range $0<\lambda<\epsilon=0.1$, this becomes

$$\delta L=4\pi\left(\frac{N}{\lambda_m}\right)^2\left\{0.011f'(o)+\int_\epsilon^{\lambda_m}\psi(\lambda)f(\lambda)d\lambda\right\} \tag{24a}$$

To compute δL by this formula, it will be recalled that N is the total number of turns each of radius a and that λ is $\frac{y}{2a}$ and λ_m is $\frac{l}{2a}$ where the length of the solenoid is l cm and y is the distance in cm from one end to a variable point and the method of constructing and plotting the small function $f(\lambda)$ is as follows: The observed displacement in cm relative to the ideal helix of a turn at distance y from one end being the small function of y, $\delta(y)$, (which is reckoned as positive when the displacement is in the direction of increasing y), we define $f_1(y)$ by $f_1(y)=\delta(y)-\delta(l-y)$ and then make the transformation $y=2a\lambda$ representing the function $f_1(y)=f_1(2a\lambda)$ by the new symbol $f(\lambda)$. This may be plotted as a function of λ and the ordinates when multiplied by the ordinates of the curve Figure 1 for $\psi(\lambda)$ give the integrand of the integral in (24) or (24a). If this integrand, $\psi(\lambda)f(\lambda)$, be plotted as a function of λ, the area under the curve can be found by

graphical integration and represents the integral desired in (24). Since λ is dimensionless and $\delta(y)$ and $f(\lambda)$ and $f'(\lambda)$ are given in centimeters, the change of inductance δL given by formulas (16), (24) or (24a) will be measured in absolute c. g. s. electromagnetic units or centimeters. (1 cm $=10^{-9}$ henries.)

2. SECOND METHOD

The procedure outlined above is applicable when $f(\lambda)$ is any function which is finite and has a finite slope at $\lambda=0$. If $f(o)$ is not zero, an improper integral is involved and this method of evaluating the integral analytically over a small initial range must be used as graphical integration could give no certainty in the case of a curve going to infinity at $\lambda=0$. Since, however, the function $f(\lambda)$ always vanishes at $\lambda=0$ and has a finite initial slope, the integrand $\psi(\lambda)f(\lambda)$ is always finite (in fact zero) at $\lambda=0$, and there is no practical difficulty in evaluating it graphically over the entire range. The practical difficulty is in plotting it right down to the point $\lambda=0$. This may be overcome by obtaining an asymptotic expansion for $\psi(\lambda)$ in the neighborhood of $\lambda=0$. Such an expansion is given in Bureau of Standards Scientific Paper No. 537 on page 449, formula (56) by which

$$\pi\Phi_1(\mu)=\left[1+\frac{3}{4}(1-\mu^2)\right]ln\frac{4}{\sqrt{1-\mu^2}}-2-\frac{3}{4}(1-\mu^2)$$

in which additive terms of the order of $(1-\mu^2)\log\frac{1}{1-\mu^2}$ have been neglected. Since $1-\mu^2=\frac{\lambda^2}{1+\lambda^2}$ this becomes

$$\psi(\lambda)=\left(1+\frac{3}{4}\lambda^2\right)ln\frac{4}{\lambda}-2-\frac{1}{4}\lambda^2 \qquad (25)$$

which may be used for values of λ less than 0.1 with an absolute error which is then always less than $0.1^4 ln\ 10=0.00023$.

If we use (25) for computing the integrand $\psi(\lambda)f(\lambda)$ of equation (16) in the small range, say, $0<\lambda<0.1$ then formula (16) may be readily evaluated graphically.

In the first example below, the curve for $f(\lambda)$ is practically a straight line through the origin for $0<\lambda<0.1$ and the formula (24a) has been found most convenient. In the second example, the second method is used.

Before taking up these numerical examples, the method should be described by which the value of $\delta(y)$ was inferred from the observations. As this method was somewhat indirect, new measurements are being considered by which $\delta(y)$ may be measured directly with reference to a standard of length by means of a cathetometer.

We define the ideal solenoid of constant pitch as one of the same number N of turns whose beginning and end coincide with the actual one. Taking the y-axis as the axis of the cylinder with the origin at one end, let $\delta(y)$ be the small displacement in the y-direction which deforms the element of the ideal winding, which is distant y from the end of the coil into its actual position. Evidently $\delta(y)$ is zero at both ends; that is

$$\delta(o)=\delta(l)=0 \qquad (26)$$

Since the cylindrical form is of quartz, it may be assumed to have the same length l when mounted on the lathe for winding and comparison with the screw as it was when finally set up for measurement of its length and diameter.

The nearest substitute for the ideal coil in terms of which the actual one may be calibrated is the screw. The displacement $\Delta(y)$ which would deform an element of the screw thread into the position of the corresponding element of the actual winding was determined as a function of y by means of an optical lever on the carriage which made contact with the side of the wire. As the coil was slowly rotated and the lever carried forward on the screw, four observations were taken for each turn—4,000 readings in the case of the quartz cylinder with 1,000 turns. The scale deflections, multiplied by the calibration constant of the lever, gave $\Delta(y)$. These measurements were taken immediately after winding, with the cylinder geared to the screw exactly as in the windings, so that the element of winding was compared with practically the same part of the screw that was used in winding it. Hence, if the wire had not rolled in going on to the cylinder its pitch should have possessed practically the same variations as the screw and no deflection of the optical lever should have been observed in moving from one end to the other, even though the screw were variable in pitch. Deflections $\Delta(y)$ were observed, however, and these were reasonably concordant with a similar set of observations (which were taken on one coil) in which the optical lever was replaced by a micrometer microscope The value of $\Delta(y)$ was sometimes positive and sometimes negative, but never more than 2 per cent of the pitch or distance between two turns, which was 0.1 cm in the case of the quartz cylinder of 1,000 turns, whose length was very approximately 100 cm. The displacements $\delta(y)$ and $\Delta(y)$ are reckoned as positive when they are in the direction of increasing y.

If we let $\Delta_s y$ denote the displacement (in the $+y$ direction) which would deform the ideal helix into the screw, then

$$\delta(y)=\Delta(y)+\Delta_s(y) \tag{27}$$

Now if the screw is assumed to have a constant but unknown pitch at the time of comparison, then

$$\Delta_s(y)=A+By \text{ where } A \text{ and } B \text{ are constants} \tag{28}$$

the latter depending upon the temperature. A change in the value of A merely shifts the screw as a rigid body and is irrelevant. Combining (27) and (28) gives

$$\delta(y)=\Delta(y)+A+By \tag{29}$$

The constants A and B are determined by the two conditions (26) that $\delta(o)=\delta(l)=0$. They are

$$A=-\Delta(o)$$

$$B=\frac{1}{l}[\Delta(o)-\Delta(l)]$$

so that (29) becomes

$$\delta(y)=\Delta(y)-\left[\frac{\Delta(l)-\Delta(o)}{l}y+\Delta(o)\right] \tag{30}$$

The observations are given in the form of a curve in which is plotted as a function of y from $y=0$ to $y=l$, the small observed function $\Delta(y)$, which is the displacement of the winding relative to the screw. The equation (30) then gives the desired function $\delta(y)$ representing the displacement which deforms the ideal solenoid into the actual one. The curve for $\delta(y)$ may be plotted without computation by drawing a straight line through the end points of the curve for $\delta(y)$. This is the straight line whose ordinates are represented by the bracket which is subtracted from $\Delta(y)$ in equation (30). Hence, the vertical distance of the curve for $\Delta(y)$ above this straight line represents $\delta(y)$. (See fig. 2.)

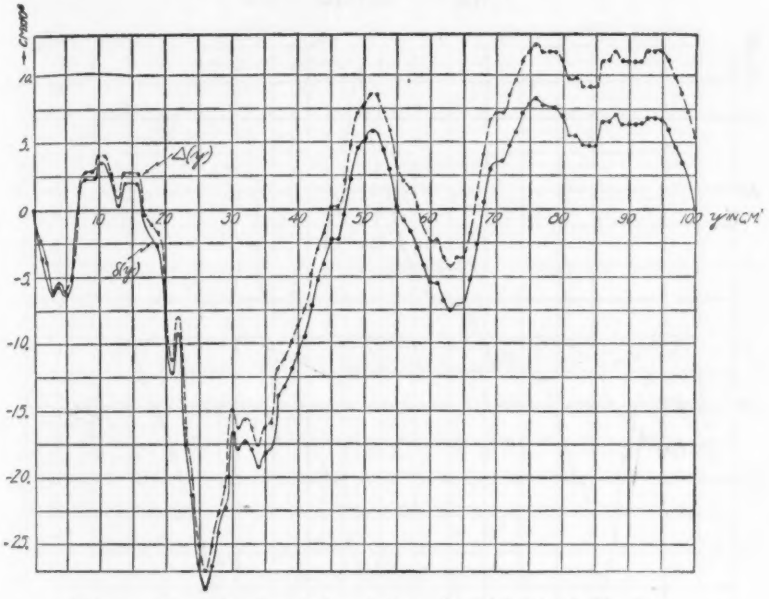

FIGURE 2.—*The observed variations in pitch of coil No. 1*

IV. NUMERICAL EXAMPLES

1. FIRST EXAMPLE

This is the case of a single layer helix of 1,000 turns of length $l=100$ cm wound upon a quartz cylinder whose radius a is 14 cm, so that $N=1{,}000$ and $\lambda_m=\frac{100}{28}=3.57$ and formula (24a) becomes

$$\delta L=\frac{4\pi(10)^6}{(3.57)^2}\left\{0.011\,f'(o)+\int_{.1}^{3.57}4(\lambda)f(\lambda)d\lambda\right\}$$

The observed variation in pitch is shown in Figure 2 by the curve which gives $\Delta(y)$ the displacement which transforms the screw thread into the actual winding. The curve in this figure for $\delta(y)$ was obtained graphically as explained since $\delta(y)$ is the height of the $\Delta(y)$ curve above the straight line connecting the ends of the latter. The $\delta(y)$ curve represents the displacement which would deform the ideal helix into the actual windings. From $\delta(y)$ the function $f_1(y)=$

$\delta(y)-\delta(l-y)$ was constructed and plotted in Figure 3 as $f(\lambda)$ where $\lambda=\frac{y}{28}$. In Figure 3 is also shown the integrand $\psi(\lambda)f(\lambda)$, the factor ψ being taken from the curve of Figure 1. The area under the latter curve of Figure 3 was found by use of the integraph to be

$$\int_{0.1}^{3.57}\psi(\lambda)f(\lambda)d\lambda=-4.7(10)^{-4} \text{ with error } < 1 \text{ per cent of itself.}$$

The unit is here the centimeter of inductance (10^{-9}), not area on the paper. The initial slope of the curve $f(\lambda)$ in Figure 3 is

$$f'(0)=-105(10^{-4}) \text{ cm}$$

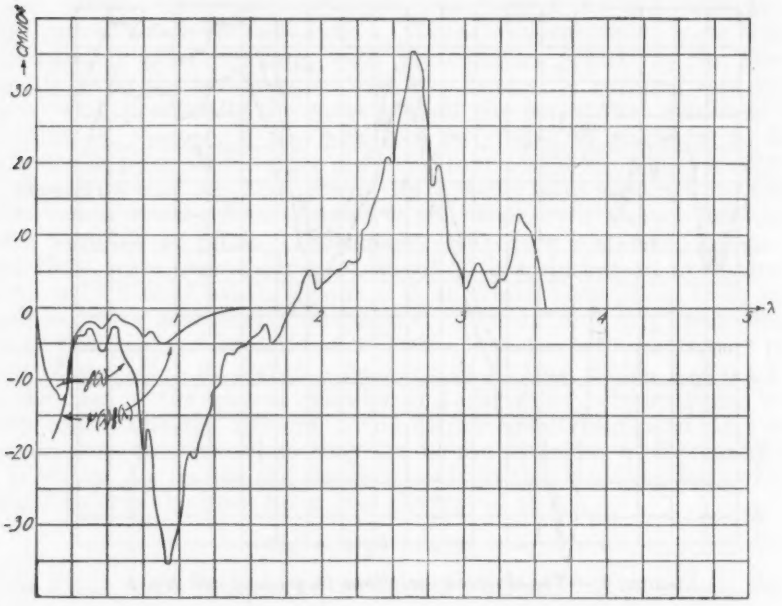

FIGURE 3.—*The functions $f(\lambda)$ and $\psi(\lambda)f(\lambda)$ for coil No. 1*

Hence formula (24) becomes

$$\delta L=-\frac{400\pi}{(3.57)^2}\{1.15+4.7\}=-580 \text{ cm}$$

which must be subtracted from the value L_o which is computed on the assumption of constant pitch. Since L_o is approximately 68×10^6 cm, this correction is about 8 parts in 1,000,000.

2. SECOND EXAMPLE

This is the case of a single-layer helix of 270 turns with the same nominal pitch (0.1 cm) as in the preceding case, but wound upon a cylinder of pyrex glass, the mean diameter of the coil being $2a=44.56$ cm, so that since $l=27$ cm, $\lambda_m=\frac{27}{44.56}=0.605$. In this case there were two types of observations whose discrepancy served to indicate the

probable total error of the method. The first was by means of the optical lever; the second was by means of readings taken with a micrometer microscope. The two sets of data are shown in Figure 4,

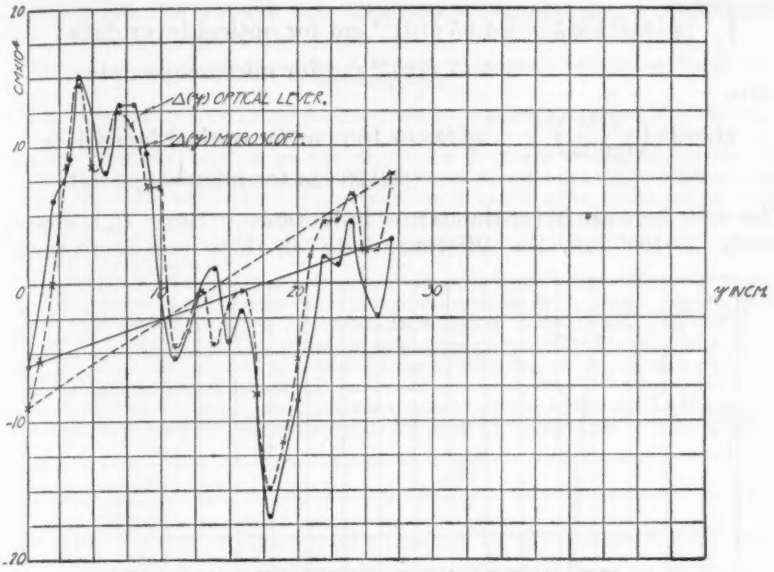

FIGURE 4.—*Observed variations in pitch of coil No. 2*

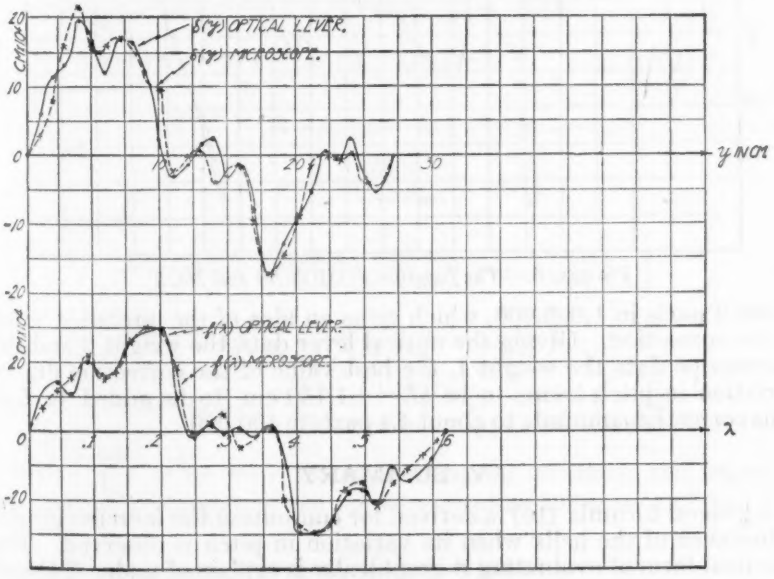

FIGURE 5.—*The functions* $\delta(\lambda)$ *and* $f(\lambda)$ *for coil No. 2*

which gives Δy in the two cases. The corresponding $\delta(y)$'s were constructed graphically and shown in the upper curves of Figure 5 and the $f(\lambda)$'s in the lower curves. In Figure 6 are shown the two

curves for $\psi(\lambda)f(\lambda)$, these being constructed by the use of formula (25) for values of λ less than 0.1. The area under these two curves was found by the use of an integraph and gave

$$\int_0^{0.605} \psi(\lambda)f(\lambda)d\lambda = +4.65\ (10)^{-4} \text{ cm for optical lever data}$$
$$= +4.47\ (10)^{-4} \text{ cm for microscope data}$$

Hence

$$\delta L = 4\pi\left(\frac{270}{0.605}\right)^2 \int_0^{0.605} \psi f d\lambda = 1{,}160 \text{ cm for optical lever data}$$
$$= 1{,}120 \text{ cm for microscope data}$$

(The units here are in centimeters of inductance.) Since L_o is approximately $26(10)^6$ cm, the difference between these two corrections is

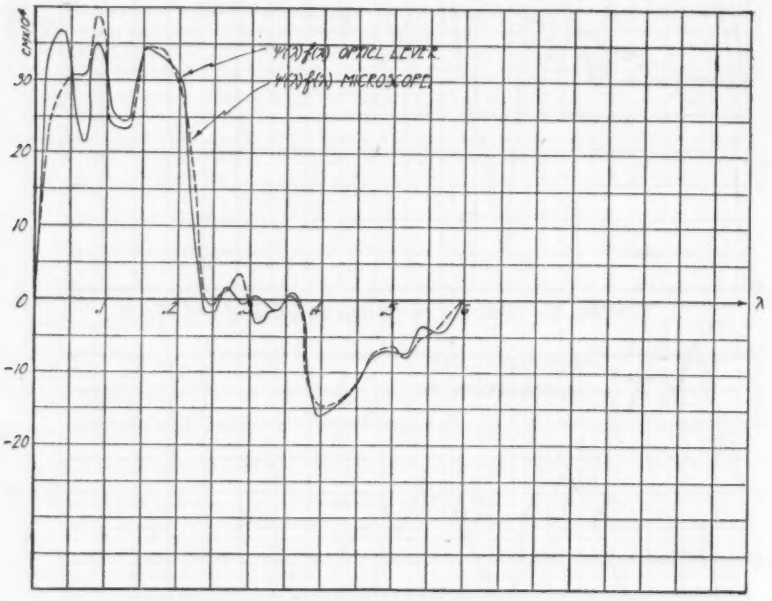

FIGURE 6.—*The function $\psi(\lambda)f(\lambda)$ for coil No. 2*

about 2 parts in 1,000,000, which gives an idea of the probable error in the correction. Giving the optical lever data the weight 2 and the microscope data the weight 1, the best value of the correction due to variation in pitch seems to be $\delta L = +1{,}150$ cm (to be added to L_o). This correction amounts to about 4.4 parts in 100,000.

V. SUMMARY

A general formula (16) is derived for computing the increase in self-inductance of the helix when its variation in pitch is observed. The practical form of evaluating it graphically is explained under (24) and (24a), and also in connection with equation (25). The directions for constructing the observational function are summarized after formula (24a). The application shows that this correction may amount to 4 or 5 parts in 100,000, which shows that it must be taken account of in absolute measurements which use the coils as standards whose inductance may be computed from their geometric dimensions.

VI. APPENDIX

1. AN INDEPENDENT METHOD OF DERIVING THE EFFECT OF SMALL VARIATIONS IN PITCH ON THE INDUCTANCE OF A STANDARD SOLENOID

(The following method was derived by F. W. Grover during the editorial reading of the preceding paper)

The inductance of a coil may be obtained by summing the self-inductances of the turns and the mutual inductances of all the pairs of turns of which the coil is composed. We will assume, as has been done in the preceding paper, that the coil is made up of parallel, coaxial, circular turns of wire; that is, the helicity will be neglected. Thus the effect of irregularities in the winding pitch will be taken into account by supposing each turn to be displaced in the axial direction by an amount equal to the average of the displacements of all the elements of the turn from their ideal positions.

It is evident that the self-inductance of an individual turn will not be altered by such a displacement. The mutual inductances of the various pairs of turns are, on the contrary, changed by the displacements of the wires from their ideal positions, and the algebraic sum of the changes of mutual inductance of all the pairs of turns of the coil will give the change of inductance of the coil, due to the assumed irregularities of winding.

If two turns, whose axial coordinates are y and $(y+\Delta y)$ in the ideal coil are given displacements δ_1 and δ_2, respectively, their mutual inductance suffers a change equal to

$$\delta M = -(\delta_1 - \delta_2)\frac{dM}{dy} \tag{1}$$

Furthermore, $\frac{dM}{dy}$ will be the same for all pairs of turns which are equally spaced in their ideal positions. Applying these considerations to the observed displacements $\delta_1, \delta_2, \delta_3, \ldots \delta_n$ of all the turns of a coil of N turns, wound with an average pitch g, the inductance of the coil is changed by an amount

$$\begin{aligned}\delta L = \Sigma \delta M = -2\Big[&\left(\frac{dM}{dy}\right)_1 \{(\delta_1-\delta_2)+\delta_2-\delta_3)+\cdots+(\delta_{n-1}-\delta_n)\} \\ &+\left(\frac{dM}{dy}\right)_2 \{(\delta_1-\delta_3)+(\delta_2-\delta_4)+\cdots+(\delta_{n-2}-\delta_n)\} \\ &+\cdots+\left(\frac{dM}{dy}\right)_{n-1}(\delta_1-\delta_n)\Big]\end{aligned} \tag{2}$$

or, rearranging

$$\begin{aligned}\delta L = -2[&(\delta_1-\delta_n)\left\{\left(\frac{dM}{dy}\right)_1+\left(\frac{dM}{dy}\right)_2+\cdots+\left(\frac{dM}{dy}\right)_{n-1}\right\} \\ &+(\delta_2-\delta_{n-1})\left\{\left(\frac{dM}{dy}\right)_2+\left(\frac{dM}{dy}\right)_3+\cdots+\left(\frac{dM}{dy}\right)_{n-2}\right\}+\cdots \\ &+(\delta_r-\delta_{n-r+1})\left\{\left(\frac{dM}{dy}\right)_r+\left(\frac{dM}{dy}\right)_{r+1}+\cdots+\left(\frac{dM}{dy}\right)_{n-r}\right\}\Big]\end{aligned} \tag{3}$$

in which $\left(\frac{dM}{dy}\right)_p$ is the rate of change of the mutual inductance with respect to their axial distance, apart, of two turns separated by a distance pg. The final term in (3) is

$$(\delta_{\frac{n}{2}}-\delta_{\frac{n}{2}+1})\left(\frac{dM}{dy}\right)_{\frac{n}{2}}, \text{ if } N \text{ is even}$$

and

$$(\delta_{\frac{n-1}{2}}-\delta_{\frac{n+3}{2}})\left(\frac{dM}{dy}\right)_{\frac{n-1}{2}}, \text{ if } N \text{ is odd.}$$

The calculation of δL is thus seen to depend upon the calculation of $\left(\frac{dM}{dy}\right)$ for pairs of coaxial circular filaments, with axial separations g, $2g$, $3g$, etc. Since the force between two filaments carrying unit current is $-\left(\frac{dM}{dy}\right)$, the terms of equations (2) and (3) are seen to represent work done by the electromagnetic forces during the deformation from the ideal winding, a result agreeing with equation (1) of the text.

Except for turns very close together, the values of the $\left(\frac{dM}{dy}\right)$ can not be expressed by a single series expression. However, the well-known elliptic integral formula of Maxwell, Elect. and Mag. volume 2, page 339, is universally applicable, or more conveniently, numerical values may be interpolated from the tables of Nagaoka and Sakurai, Institute of Physical and Chemical Research, Table 2, Tokyo, 1927.

The calculation of δL for short coils, or coils of only a few turns may readily be carried out by the use of formula (3) and such tables. For a coil of many turns, however, this process would become very laborious. In such cases the winding pitch is small compared with the dimensions of the coil, and $\left(\frac{dM}{dy}\right)$ changes slowly with the spacing of the turns. Thus it is possible to transform the summation of equation (3) into an integration over the length of the coil, and it will be shown that this leads to Doctor Snow's equation (13).

To prove this, we note that the displacements of the turns enter in (3) in the form $\delta(y)-\delta(l-y)=f_1(y)$, so that on summing along the coil, under the assumption that $\Delta y=g$ is very small, each term of (3) takes the form $\frac{1}{g}[\delta(y)-\delta(l-y)](M_y-Ml-_y)$, where M_y and M_{l-y} are the mutual inductances of equal coaxial circles, separated by axial distances y and $(l-y)$, respectively.

Thus, if we remember that the winding density is $\frac{N}{l}$ turns per cm. of axial length, equation (3) becomes

$$\delta L=\frac{2}{g}\int_0^{l/2}\frac{N}{l}f_1(y)\ (M_y-M_{l-y})dy \tag{4}$$

It is, however, to be noted that the function $\pi\varphi_1(\mu)$, of equation (15), is a factor in Maxwell's elliptic integral formula for the mutual inductance of equal coaxial circles (loc. cit.), so that we may write

$$\frac{M_y}{4\pi a}=\psi(\lambda) \tag{6}$$

and, therefore,

$$\delta L=\frac{8\pi Na}{gl}\int_0^{l/2}f_1(y)[\psi(\lambda)-\psi(\lambda_m-\lambda)]dy \tag{7}$$

The second integral in this equation may be transformed by changing the variable to $y'=l-y$, so that it takes the form $\int_{\frac{l}{2}}^{l}f_1(y)\psi(\lambda)dy$. Thus (7) becomes finally

$$\delta L=\frac{8\pi aN^2}{l^2}\int_0^{l}f_1(y)\psi(\lambda)dy \tag{8}$$

which is exactly the equation (13) of the paper, since $\pi\varphi_1(\mu)=\psi(\lambda)$.

The alternative method is thus seen to lead to exactly the same correction formula for the inductance change due to variations in winding pitch as was found by Snow's more general solution of the problem in the preceding paper.

WASHINGTON, September 15, 1930.

HEAT CONTENT VALUES FOR AQUEOUS SOLUTIONS OF THE CHLORIDES, NITRATES, AND HYDROXIDES OF HYDROGEN, LITHIUM, SODIUM, AND POTASSIUM AT 18° C.

By Frederick D. Rossini

ABSTRACT

The existing data on the heats of dilution of the chlorides, nitrates, and hydroxides of hydrogen, lithium, sodium, and potassium at various temperatures and concentrations have been converted to one temperature, and a series of values for the concentration range from infinite dilution to about 2 molal have been obtained. The extrapolation to infinite dilution has been made with the aid of the Debye-Hückel theory of strong electrolytes.

The data, exhibited in tabular and graphic form, give values for $\Phi_L - \Phi_L^\circ$, the relative apparent molal heat content of the solute, $\overline{H}_2 - \overline{H}_2^\circ$, the relative partial molal heat content of the solute, and $\overline{H}_1 - \overline{H}_1^\circ$, the relative partial molal heat content of the H_2O. The procedure employed in calculating the above quantities is given in detail.

CONTENTS

	Page
I. Definitions	791
II. Introduction	792
III. Methods of calculation and treatment of the data	796
IV. The available data	800
V. The calculated results	801
VI. Discussion	803

I. DEFINITIONS

In this discussion the nomenclature of Lewis and Randall[1] will, in the main, be followed:

m is the molality in moles of solute per 1,000 g H_2O.

The subscripts 1 and 2 refer to the solvent and solute, respectively.

The superscript zero on any symbol refers to the given property at infinite dilution.

H (printed in italic caps) is the symbol for the total heat content of a given solution.

$\overline{H}_1$ and $\overline{H}_2$ (printed in italic caps with bar) are the partial molal heat content [2] of the solvent and of the solute, respectively, and are defined by the following equations:

$$\overline{H}_1 = \left(\frac{\delta H}{\delta n_1}\right)_{n_2,\, P,\, T} \tag{1}$$

$$\overline{H}_2 = \left(\frac{\delta H}{\delta n_2}\right)_{n_1,\, P,\, T} \tag{2}$$

[1] Lewis and Randall, Thermodynamics, Chap. VIII. McGraw-Hill Book Co., New York; 1923.

[2] In the partial molal symbols, the use of the italic cap letter indicates a molal property while the overhead bar is the differential mark.

where n_1 and n_2 are the number of moles of the solvent and solute, respectively.

Φ_h is the apparent molal heat content of the solute.

$MX \cdot n_1H_2O$ designates a solution composed of 1 mole of the solute MX and n_1 moles of the solvent H_2O.

The heat content of any solution is given by the equation:[3]

$$H = n_1\overline{H}_1 + n_2\overline{H}_2 \tag{3}$$

or by definition of Φ_h,

$$H = n_1\overline{H}_2^\circ + n_2\Phi_h \tag{4}$$

For the reaction

$$n_2MX \cdot n_1H_2O + (\infty - n_1)H_2O = n_2MX \cdot \infty H_2O \tag{5}$$

$$\Delta H = [n_2\overline{H}_2^\circ + \infty\overline{H}_1^\circ] - [n_2\overline{H}_2 + n_1\overline{H}_1 + (\infty - n_1)\overline{H}_1^\circ] = n_2(\overline{H}_2^\circ - \overline{H}_2) + n_1(\overline{H}_1^\circ - \overline{H}_1) \tag{6}$$

or, using the apparent molal heat content function, for the same reaction,

$$\Delta H = [n_2\Phi_h^\circ + \infty\overline{H}_1^\circ] - [n_2\Phi_h + n_1\overline{H}_1^\circ + (\infty - n_1)\overline{H}_1^\circ] = n_2(\Phi_h^\circ - \Phi_h) \tag{7}$$

Combination of equations (6) and (7) gives

$$n_2(\Phi_h - \Phi_h^\circ) = n_2(\overline{H}_2 - \overline{H}_2^\circ) + n_1(\overline{H}_1 - \overline{H}_1^\circ) \tag{8}$$

or

$$\Phi_h - \Phi_h^\circ = \overline{H}_2 - \overline{H}_2^\circ + \frac{n_1}{n_2}(\overline{H}_1 - \overline{H}_1^\circ) \tag{9}$$

$\Phi_h - \Phi_h^\circ$ will be called the relative apparent molal heat content[4] of the solute; $\overline{H}_2 - \overline{H}_2^\circ$, the relative partial molal heat content of the solute[5], and $\overline{H}_1 - \overline{H}_1^\circ$, the relative partial molal heat content of the solvent.

II. INTRODUCTION

Values for $\Phi_h - \Phi_h^\circ$, $\overline{H}_2 - \overline{H}_2^\circ$, and $\overline{H}_1 - \overline{H}_1^\circ$ are needed in many thermodynamic calculations involving aqueous solutions. If values are known for the relative apparent molal heat content of the solute, and for the heat change in a given reaction at one concentration, one can calculate the heat change for the given reaction at any desired concentration.

The partial molal heat content of the solute and of the H_2O serve as a measure of the change of the respective partial molal free energies with temperature, according to the thermodynamic formula

$$\frac{d}{dT}\left(\frac{\overline{F} - \overline{F}^\circ}{T}\right) = -\frac{\overline{H} - \overline{H}^\circ}{T^2} \tag{10}$$

[3] See Chap. IV of reference 1.

[4] See footnote 3.

[5] Lewis and Randall (see footnote 1, p. 791) use the symbol L_2 for this property, but in order to better keep in mind the physical significance of it, we shall use the complete designation

One application of this formula is in the calculation of activity coefficients from freezing point data, where the value for $\overline{H}_1-\overline{H}_1°$ is needed.

In order to evaluate $\Phi_h-\Phi_h°$, $\overline{H}_2-\overline{H}_2°$, and $\overline{H}_1-\overline{H}_1°$, there must be available data on heats of dilution, or heats of solution, extending to very small concentrations from which extrapolation to infinite dilution will introduce no appreciable uncertainty. Until recently, the only extensive data on the heats of dilution of uni-univalent electrolytes in aqueous solution were those of Richards and Rowe,[6] who measured heats of dilution from $MX \cdot 25\ H_2O$ to $MX \cdot 400\ H_2O$, and those of Pratt,[7] who covered about the same range of concentration but at many more temperatures. Without additional information, the extrapolation from $MX \cdot 400\ H_2O$ to $MX \cdot \infty\ H_2O$ is, however, over too large a gap to bridge with any measure of certainty. Later, Richards and coworkers extended the data on HCl to $800\ H_2O$ and on NaOH to $3{,}200\ H_2O$. Following 1927, there began to appear the data of Lange [8] and coworkers, who measured the heats of dilution of salts at extremely small concentrations.

However, the Richards data were obtained at 16° to 20° C., while the Lange measurements were made at 25° C. Inasmuch as the temperature coefficient of the heat of dilution is rather large, correlation of the two sets of data with those of Pratt would be impossible without sufficiently accurate data on heat capacities in the given solutions. These data are available from values which have been compiled by the present author,[9] chiefly from the experimental data of Randall and Rossini,[10] and Richards and coworkers.[11]

For extrapolating the data to infinite dilution, a new tool has been made available with the extension to heats of dilution of the Debye-Hückel [12] theory of strong electrolytes. This extension [13] involves simply taking the temperature coefficient of the original expression given by Debye and Hückel. That the heat of dilution of strong electrolytes in the region of very small concentrations follows more or less closely the predictions of this theory was first shown by the work of Nernst and Orthmann,[14] and Lange and Messner,[15] and later by Lange [16] and others.

A short derivation of the equations expressing the change of the apparent and partial molal heat content with concentration, as derived theoretically from the Debye-Hückel theory, is given here.

Consider the two systems A and B. A is an infinitely dilute solution and B is a dilute solution of molality m. The difference in the free energy of 1 mole of solute in the two systems is

$$\Delta F = \overline{F}_2 - \overline{F}_2° \qquad (11)$$

[6] Richards and Rowe, J. Am. Chem. Soc., **43**, p. 770; 1921.
[7] Pratt, J. Frank. Inst., **185**, p. 663; 1918.
[8] Lange, Fortschritte der Chemie, Physik, und physikalische Chemie, **19**, No. 6, p. 1; 1928.
[9] These data will appear in B. S. Jour. Research, 1931.
[10] Randall and Rossini, J. Am. Chem. Soc., **51**, p. 323; 1929.
[11] Richards and Hall, Mair, Gucker, Dole, J. Am. Chem. Soc., **51**, pp. 507, 712, 727, 731, 740, and 794; 1929. Richards and Rowe, J. Am. Chem. Soc., **43**, p. 770; 1921.
[12] Debye and Hückel, Physikalische Zeit., **24**, p. 185; 1923. Debye, ibid., **25**, p. 97; 1924.
[13] Gross and Halpern, Physikalische Zeit., **26** p. 403; 1925. Bjerrum, Z. physik. Chem. **119**, p. 156; 1926. Gross, Monatshefte f. Chemie, **48**, p. 243; 1927. Lewis and Randall, "Thermodynamics," German translation by Redlich, Berlin; 1927.
[14] Nernst and Orthmann, Sitzb. Preuss. Akad. Wiss., p. 51; 1926.
[15] Lange and Messner, Z. Elektrochem., **33**, p. 431; 1927.
[16] For a complete list of this work see Lange, Z. Elektrochem., **36**, p. 772; 1930.

Following Debye and Hückel, this free energy difference may be separated into two parts: (1) The "classical" or that due to the free energy change with concentration where the molecules of solute are considered as particles of an "ideal" solution, and (2) the "electrical" or that due to the free energy change resulting from the electrical forces of the ions. Then

$$\overline{F}_2-\overline{F}_2^\circ=[\overline{F}_{2\,(\text{class.})}-\overline{F}_2^\circ{}_{(\text{class.})}]+[\overline{F}_{2\,(\text{elec.})}-\overline{F}_2^\circ{}_{(\text{elec.})}] \tag{12}$$

For very low concentrations, one may write

$$\overline{F}_2-\overline{F}_2^\circ=R\ T\ ln\ m+\left[-\frac{N^{3/2}\ e^3}{D^{3/2}\ T^{1/2}}\left(\frac{\pi}{1{,}000\ k}\right)^{1/2}(\Sigma\nu_i z_i^2)^{3/2}m^{1/2}\right] \tag{13}$$

where the last term is that given by Debye and Hückel for the change in "electrical" free energy for the very dilute range with the exception that m has been substituted for the concentration. In this expression N is Avogadro's number, e is the electronic charge, D is the dielectric constant of the medium, k is Boltzmann's constant, T is the absolute temperature, z is the charge on the ith kind of ions whose number per molecule of solute is ν, and m is the molality as already defined.

By operating upon equation (13) according to the thermodynamic relation expressed by equation (10)

$$\frac{d}{dT}\left(\frac{\overline{F}_2-\overline{F}_2^\circ}{T}\right)=-\frac{\overline{H}_2-\overline{H}_2^\circ}{T^2} \tag{10}$$

one obtains the expression

$$\overline{H}_2-\overline{H}_2^\circ=-\tfrac{3}{2}\frac{N^{3/2}e^3}{D^{3/2}T^{1/2}}\left(\frac{\pi}{1{,}000\ k}\right)^{1/2}\left(1+\frac{T\,dD}{D\,dT}\right)\ (\Sigma\nu_i z_i^2)^{3/2}\ m^{1/2} \tag{14}$$

New data on the dielectric constant of water and its temperature coefficient have recently been published.[17] These have been reviewed and compared with the existing data [18] by Lange and Robinson.[19] Following the suggestion of these latter authors, the values for D and $\frac{dD}{dT}$ used in the present work were obtained by averaging the values of Drude, Wyman, and Drake, Pierce, and Dow. This gives the following values for 18° C.

$$D=81.15 \qquad \frac{dD}{dT}=-0.37$$

Then, for a uni-univalent electrolyte at 18° C., evaluation of equation (14) gives

$$\overline{H}_2-\overline{H}_2^\circ=653\ m^{1/2}\ \text{calories per mole of solute} \tag{15}$$

[17] Drake, Pierce, and Dow, Phys. Rev., **35**, p. 613; 1930. Wyman, Phys. Rev., **35**, p. 623; 1930. Cuthbertson and Maass, J. Am. Chem. Soc., **52**, p. 483; 1930.
[18] Drude, Wied. Ann., **59**, p. 48; 1896. Kockel, Ann. Physik., **77**, p. 430; 1925.
[19] Lange and Robinson, J. Am. Chem. Soc., **52**, p. 2811; 1930.

This expression gives the variation with concentration of the relative partial molal heat content of the solute from the region of very low concentration to infinite dilution.

The expression for the like property of the solvent, H_2O, can be deduced from the partial molal equation.[20]

$$55.508\ d\bar{H}_1 + m\ d\bar{H}_2 = 0 \tag{16}$$

On substituting in equation (16) the value for $d\bar{H}_2$ obtained by differentiating equation (15), and then integrating, one obtains for an aqueous solution of a uni-univalent electrolyte at 18° C.

$$\bar{H}_1 - \bar{H}_1^\circ = -\frac{(\bar{H}_2 - \bar{H}_2^\circ)\ m}{3\ (55.508)} = -\frac{653\ m^{3/2}}{3\ (55.508)} \tag{17}$$
$$= -3.92\ m^{3/2} \text{ calories per mole of } H_2O$$

For a solution composed of m moles of solute and 1,000 g or 55.508 moles of H_2O, equation (9) may be written

$$\Phi_h - \Phi_h^\circ = \bar{H}_2 - \bar{H}_2^\circ + \frac{55.508}{m}(\bar{H}_1 - \bar{H}_1^\circ) \tag{18}$$

Substituting into equation (18), $-\frac{(\bar{H}_2 - \bar{H}_2^\circ)\ m}{3\ (55.508)}$ for $(\bar{H}_1 - \bar{H}_1^\circ)$ (from equation (17)) gives

$$\Phi_h - \Phi_h^\circ = \frac{2}{3}(\bar{H}_2 - \bar{H}_2^\circ) \tag{19}$$

This relation always holds whenever a partial molal property of the solute is directly proportional to $m^{1/2}$.

Evaluating equation (19), one obtains

$$\Phi_h - \Phi_h^\circ = 435\ m^{1/2} \text{ calories per mole of solute} \tag{20}$$

This equation gives the theoretical variation of the relative apparent molal heat content with concentration in the very dilute region for a uni-univalent electrolyte at 18° C., and is the device used in this paper to extrapolate the experimental data from regions of low concentration to infinite dilution.

The uncertainty in the value of the numerical cœfficient in equation (20) is in large part due to the uncertainty in the value of $\frac{dD}{dT}$ used in evaluating equation (14). If the uncertainty [21] in the value of $\frac{dD}{dT}$ is taken as about 3 per cent, the resulting uncertainty in the value of the numerical cœfficient in equation (20) is about 50 calories. However, since this equation is used in extrapolating only over a small range, the uncertainty due to lack of knowledge of the exact value of this cœfficient introduces a possible error in the extrapolated values of only several calories in most cases. As can be seen from an inspection of Figures 1, 2, and 3, where are plotted the experimentally

[20] See footnote 3, p. 792.

[21] See footnote 19, p. 794.

observed values for the heats of dilution, the error in locating the intercept at infinite dilution is due more to lack of knowledge of the exact position of the curve in the region of low concentration than to the selection of the slope used in extrapolation.

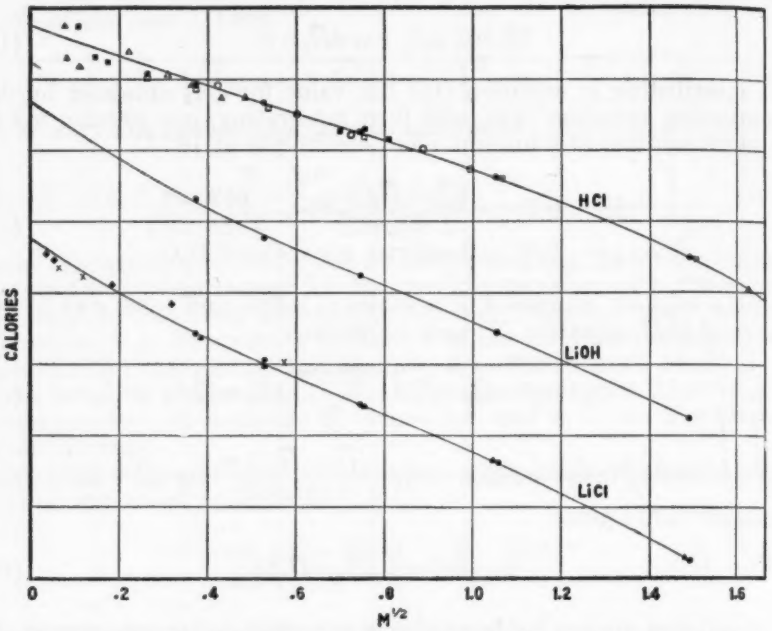

FIGURE 1.—*Plot of the experimental data on the heats of dilution of HCl, LiCl, and LiOH*

The data have been calculated to 18°C., in calories per mole of solute.

The ordinate scale measures the apparent molal heat content in calories per mole while the abscissa scale gives the square root of the molality. Each unit of the ordinate scale is for HCl, 200 calories, and for LiCl and LiOH, 100 calories.

The data of the various investigators are:

● Richards and Rowe.
□ Richards, Mair, and Hall.
■ Muller.
△ Steinwehr.
○ Wrewsky and Savaritzky.
◆ Nernst and Orthmann.
× Nernst and Naudé.
▲ Lange and Durr.

III. METHODS OF CALCULATION AND TREATMENT OF DATA

The starting point for the evaluation of $\Phi_h - \Phi_h^\circ$, $\overline{H}_2 - \overline{H}_2^\circ$, and $\overline{H}_1 - \overline{H}_1^\circ$ lies in equatior. (7) where the quantity ΔH can be determined by proper extrapolation of the experimental data to infinite dilution. This may be illustrated by the following procedure:

Given the solution $HCl \cdot 25H_2O$. The heat content of this solution is

$$H = \overline{H}_2 + 25\overline{H}_1 \tag{21}$$

or

$$H = \Phi_h + 25\overline{H}_1^\circ \tag{22}$$

The heat change which occurs when this solution is diluted, for example with an equal amount of H_2O, is measured. We have the reaction

$$HCl \cdot 25H_2O + 25H_2O = HCl \cdot 50H_2O \qquad (23)$$

The heat content of the newly formed solution is H′.

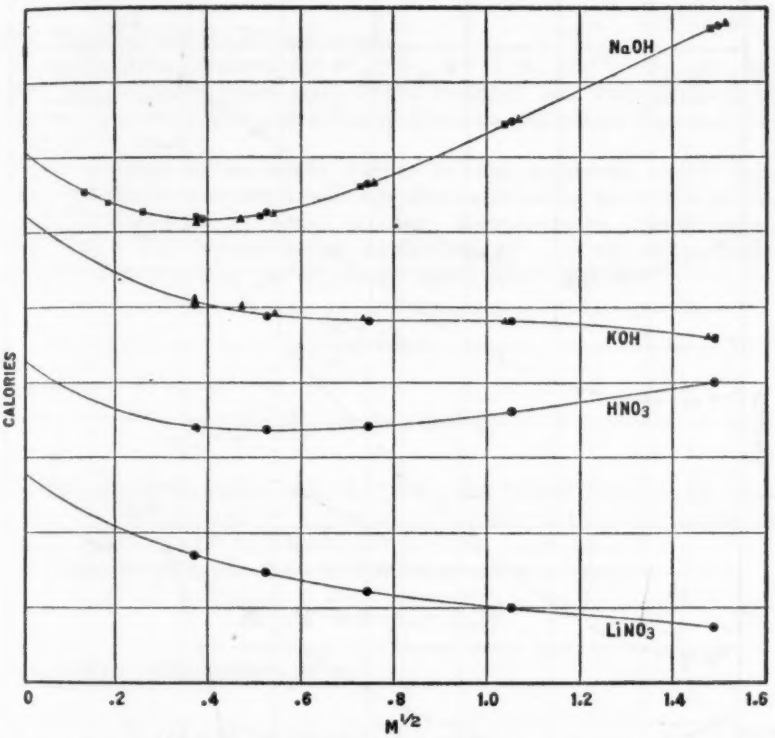

FIGURE 2.—*Plot of the experimental data on the heats of dilution of NaOH, KOH, HNO_3, and $LiNO_3$*

The data have been calculated to 18°C., in calories per mole of solute.
The ordinate scale measures the apparent molal heat content in calories per mole while the abscissa scale gives the square root of the molality. Each unit of the ordinate scale is 100 calories.
The data of the various investigators are:
● Richards and Rowe. ■ Richards and Gucker. ▲ Pratt.

Then

$$\Delta H = \Phi'_h + 50\overline{H}_1^\circ - [(\Phi_h + 25\overline{H}_1^\circ) + 25\overline{H}_1^\circ] = \Phi_h' - \Phi_h \qquad (24)$$

One then proceeds to measure the heat change when this new solution is further diluted:

$$HCl \cdot 50H_2O + 50H_2O = HCl \cdot 100H_2O \qquad (25)$$

This gives

$$\Delta H = \Phi_h'' - \Phi_h' \qquad (26)$$

Combining with equation (24), one obtains for the reaction

$$HCl \cdot 25H_2O + 75H_2O = HCl \cdot 100H_2O \quad (27)$$

the heat change

$$\Delta H = \Phi_h'' - \Phi_h \quad (28)$$

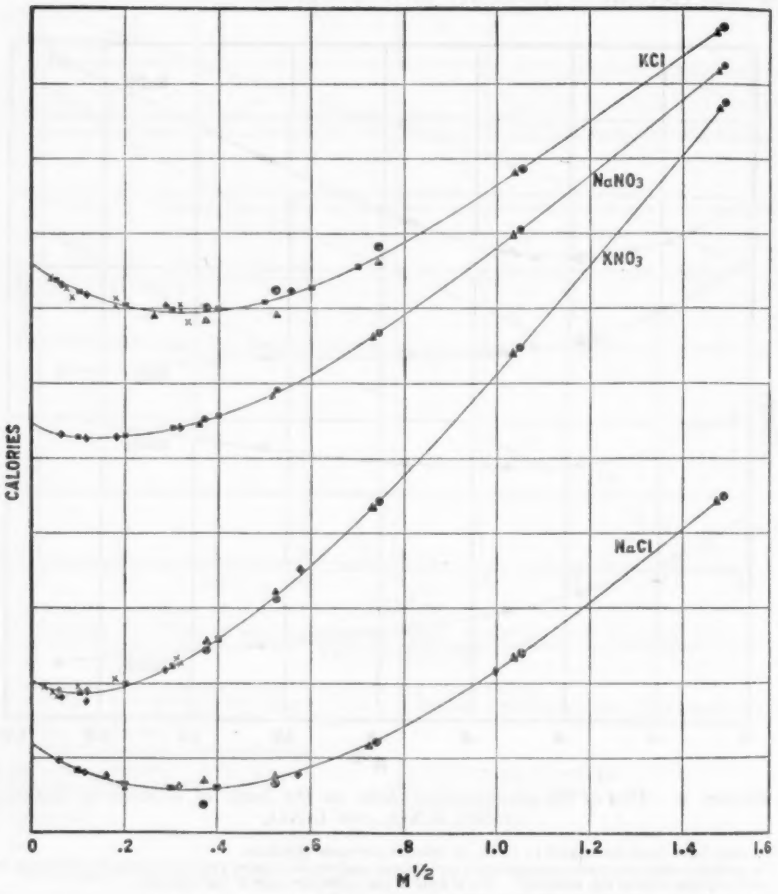

FIGURE 3.—*Plot of the experimental data on the heats of dilution of NaCl, KCl, $NaNO_3$, and KNO_3*

The data have been calculated to 18° C., in calories per mole of solute.

The ordinate scale measures the apparent molal heat content in calories per mole while the abscissa scale gives the square root of the molality. Each unit of the ordinate scale is for NaCl and KCl, 100 calories, and for $NaNO_3$ and KNO_3, 200 calories.

The data of the various investigators are:

● Richards and Rowe.
■ Lange et al.
▲ Pratt.
◆ Nernst and Naudé.
× Nernst and Orthmann.

Proceeding in this manner, one can measure, with sufficiently accurate and sensitive apparatus, heats of dilution to very small concentrations. When a proper extrapolation to infinite dilution is made, then, for the reaction

$$HCl \cdot 25H_2O + (\infty - 25)\ H_2O = HCl \cdot \infty H_2O \quad (29)$$

the heat change becomes

$$\Delta H = H^\circ - H = \Phi_h^\circ - \Phi_h \tag{30}$$

or for the reverse change

$$\Phi_h - \Phi_h^\circ = H - H^\circ \tag{31}$$

where 1 mole of solute is concerned.

When the data obtained for $\Phi'_h - \Phi_h$, $\Phi''_h - \Phi_h$, $\Phi_h''' - \Phi_h$, etc., are plotted against the square root of the molality and extrapolated by means of equation (20) to infinite dilution, values of $\Phi_h - \Phi_h^\circ$ can be read off.

Where sufficiently accurate values of the apparent molal heat capacity of the solute are available, the calculation to 18°C. of the heat of dilution data obtained at other temperatures introduces no uncertainty. The temperature coefficient of the apparent molal heat content is equal to the apparent molal heat capacity:

$$\frac{d\Phi_h}{dT} = \Phi_c \tag{32}$$

or

$$\frac{d}{dT}(\Phi_h - \Phi_h^\circ) = \Phi_c - \Phi_c^\circ \tag{33}$$

Having obtained values for $\Phi_h - \Phi_h^\circ$, the values for $\overline{H}_2 - \overline{H}_2^\circ$ and $\overline{H}_1 - \overline{H}_1^\circ$ can be derived by a procedure similar to that employed by Randall and Rossini [22] and Rossini [23] for heat capacities.

From equation (28), one may write, for m moles of solute,

$$H - H^\circ = m\,(\Phi_h - \Phi_h^\circ) \tag{34}$$

Differentiating with respect to m,

$$\frac{d}{dm}(H - H^\circ) = (\Phi_h - \Phi_h^\circ) + m\frac{d}{dm}(\Phi_h - \Phi_h^\circ) \tag{35}$$

But

$$\frac{d}{dm}(H - H^\circ) = \overline{H}_2 - \overline{H}_2^\circ \tag{36}$$

Hence

$$\overline{H}_2 - \overline{H}_2^\circ = \Phi_h - \Phi_h^\circ + m\frac{d}{dm}(\Phi_h - \Phi_h^\circ) \tag{37}$$

substituting $2m^{1/2}\,d\,m^{1/2}$ for dm, we obtain

$$\overline{H}_2 - \overline{H}_2^\circ = \Phi_h - \Phi_h^\circ + \tfrac{1}{2}m^{1/2}\frac{d}{dm^{1/2}}(\Phi_h - \Phi_h^\circ) \tag{38}$$

From a plot of values of $\Phi_h - \Phi_h^\circ$ against $m^{1/2}$, one obtains values for $\overline{H}_2 - \overline{H}_2^\circ$ from equation (38).

---

[22] See footnote 10, p. 793. [23] Rossini, B. S. Jour. Research, **4**, p. 313; 1930.

Now by equation (18)

$$\Phi_h - \Phi_h^\circ = \overline{H}_2 - \overline{H}_2^\circ + \frac{55.508}{m}(\overline{H}_1 - \overline{H}_1^\circ) \tag{18}$$

Combination of equations (38) and (18) gives

$$\overline{H}_1 - \overline{H}_1^\circ = -\frac{m^{3/2}}{2(55.508)}\frac{d}{dm^{1/2}}(\Phi_h - \Phi_h^\circ) \tag{39}$$

Values of the slope of $\Phi_h - \Phi_h^\circ$ against $m^{1/2}$ have already been obtained in evaluating $\overline{H}_2 - \overline{H}_2^\circ$. There remains only the multiplication of this slope by the coefficient, $-\frac{m^{3/2}}{2(55.508)}$, to obtain values for $\overline{H}_1 - \overline{H}_1^\circ$.

IV. THE AVAILABLE DATA

The data which have been used in this paper to carry out the procedure and calculations described in the foregoing section are plotted, for the various solutes, in Figures 1, 2, and 3. The plotted data have, of course, all been calculated to 18° C. from whatever temperature they were measured. Only those data which give heats of dilution in the range from $MX \cdot 25H_2O$ to infinite dilution were considered.

Richards and Rowe [24] measured the heats of dilution of HCl at 16° and 20° C. over the range $HCl \cdot 25H_2O$ to $HCl \cdot 400H_2O$. These same authors [25] obtained data at the same temperatures and for the same range of concentration on HNO_3, $LiNO_3$, $NaNO_3$, KNO_3, LiCl, NaCl, KCl, LiOH, NaOH, and KOH. For the purposes of the present work, the measurements at 16° and 20° C. were averaged to give the heat of dilution at 18° C.

Richards, Mair, and Hall [26] repeated the measurements on HCl and extended them to $HCl \cdot 800\ H_2O$. Richards and Gucker [27] reported new measurements on NaOH, extending the data to $NaOH \cdot 3200H_2O$.

Pratt [28] measured the heats of dilution of NaCl, KCl, $NaNO_3$, NaOH and KOH over the range of concentration $MX \cdot 25H_2O$ to about $MX \cdot 400H_2O$ at many temperatures from 0° to 33.5° C. For NaCl and KCl, data at 18° C. were available, but for the other electrolytes data for 18° C. were obtained by interpolating the measurements made by Pratt at 15° and 20° C.

Data on HCl were available from the measurements of Muller [29] at 16° C., of Steinwehr [30] at 18° C., and the data of Wrewskii and Savaritzky,[31] who measured the heat of solution of HCl gas in water at 21.5° C. for various concentrations.

In the very dilute range of concentrations there are the measurements of Lange and coworkers at 25° C. and of Nernst and coworkers

[24] Richards and Rowe, J. Am. Chem. Soc., **43**, p. 1621; 1920.
[25] Richards and Rowe, J. Am. Chem. Soc., **43**, p. 770; 1921.
[26] Richards, Mair, and Hall, J. Am. Chem. Soc., **51**, p. 727; 1929.
[27] Richards and Gucker, J. Am. Chem. Soc., **51**, p. 712; 1929.
[28] Pratt, J. Frank. Inst., **185**, p. 663; 1918.
[29] Muller, Bull. Soc. Chim., **13**, p. 1053; 1913.
[30] Steinwehr, Z. physik. Chem., **38**, p. 185; 1903.
[31] Wrewskii and Savaritzky, Z. physik. Chem., **112**, p. 90; 1924.

at 18° C. Lange and Robinson [32] obtained data on $NaNO_3$ and NaCl; Lange and Leighton,[33] on KCl; and Lange and Monheim,[34] on KNO_3. The original work of Lange and Messner [35] contained a few data on LiCl, NaCl, KCl, and KNO_3. The measurements of Nernst and Orthmann [36] include data on LiCl and KCl, while Nernst and Naudé [37] record some measurements on LiCl, NaCl, KCl, $NaNO_3$, and KNO_3.

All of the foregoing data, where obtained at other temperatures, were calculated to 18° C. by means of the apparent molal heat capacity values already mentioned.[38] The experimental data for the heats of dilution have been plotted against $m^{1/2}$ in Figures 1, 2, and 3. The extrapolation to infinite dilution has been made by the use of equation (20).

V. THE CALCULATED RESULTS

By a shift of the ordinate scale so that the intercept of the curve for the heat of dilution on the ordinate axis becomes the origin, $m=0$ and $\Phi_h-\Phi_h^\circ=0$, the curves in Figures 1, 2, and 3 give immediately values for $\Phi_h-\Phi_h^\circ$, by equation (30).

In Table 1 are given values of $\Phi_h-\Phi_h^\circ$, the relative apparent molal heat content of the solute, for the 11 different solutions at dilutions expressed in terms of the number of moles of H_2O associated with 1 mole of solute.

From the curves of $\Phi_h-\Phi_h^\circ$ against $m^{1/2}$, values of $\overline{H}_2-\overline{H}_2^\circ$, the relative partial molal heat content of the solute, were determined by means of equation (38). Then by application of equation (39) values for $\overline{H}_1-\overline{H}_1^\circ$, the relative partial molal heat content of the H_2O, were obtained. In Table 2 are given values of $\Phi_h-\Phi_h^\circ$, $\overline{H}_2-\overline{H}_2^\circ$, and $\overline{H}_1-\overline{H}_1^\circ$, for the 11 different solutions at concentrations from $m=0$ to $m=1.96$.

TABLE 1.—$\Phi_A-\Phi_A^0$, *relative apparent molal heat content, at 18° C. in g-cal.*[18] *per mole of solute* [a]

Solution ↓ MX→	HCl	LiCl	NaCl	KCl	HNO_3	$LiNO_3$	$NaNO_3$	KNO_3	LiOH	NaOH	KOH
MX· ∞ H_2O	0	0	0	0	0	0	0	0	0	0	0
MX· 6,400 H_2O	41	38	35	33	36	36	30	31	40	38	38
MX· 3,200 H_2O	58	53	45	42	48	49	34	29	55	50	52
MX· 1,600 H_2O	81	73	55	51	61	65	31	18	77	63	70
MX· 800 H_2O	115	100	61	58	74	85	18	−17	106	76	90
MX· 400 H_2O	162	132	61	58	85	108	−15	−90	141	86	113
MX· 200 H_2O	222	175	47	45	90	133	−86	−233	188	78	130
MX· 100 H_2O	305	231	−5	−13	86	157	−246	−465	243	39	137
MX· 50 H_2O	430	312	−120	−128	66	180	−520	−885	323	−45	137
MX· 25 H_2O	655	450	−330	−318	28	205	−960	−1,530	443	−173	162

[a] The composition of the solution is given in terms of the number of moles of water associated with 1 mole of solute.

[32] Lange and Robinson, Z. physik. Chem., A, **148**, p. 197; 1930.
[33] Lange and Leighton, Z. Elektrochem., **34**, p. 566; 1928.
[34] Lange and Monheim, Z. physik. Chem., A, **150**, p. 349; 1930.
[35] Lange and Messner, Naturwissenschaften, **15**, p. 521; 1927.
[36] Nernst and Orthmann, sitzb. preuss. Akad. Wiss., p. 51; 1926; p. 136; 1927.
[37] Nernst and Naudé, Z. Elektrochem., **33**, p. 532; 1927.
[38] See footnote 9, p. 793.

TABLE 2.—*Apparent and partial molal heat content of solute and partial molal heat content of H_2O in aqueous solutions of HCl, LiCl, NaCl, KCl, HNO_3, $LiNO_3$, $NaNO_3$, KNO_3, LiOH, NaOH, and KOH at 18° C*

Solute	m moles of solute per 1,000 g H_2O	$m^{1/2}$	$\Phi_A-\Phi_A^\circ$ g-cal.$_{18}$ per mole of solute	$\bar{H}_2-H_2^\circ$ g-cal.$_{18}$ per mole of solute	$\bar{H}_1-H_1^\circ$ g-cal.$_{18}$ per mole of H_2O
HCl	0	0	0	0	0
	.01	.1	44	66	−.0040
	.04	.2	88	131	−.0310
	.09	.3	131	196	−.105
	.16	.4	173	257	−.242
	.25	.5	213	310	−.437
	.36	.6	251	367	−.752
	.64	.8	327	482	−1.78
	1.00	1.0	408	623	−3.87
	1.44	1.2	500	792	−7.57
	1.96	1.4	604	983	−13.38
LiCl	0	0	0	0	0
	.01	.1	41	61	−.0036
	.04	.2	78	113	−.0252
	.09	.3	112	159	−.0762
	.16	.4	141	197	−.162
	.25	.5	168	234	−.297
	.36	.6	194	271	−.499
	.64	.8	245	347	−1.18
	1.00	1.0	297	433	−2.45
	1.44	1.2	355	537	−4.72
	1.96	1.4	419	658	−8.44
NaCl	0	0	0	0	0
	.01	.1	38	52	−.0025
	.04	02	56	66	−.0072
	.09	.3	62	64	−.0032
	.16	.4	60	47	+.037
	.25	.5	48	14	.153
	.36	.6	33	−31	.415
	.64	.8	−23	−154	1.51
	1.00	1.0	−97	−303	3.71
	1.44	1.2	−188	−477	7.50
	1.96	1.4	−287	−638	12.39
KCl	0	0	0	0	0
	.01	.1	35	49	−.0025
	.04	.2	52	63	−.0079
	.09	.3	59	63	−.0064
	.16	.4	58	51	+.020
	.25	.5	49	14	.158
	.36	.6	30	−44	.480
	.64	.8	−33	−165	1.53
	1.00	1.0	−108	−306	3.57
	1.44	1.2	−188	−442	6.59
	1.96	1.4	−277	−605	11.58
HNO_3	0	0	0	0	0
	.01	.1	38	54	−.0029
	.04	.2	64	84	−.0144
	.09	.3	79	111	−.052
	.16	.4	86	97	−.032
	.25	.5	90	96	−.027
	.36	.6	90	88	+.013
	.64	.8	84	58	.30
	1.00	1.0	70	32	.68
	1.44	1.2	54	6	1.25
	1.96	1.4	37	−32	2.44
$LiNO_3$	0	0	0	0	0
	.01	.1	38	55	−.0031
	.04	.2	69	94	−.0180
	.09	.3	93	125	−.052
	.16	.4	113	148	−.101
	.25	.5	129	166	−.167
	.36	.6	142	176	−.221
	.64	.8	162	195	−.38
	1.00	1.0	177	213	−.65
	1.44	1.2	190	224	−.88
	1.96	1.4	201	235	−1.20
$NaNO_3$	0	0	0	0	0
	.0025	.05	20	30	−.0004
	.01	.1	32	39	−.0013
	.04	.2	30	18	+.0087
	.09	.3	8	−34	.068
	.16	.4	−25	−102	.222
	.25	.5	−71	−208	.617
	.36	.6	−135	−349	1.388
	.64	.8	−290	−635	3.98
	1.00	1.0	−475	−942	8.42
	1.44	1.2	−667	−1260	15.38
	1.96	1.4	−868	−1584	25.28
KNO_3	0	0	0	0	0
	.0025	.05	20	30	−.0004
	.01	.1	32	33	−.0002
	.04	.2	13	−26	+.026
	.09	.3	−39	−136	.157
	.16	.4	−113	−276	.470
	.25	.5	−207	−456	1.122
	.36	.6	−313	−636	2.195
	.64	.8	−551	−1060	5.87
	1.00	1.0	−823	−1525	12.65
	1.44	1.2	−1108	−1993	22.96
	1.96	1.4	−1408	−2476	37.71
LiOH	0	0	0	0	0
	.01	.1	42	63	−.0038
	.04	.2	82	119	−.0267
	.09	.3	118	168	−.081
	.16	.4	150	212	−.179
	.25	.5	180	252	−.328
	.36	.6	208	286	−.506
	.64	.8	258	360	−1.18
	1.00	1.0	310	440	−2.34
	1.44	1.2	362	525	−4.23
	1.96	1.4	418	615	−6.96
NaOH	0	0	0	0	0
	.01	.1	40	57	−.0031
	.04	.2	65	84	−.0137
	.09	.3	81	97	−.026
	.16	.4	86	84	+.006
	.25	.5	81	58	.136
	.36	.6	68	20	.311
	.64	.8	26	−75	1.16
	1.00	1.0	−30	−170	2.52
	1.44	1.2	−86	−254	4.36
	1.96	1.4	−143	−319	6.21
KOH	0	0	0	0	0
	.01	.1	40	58	−.0032
	.04	.2	74	103	−.0218
	.09	.3	99	131	−.052
	.16	.4	117	145	−.081
	.25	.5	129	148	−.086
	.36	.6	133	147	−.091
	.64	.8	137	137	.000
	1.00	1.0	137	139	−.036
	1.44	1.2	142	164	−.57
	1.96	1.4	154	207	−1.87

The data for $\Phi_h - \Phi_h^\circ$ and $\overline{H}_2 - \overline{H}_2^\circ$ are plotted against $m^{1/2}$ in Figures 4 and 5, respectively, while Figure 6 shows values of $\overline{H}_1 - \overline{H}_1^\circ$ plotted against $m^{3/2}$.

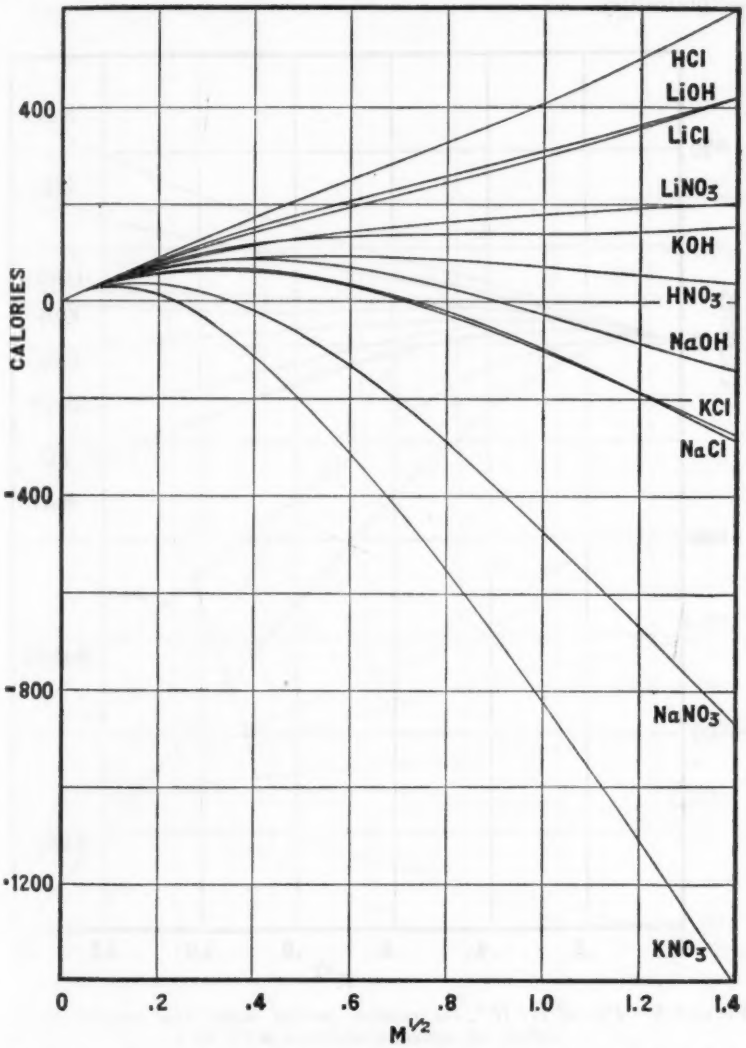

FIGURE 4.—*Plot of $\Phi_h - \Phi_h^\circ$, the relative apparent molal heat content of the solute, in aqueous solutions at 18° C.*

The ordinate scale gives $\Phi_h - \Phi_h^\circ$ in calories per mole of solute while the abscissa scale gives the square root of the molality.

VI. DISCUSSION

The character of the family of curves shown in Figure 4, in which the relative apparent molal heat content is plotted against the square

root of the molality, has already been discussed, in the very dilute region by Lange[39] and coworkers, and in the more concentrated range by Richards and Rowe.[40] The curves in Figures 5 and 6, showing the relative partial molal heat content of the solute and of the H_2O, are self-explanatory.

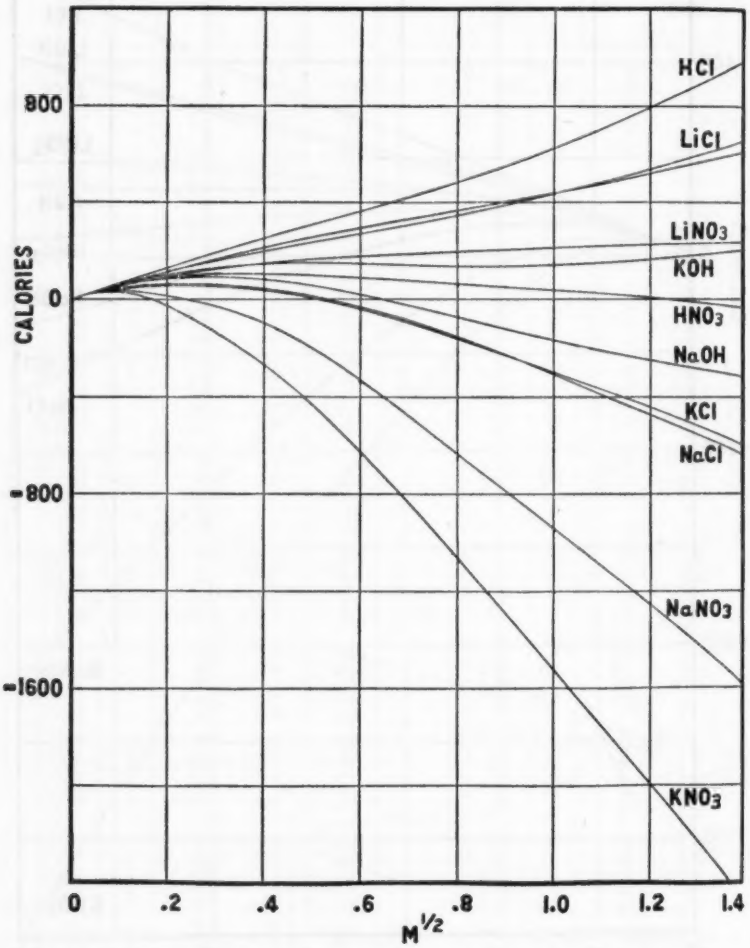

FIGURE 5.—*Plot of $\bar{H}_2-\bar{H}_2°$, the relative partial molal heat content of the solute, in aqueous solutions at 18° C.*

The ordinate scale gives $\bar{H}_2-\bar{H}_2°$ in calories per mole of solute while the abscissa scale gives the square root of the molality.

The usefulness of a complete compilation of values of $\Phi_h-\Phi_h°$, $\bar{H}_2-\bar{H}_2°$, $\bar{H}_1-\bar{H}_1°$, for the given concentration range will be apparent to whoever has need of such data in the calculation of heats of reaction at various concentrations from a heat of reaction measured at

[39] See footnote 16, p. 793. [40] See footnote 6, p. 793.

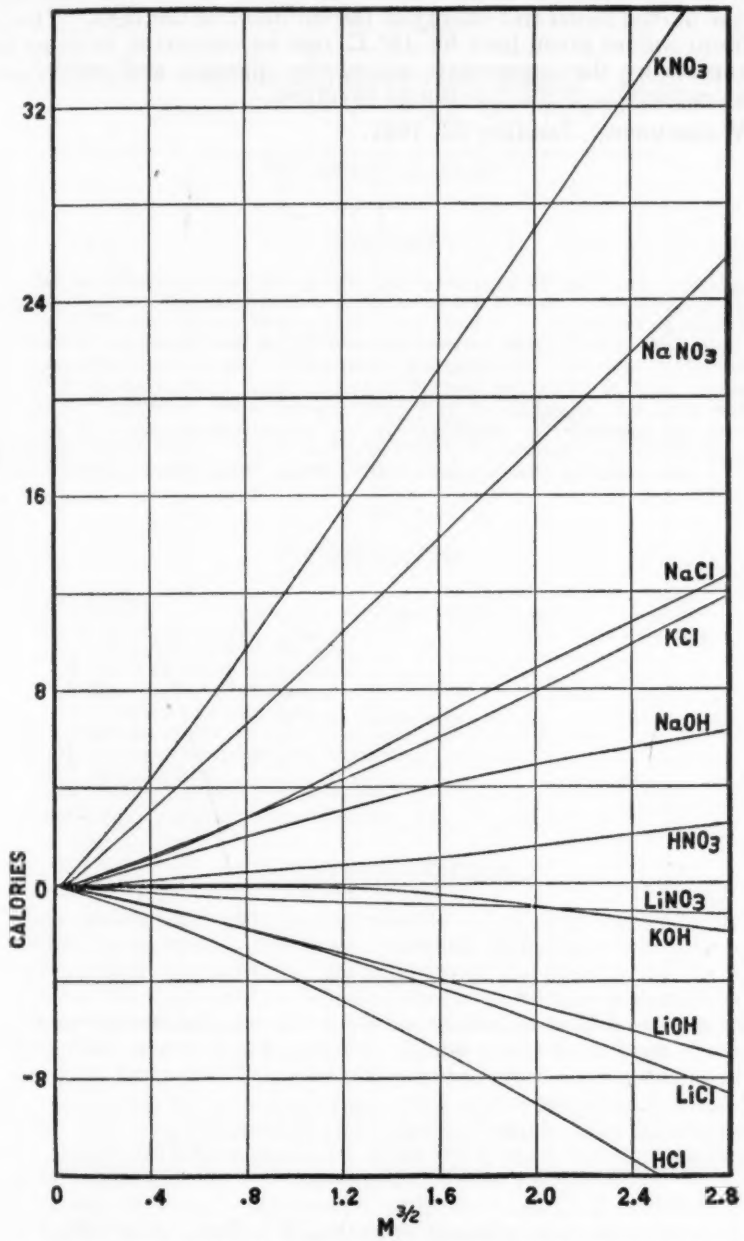

FIGURE 6.—*Plot of* $\overline{H}_1-\overline{H}_1°$, *the relative partial molal heat content of the* H_2O, *in aqueous solutions at 18° C.*

The ordinate scale gives $\overline{H}_1-\overline{H}_1°$ in calories per mole of H_2O while the abscissa scale gives the 3/2 power of the molality.

one concentration, or in the calculation of the temperature coefficient of the partial molal free energy of the solute or of the H_2O. The heat content values given here for 18° C. can be converted to other temperatures by the appropriate use of the apparent and partial molal heat capacities of the substances involved.

WASHINGTON, January 23, 1931.

ACCURATE MEASUREMENT OF SMALL ELECTRIC CHARGES BY A NULL METHOD [1]

By Lauriston S. Taylor

ABSTRACT

In the use of an electrostatic system for measuring charges and currents, it is necessary to know the electrostatic capacity of the system. For small capacities the error in this measurement may easily be 1 per cent. There is here described a new method for calibrating a null system in such a manner that the capacity of the leads does not enter and which, therefore, permits a reduction in the calibration error to one-tenth. When a system is once calibrated in the manner described, any unknown capacity whatever may be added to the leads without affecting the measurement of the desired quantities. Expressions are given for the sensitivity of the system in terms of readily measured quantities. Applications to the measurements of current, charge and capacity are discussed.

CONTENTS

	Page
I. Introduction	807
II. Theory of method	808
1. Measurement of charge	808
2. Calibration of condenser	809
3. Sensitivity of system	810
4. Method of operation	811
III. Experimental study	813
1. Description of system as used	813
2. Calibration	814
3. Factors affecting sensitivity	816
IV. Application to current measurements	817

I. INTRODUCTION

When making accurate measurements of small charges or currents by electrostatic means one of the greatest difficulties encountered is that of correctly determining the capacity of the system. This is due largely to the inability, without taking elaborate precautions, to determine corrections for the capacity of the leads from the capacity bridge to the electrometer system. These errors have been discussed in detail by Rosa and Dorsey [2] who showed that for capacities of the order of 500 cm they might be as much as 1.0 per cent. This difficulty has been encountered in endeavoring to make accurate measurements of the ionization produced in air by X rays, in connection with the international unit of X-ray quantity—the roentgen.

Investigators have used several different means of measuring the small currents involved. The factors favoring the use of an electrostatic measuring system have been discussed and it has been shown [3] [4] that the null electrostatic method, in that it does not introduce field

[1] See footnote, Radiology, **16**, p. 9; 1931.
[2] E. B. Rosa and N. E. Dorsey, B. S. Bull., **3**, p. 433.
[3] G. Failla, Am. J. Roent., **21**, p. 47; 1929.
[4] L. S. Taylor, B. S. Jour. Research, **2** (RP56), p. 771; 1929.

distortion in the ionization chamber, has an advantage over deflection methods. An additional difficulty in deflection electrostatic systems of small capacity arises from the motion of the leaf or fiber altering the capacity and thereby the calibration.

In null electrostatic measuring systems the potential of the electrometer and collecting system is maintained at some constant value—usually zero with respect to ground—by one of three methods. One method of accomplishing this is by communicating to the collector system an evaluated charge or current opposite in sign to that measured. Failla [5] and Jaeger [6] have devised sources of current for this purpose which serve as working standards. For absolute measurements this method is impractical because the working standard requires a calibration in kind. In the second method, the charge accumulated on the collector system is compensated by increasing its capacity to maintain the potential constant. Aside from the mechanical difficulties involved in a circuit of this kind, it has the disadvantage necessitating an elaborate calibration. In a third method, sometimes known as the Townsend method,[7] the communicated charge is entirely localized in a condenser of constant known capacity, but varied potential difference as determined by a voltmeter. In this, the greatest source of uncertainty is the voltmeter while in the second method it is the variable condenser. Since, in general, a variable condenser suitable for such purposes is a less dependable instrument than a voltmeter, the third method is from this standpoint distinctly preferable to the second.

II. THEORY OF METHOD

1. MEASUREMENT OF CHARGE

Given a circuit as represented in Figure 1, an unknown charge is communicated to the system containing an accurately known capacity C_1 and the unknown remainder C (which represents the capacity of the leads, ionization chamber, and electrometer, together with a calibrated variable capacity which will be described below). One plate of C is connected to earth, while the corresponding plate of C_1 is connected to a potentiometer circuit so as to bring it to any desired potential above or below that of the earth. As indicated by the deflection of the electroscope E this communicated charge raises the insulated side to a calibrated potential v relative to the earth as zero. Calibration of the electroscope is readily carried out by closing the key K and shifting the potentiometer contact to give any desired potential v which is read directly on the voltmeter. (The electroscope can at the same time be adjusted so that the deflection is at the most sensitive part of the scale.) With the electroscope at v, K is opened and an unknown charge Q communicated to the system through, say, the ionization chamber I. This requires the potentiometer contact to be shifted to V in order to bring back to, or maintain the potential of the system, at the calibrated value v, as indicated by the electroscope.

Since v is unchanged by this operation the charge on the part of the system of capacity C remains unchanged, hence the entire charge Q

[5] G. Failla, Radiology, **15**, p. 437; 1930.
[6] R. Jaeger, Strahlentherapie, **33**, p. 542; 1929.
[7] J. S. Townsend, Phil. Mag., **6**, p. 598; 1903.

is accumulated on C_1. Its magnitude is readily obtained from the measured values; that is

$$Q = C_1 (v - V) \tag{1}$$

2. CALIBRATION OF CONDENSER

The difficult part of this method lies in the accurate calibration of C_1. To present an adequate method of calibration is the prime object of the present communication.

C is here made up, in part, by an accurately calibrated variable condenser connected into the system as dotted in the figure. The total capacity in situ of this condenser is not accurately known because the leads, etc., introduce an uncertainty. However, its capacity differences are very accurately known.

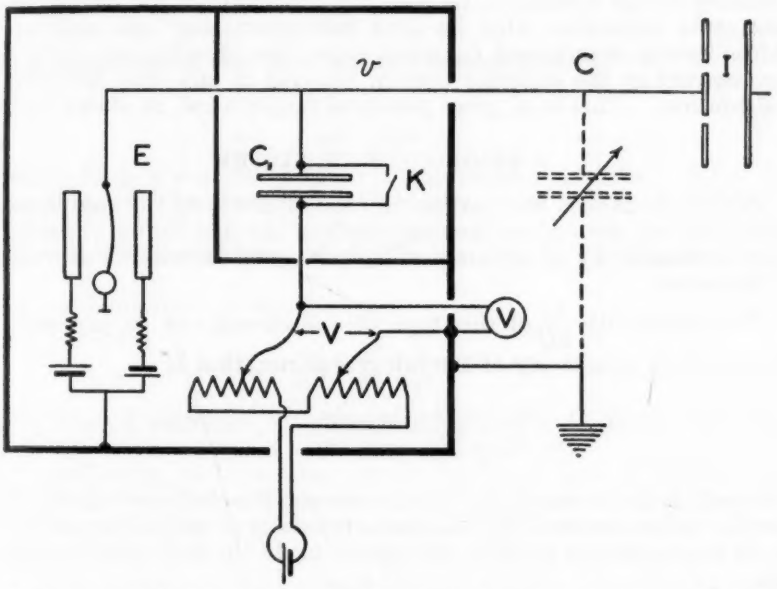

FIGURE 1.—*Null electrostatic system for measuring small charges or currents*

The part within the heavy lines is referred to as the "isolated system" and is so constructed that all capacities remain fixed.

Starting now with the system uncharged (that is, when V is zero, K is first closed then opened again), the potentiometer contact is shifted to a value V such that the electroscope indicates accurately any convenient potential v. Since no charge has been communicated to the system by this operation the induced charge $(-Q)$ on the unknown capacity C_1 must be exactly equal and opposite to that (Q) on the unknown remainder of capacity C.

Since

$$-Q = C_1 (v - V)$$

and

$$Q = Cv$$

it follows that

$$C_1(V - v) = Cv \tag{2}$$

The experiment is now repeated with C changed by an accurately known increment to a new value C', and V, consequently to a new value V'.
In this case

$$C_1 (V'-v) = C'v \tag{3}$$

Subtracting equation (3) from equation (2), C_1, the desired quantity, is obtained in terms of the accurately known magnitude $(C-C')$, namely

$$C_1 = (C-C') \frac{v}{V-V'} \tag{4}$$

from which expression all extraneous capacity, such as the ionization chamber, electroscope, and leads are wholly eliminated. Since the capacity of the system varies with the deflection of the electrometer, the same deflection must be used throughout any one calibration. After having determined C_1, other capacities of unknown value may be inserted in the collector system without in any way affecting its calibration. This is of great practical importance, as shown later.

3. SENSITIVITY OF SYSTEM

Although, as seen in equation (1), the quantity of the charge measured does not depend on the magnitude of the distributed capacity C, yet the sensitivity of the measuring system must obviously decrease as C increases.

The sensitivity $\frac{\Delta s}{\Delta Q}$ of this type of null circuit can be expressed in terms of the sensitivity of the integral parts; that is

$$\frac{\Delta s}{\Delta Q} = \frac{\Delta s}{\Delta v} \cdot \frac{\Delta v}{\Delta Q} \tag{5}$$

where Δs is the increment in scale divisions of the electrometer deflection for a given increment ΔQ of the imparted charge; and at the same time Δv is the increment in volts corresponding to the deflection increment Δs.

The electrometer sensitivity, $\frac{\Delta s}{\Delta v}$, is a magnitude which is obtainable separately, is in no way dependent upon the remainder of the system, and may be considered as known. As to the other factor, $\frac{\Delta v}{\Delta Q}$, the sensitivity of the compensating system, we have (from the general law $Q=CV$) $\Delta Q = C\Delta V$. Any error Δv in the adjustment of the potential v introduces an error ΔQ, which is given in this case by

$$\Delta Q = (C_1 + C)\Delta v \tag{6}$$

That is, the error in the determined magnitude Q is proportional to the total capacity of the system.

The uncertainty, Δv, may readily be obtained by comparing the electroscope independently with an adequate voltmeter; the value

of C_1 is supposed to be accurately known; leaving C, which includes all capacity of the circuit external to C_1 to be evaluated in terms of observed magnitudes.

From equation (2)

$$\frac{C_1+C}{C_1}=\frac{V}{v} \tag{7}$$

hence equation (6) may be rewritten

$$\Delta Q=C_1\frac{V}{v}\Delta v \tag{8}$$

which in turn, since from equation (7) $\frac{V}{v}$ is a constant (say k) of the system as given, may be written

$$\Delta Q=C_1k\Delta v$$

The sensitivity of the compensating system is then

$$\frac{\Delta v}{\Delta Q}=\frac{1}{C_1k} \tag{9}$$

in which $1/k$ is a *sensitivity factor* of the system as given. Since C_1 is constant and known from (4) we have now expressed the sensitivity $\frac{\Delta v}{\Delta Q}$ without C being explicitly involved. The working sensitivity of equation (5) then becomes

$$\frac{\Delta s}{\Delta Q}=\frac{\Delta s}{\Delta v}\cdot\frac{1}{C_1k} \tag{10}$$

which, since k increases with the stray capacity C, shows that the sensitivity decreases as the stray capacity increases.

By considering all capacities outside the heavy lines of Figure 1 to be removed from the system, we may determine a value of the sensitivity factor k_o which is characteristic of the isolated part. Thus

$$k_o=\frac{V_o}{v_o} \tag{11}$$

serves in practice as a ready control of the system.

4. METHOD OF OPERATION

Referring to equation (4), only two capacities whose difference is accurately known are required for the calibration of C_1. If, however, a variable capacity C having a number of accurately known capacity differences be used for the calibration, the following graphical analysis which gives equal weight to all observations shows readily how to obtain the magnitude of any of the capacities in the system, including C_1.

Remembering that $\frac{V}{v}=k$, we have from equation (7)

$$C=C_1k-C_1 \tag{12}$$

showing a linear relationship between C and k. Here it is seen that C_1 may be obtained either from the slope or from the C intercept; also that $k=1$ when $C=0$; and finally that for $k=k_o$, C takes on a derived value which will later be found serviceable in the analysis.

In plotting C against k, as in Figure 2, the capacity differences for various settings of C being accurately known while the absolute capacity is yet undetermined, we are unable to assign C its correct coordinate position at the start but merely a place, say a. Then, for a C scale, may be chosen coordinates representing *capacity differences* employed without regard to the location $C=0$.

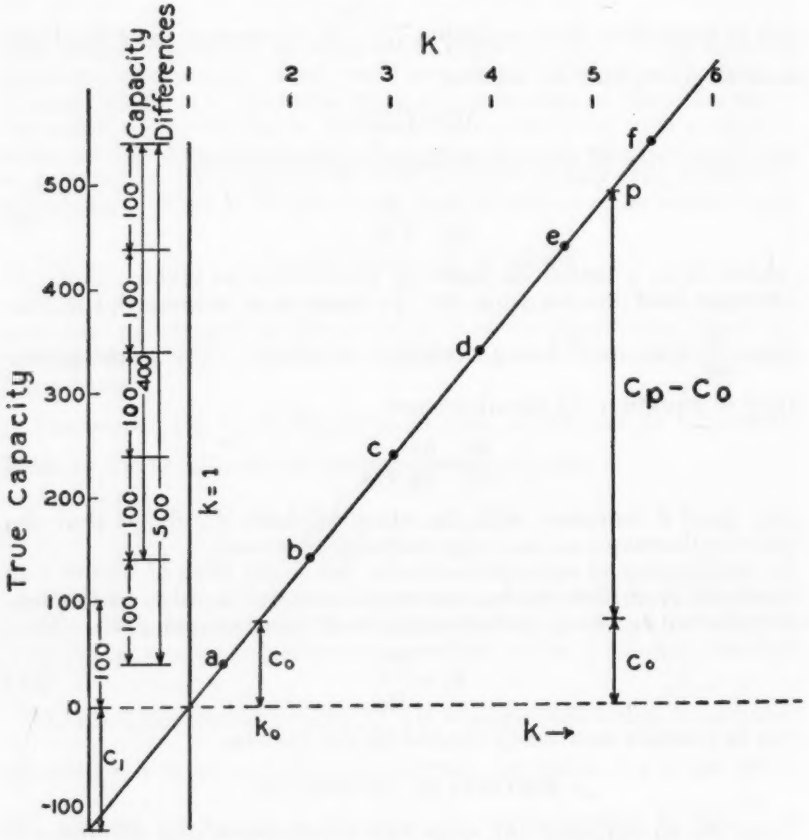

FIGURE 2.—*Schematic method of evaluating fixed capacity* C_1

The next point b corresponding to a known capacity change from a is then plotted with reference to a, etc. A straight line drawn through the plotted points must also pass through the point $k=1$, $C=0$ and thus locate the origin. Having determined the position $C=0$ it is now possible to read off the graph the value of the other capacities in the circuit. For example, the isolated system has a determined sensitivity factor k_o so that referring to (12) the corresponding ordinate C_o gives what will be called the stray capacity of the isolated system. Similarly, the difference between the ordinate

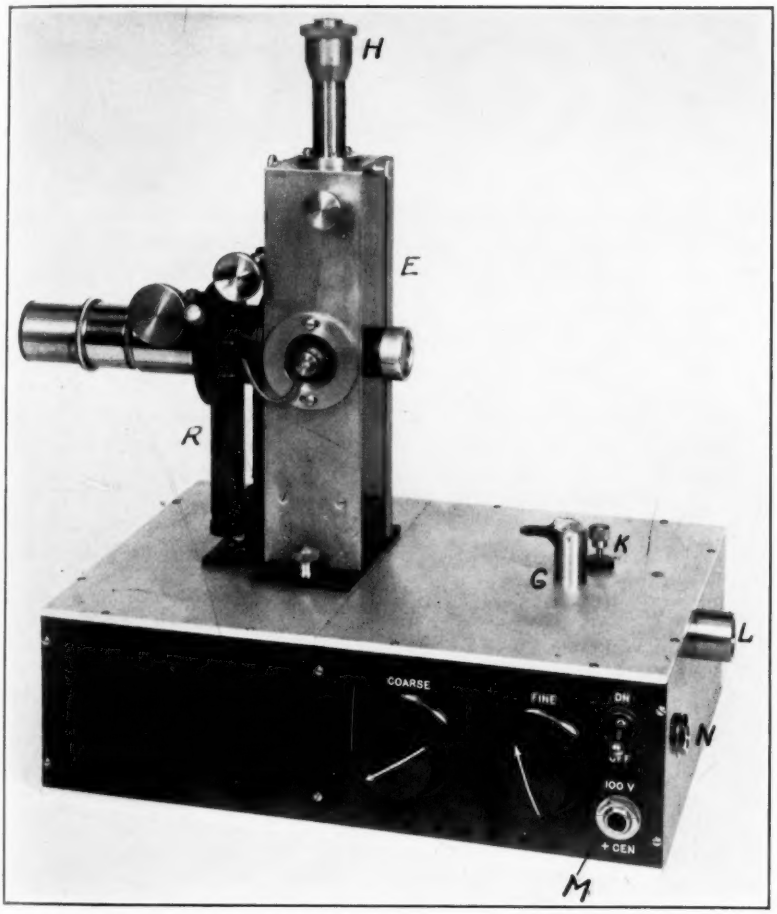

FIGURE 3.—*Photograph of "isolated system" as used in the study*

UNIV OF MICH

C_o and that C_p at any other point P on the curve gives the corresponding capacity of the external system.

Obviously such a system is applicable to the accurate measurement of any inserted capacity; for example, $(C_p - C_o)$. We will consider C as made up of the stray capacity C_o of the isolated system and the total external capacity C_{ext}. Then equation (12) becomes

$$C_1 k = C_1 + C_o + C_{ext} \tag{13}$$

In this C_1 is determined by equation (4), C_{ext} is removed, and C_o is determined from the relation

$$C_1 k_o = C_1 + C_o \tag{14}$$

Combining these

$$C_{ext} = C_1 (k - k_o) \tag{15}$$

For any given measuring system, C_1 and C_o and k_o remain fixed so that the measurement of any capacity, such as C_{ext}, requires but a determination of k with the external capacity inserted.

III. EXPERIMENTAL STUDY

1. DESCRIPTION OF SYSTEM AS USED

We will now examine a specific null circuit represented in general by the diagram in Figure 1 and for the isolated part in Figure 3. In this latter, E is a string electrometer of the general Edelmann type in which the deflection of a very fine platinum (Wollaston) wire, under an adjustable tension between the charged knife-edges, is observed by a suitable microscope. The potential on these knife-edges is supplied, through very high protective resistances R, by two 22.5 volt batteries. For any given potential on the knife-edges, the voltage sensitivity $\frac{\Delta s}{\Delta v}$ of the electrometer is adjusted by varying the tension on the fiber by the micrometer head, H. The sensitivity of this particular instrument can be readily changed from 100 divisions per volt to 0.01 division per volt.

The resistances of the compensating potentiometer are operated by the knobs "coarse" and "fine" on the front of the aluminum box container. Potentiometer, charging batteries, compensating condenser C_1 and the necessary leads are all contained in this box, the electrometer circuit being led out through an amber bushing L. All parts are carefully shielded electrostatically. G is a grounding key and K a switch to short circuit C_1 (for the purpose of calibrating the electrometer). Leads to the potentiometer battery and the voltmeter are in the form of jack and plug at M and N, respectively.

TABLE 1

VARIABLE CONDENSER ALONE

Nominal capacity C	k	Average deviation from mean	Deviation from mean
1	2	3	4
			Per cent
[1] 0.0	1.057	0.0015	0.14
43.8	1.120	.0016	.14
97.6	1.185	.0018	.15
175.9	1.279	.0008	.06
254.5	1.378	.0021	.15
313.5	1.470	.0014	.09
412.0	1.569	.0018	.12
490.6	1.666	.0009	.05
		Average...	.11
VARIABLE CONDENSER + RUBBER CABLE			
[2] 215.2	1.968	0.008	0.36
313.5	2.075	.005	.24
412.0	2.232	.006	.32
		Average...	.31
VARIABLE CONDENSER, HIGH VOLTAGE			
117.1	1.207	0.005	0.41
195.6	1.303	.003	.23
274.1	1.397	.002	.14
352.8	1.495	.005	.33
431.7	1.590	.004	.25
		Average...	.27

[1] Variable condenser actually removed and L covered.
[2] Capacity of variable condenser only. Full value of C is this plus the unknown capacity of the cable.

2. CALIBRATION

The capacity used for the calibration of C_1 was a precision variable condenser of well-known make; the voltmeter was of the laboratory standard type; the capacity differences and voltmeter were calibrated with an accuracy of one-tenth per cent by the electrical division of this bureau.

The accuracy of the results obtainable under working conditions is best brought out graphically. The factor k (equation (9)) may be obtained from the slope of the curve V plotted against v—a series of which curves are given in Figure 4 for several different settings of the variable condenser C.

The first part of Table 1 gives results of a number of determinations of k for different nominal values of the external capacity C, in which the variable condenser was connected to the terminal L by a well insulated and shielded conductor of unknown capacity. The average deviation of five determinations of each k is seen to be within the one-tenth per cent accuracy of the measuring instruments.

Plotting (circles, fig. 5, Curve I) these values of k as abscissae and the corresponding variable condenser values as ordinates, it is found

that all of the points lie close on a straight line. According to (12) the slope $\frac{\Delta C}{\Delta k}$, which is obtainable in terms of the accurate differences in capacity, gives C_1 as 809.2 ± 0.4 $\mu\mu f$.

Having removed the condenser C and covered the amber bushing L with a cap, the sensitivity factor k_o for the electrometer-condenser system alone was found to be 1.057 ± 0.0005.

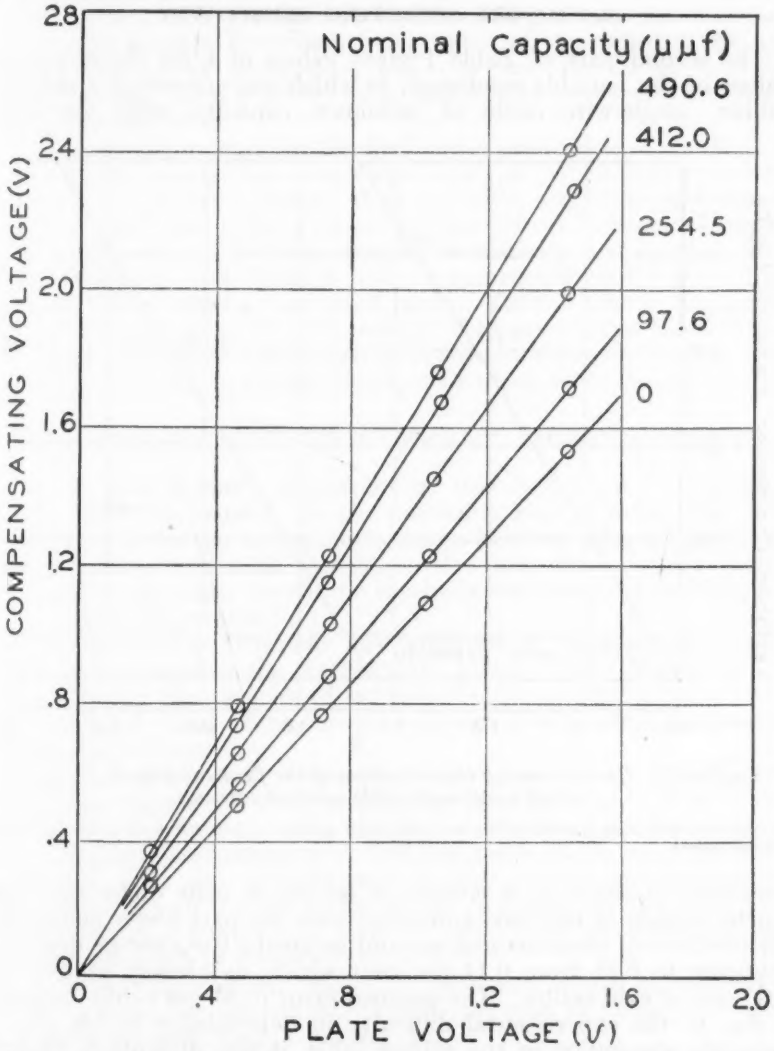

FIGURE 4.—*Curves showing the evaluation of the sensitivity factor k over a range of potentials*

This curve might be given its coordinate position on a C–k plot by extending it to the point $k=1$; hence, also, the ordinate value $C=0$—located as seen at -48 on the variable condenser scale. The value of the internal lead capacity C_o may be read from the curve at the point

$k=1.057$, thus giving $C_o=46\ \mu\mu f$. Likewise the value of C_p, at the point P for example, is found to be $460\ \mu\mu f$.

These capacity values may be calculated more accurately from equations (14) and (15). Using equation 14 for $k_o=1.057$ we find $C_1+C_o=855.3\ \mu\mu f$ where, since $C_1=809.2\ \mu\mu f$, we have $C_o=46.1\ \mu\mu f$. The capacity at C_p, for which $k=1.569$, is obtained by substituting the values of k and k_o in equation (15) giving $C_p=459.8\ \mu\mu f$.

3. FACTORS AFFECTING SENSITIVITY

The second part of Table 1 gives values of k for three nominal values of the variable condenser, to which was connected a shielded, rubber, single-wire cable of unknown capacity, with the shield

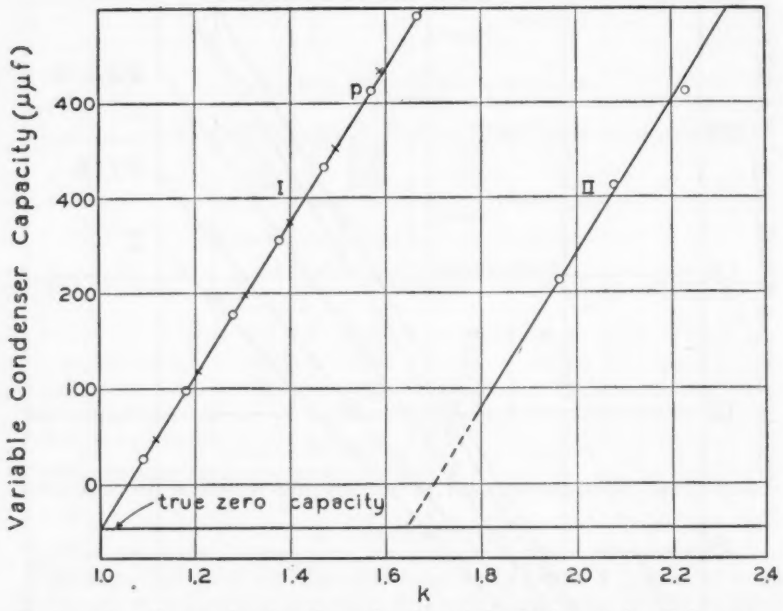

FIGURE 5.—*Curves showing the evaluation of the fixed capacity C_1 by means of an accurate variable external capacity*

Curve I (circles) using low voltage, (crosses) using high voltage. Curve II using a rubber cable in the external system.

grounded to serve as a condenser having a poor dielectric. The fourth column of this part compared with the part above shows that the precision of measurement was not so good—the average deviation changing to 0.31 from 0.11 per cent which, as already stated, was the error of calibration. The greatest error (0.31 per cent), however, is due to the experimental difficulty in determining k; for, due to dielectric absorption in the rubber cable, it was difficult to fix with accuracy upon the V necessary to apply to C_1 to induce a definite potential v 0 on the electrometer.[8]

Reference to the corresponding Curve II in Figure 5 shows the same effect in that the plotted points determined with the cable in the sys-

[8] This absorption is not operative when using, as in current measuring, the system at $v=0$.

tem do not fall closely on the straight line drawn parallel to Curve I. The superiority of conditions when all questionable external capacity is removed while calibrating C_1[9] is obvious—a conclusion supported also by the fact that, when the cable was replaced by a highly insulated condenser of about the same capacity, the points fell well along a straight line, the slope of which represented satisfactorily the capacity as checked by other means. Furthermore, the average deviation from the mean for the values of k made with the well insulated unknown was 0.12 per cent as against 0.31 per cent for the cable. This small average deviation, being again of the order of the error of the instrument calibration, indicates that the larger deviation (0.31 per cent) for the rubber cable was due to absorption and not to the magnitude of C.

In the measurements for the first and second parts of Table 1, the electrometer sensitivities were, respectively, about 13 and 17 divisions per volt; v was never greater than 1.5 volts, and, consequently, the external condenser offered no difficulties due to leakage. However, with v increased to 80 volts and the sensitivity decreased to about 0.3 division per volt, leakage became appreciable and k was subject to error as indicated in the third part of Table 1 where the average deviation was 0.27 per cent as against 0.11 per cent in the first part. The values obtained are plotted as crosses on Curve I (fig. 5). Such conditions should, of course, be avoided when determining C_1.

IV. APPLICATION TO CURRENT MEASUREMENTS

In the measurement of current by this method, a time measurement, of course, enters. In the particular case of measuring X-ray intensities, a shutter in the X-ray beam between tube and ionization chamber is so controlled that it remains open for a definite interval of time during which the charge is wholly compensated, holding $v=0$, by varying the potential on C.[10] [11]

In practice it is extremely advantageous to use a shielded rubber cable for connecting the electrometer to the source of current. As shown above, the presence of unknown lead capacities does not affect the measured value of the charge, although it does affect the accuracy of the measurement.

The effect of poor insulation may be eliminated by choosing such conditions that $v=0$ with respect to the shielding. This confines leakage to the condenser C_1, and it is a relatively simple matter to construct this fixed capacity so that leakage between its plates will be negligible. In the isolated part of the system here described, a 20-volt charge on the condenser leaked to ground at the rate of only 3 per cent in 8 hours; but, with a rubber cable attached, the same leakage occurred in about 10 minutes.

To obtain the desired sensitivity with any length of cable added to the system, the electrometer sensitivity may be changed in accord with k as brought out in equation (9).

To test the effect of a poor dielectric in the external condenser, two sets of intensity measurements were made of the same X-ray

[9] It is of interest to note that using equation (15), the capacity of the cable was found to be 522 $\mu\mu$f as compared with 526 $\mu\mu$f obtained with a capacity bridge calibrated with an accuracy of 1 per cent.
[10] D. L. Webster and A. E. Henning, Phys. Rev., **21**, p. 301; 1923.
[11] L. S. Taylor, B. S. Jour. Research, **2** (RP56), p. 771; 1929.

beam, using a standard X-ray ionization chamber.[12] In the first set, the electrometer and ionization chamber were connected by an amber insulated conductor having a capacity of about 206 $\mu\mu$f and negligible leakage. In the second set, the connection was by the shielded rubber cable having a capacity of about 525 $\mu\mu$f. For this the electrometer sensitivity was adjusted to accord with the change in k, approximately double that of the first case. The respective average deviations from the mean of 10 observations for each of the two cases were found to be 0.33 and 0.32 per cent, respectively, the averages of the two runs differing by 0.13 per cent. These deviations from the mean were no more than should be expected from the X-ray intensity variations.

In a null circuit previously described by the author [13] the expression for the magnitude of the ionization current involved the total capacity C_T of the system instead of simply C_1 as above. The fact that the total capacity C_T can not be measured accurately (with a bridge, as previously done) renders the other method less satisfactory than the present one. Intensity measurements of the same X-ray beam by the two outfits showed a difference of nearly 1 per cent which is principally attributed to the error in the measurement of C_T. Compared with the average deviation above of one-third this magnitude for both the highly insulated and the cable connected systems, the superiority of the method here presented is evident.

WASHINGTON, December 30, 1930.

---

[12] L. S. Taylor and G. Singer, B. S. Jour. Research, **5** (RP211), p. 507; 1930.
[13] L. S. Taylor, B. S. Jour. Research, **2** (RP56), p. 771; 1929.

LIGHT SENSITIVITY OF ROSIN PAPER-SIZING MATERIALS[1]

By Arthur E. Kimberly[2] and J. F. G. Hicks[2]

ABSTRACT

The effect of light upon rosin, and compounds of rosin formed during the rosin sizing of paper has been studied, both in air and in an atmosphere of nitrogen, a relatively inert gas. The source of light used was an inclosed carbon arc. Commercial rosin and bleached rosin as well as resinates of sodium, aluminum, and iron, and rosin size contaminated with ferrous and ferric iron were exposed to the rays of the arc in quartz tubes. The fact that changes occur in an inert atmosphere, such as nitrogen, indicates that the presence of oxygen is not necessary to the chemical alteration of rosin when exposed to the action of light.

The more important conclusions of this investigation follow: Rosin, both bleached and unbleached, is sensitive to light, darkening under the action of the rays. Ferrous resinate, and rosin size contaminated with ferrous iron are also light sensitive probably because of the ease with which the ferrous iron is oxidized by light. Ferric resinate, aluminum resinate, and sodium resinate have no effect upon rosin size in so far as light sensitivity is concerned. The yellowing of paper with age may be explained in terms of the light sensitivity of rosin and of ferrous iron.

CONTENTS

	Page
I. Introduction	819
II. Experiments performed	822
1. Effect of light upon rosin	822
2. The effect of light upon resinates of sodium, aluminum, ferrous iron, and ferric iron	823
3. The effect of light upon rosin size contaminated with ferrous and ferric iron, singly and together	825
III. Discussion of experimental results	826
1. Effect of light upon rosin	826
2. Effect of light upon resinates of sodium, aluminum, and iron	827
3. The effect of light upon rosin size contaminated with ferrous and ferric iron	827
IV. Summary	827

I. INTRODUCTION

Light, according to the literature, is an important factor in the deterioration of high-grade papers, as is most frequently noticed in libraries or similar depositories of records. The term "high grade" is used in this instance to distinguish papers containing no ground wood fibers from those containing ground wood fibers. The change in color occasioned by the action of light upon papers containing ground wood has been attributed[3] to the oxidation of the lignins contained in such fibers. In order to ascertain the effect of light upon the ma-

[1] This series of investigations is being made at the request of the American Library Association, and is financed by a grant from the Carnegie Institution. The experimental work is being performed at the National Bureau of Standards.

[2] Research associate, National Research Council.

[3] Klason, P.: Svensk Pappierstidning. See translation by C. E. Bandelin, Paper Trade J., 57, pp. 17, 46; 1913. Compare Cross, C. F., Roy. Soc. Arts J., 45, p. 684; 1897.

terials comprising the rosin sizing used in the manufacture of papers containing no ground wood, as distinguished from the effect of light upon the paper fibers themselves,[4] this phase of an investigation of the impermanency of records was inaugurated.

Klemm [5] indicated that the yellow discoloration in paper was due to what he called "rosin-iron soaps," and that the intensity of the discoloration was generally proportional to the quantity of iron present. Schwalbe [6] found that rosin itself was very sensitive to both light and air, and that a rosin-sized paper, upon exposure to direct sunlight, underwent a rapid loss of sizing. Schoeller [7] indicated that all papers turned yellow to a greater or lesser extent, with passage of time, more especially those which had been sized with rosin. He further indicated that the darkening of rosin itself was due to polymerization or auto-oxidation, and that the discoloring of papers would be prevented by "bleaching" the rosins used in size making with an oxidizing agent.[8] Zschokke,[9] working independently of Schoeller, showed results which partially agreed with those of Schoeller, but asserted that the color changes in paper are due to the effects of heat and light. He further disagrees with Klemm [10] as to the direct relation between degree of discoloration and iron content of paper. At about the same time, Klason [11] showed that rosin rapidly takes up atmospheric oxygen in the presence of sunlight, and only very slowly, if at all, in the dark. Haas [12] recommended the use of "alum free from iron," and of "bleached rosin" to prevent the deterioration of paper. Hitchins [13] showed that all rosin-sized papers will yellow with passage of time, that mere traces of iron will influence the depth of color produced, and that the iron content of a rosin-sized paper is therefore a very important factor. In addition to this somewhat contradictory collection of data, one finds in the journals relating to the paper industry several articles which appear to be résumés, translations or rewritings of the work just cited.[14 15 16 17] It appears that but little attempt has been made to connect the various color changes of rosins just described with the actual discoloring of paper,[18] or to correlate the discoloration of sizes and of paper.[19 20] One does not find any attempt to distinguish between the behavior of ferrous compounds, ferric compounds, or mixtures of the two, in connection with the term "iron" as related to the discolorations discussed.

Because of the indefinite state of the knowledge concerning the cause of the discoloration of rosins and rosin sizes, and the relation

---

[4] Trans. Inst. Rubber Ind., **5**, p. 31; 1929; also Rubber Chem. and Tech., **3**, pp. 1, 57; 1930. See also References 1, 3, and 4.
[5] Klemm Papier, Ztg. Jahrg. **27**, 1902, pp, 961–963.
[6] Schwalbe Wochbl, Papierfabr., **38**, pp. 1303–1306; 1907.
[7] Schoeller Wochbl, Papierfabr., **43**, p. 3222 et seq.; 1912 (serial).
[8] Schoeller's German Patent, Bleaching of Rosin, No. 257158; 1912.
[9] Zschokke Wochbl, Papierfabr., **44**, p. 2976 et seq.; 1913 (serial).
[10] See footnote 5.
[11] See translation by C. E. Bandelin, Paper Trade J., **57**, pp. 17, 46; 1913. Compare also Briggs, Chemical World **2**, p. 119; 1913.
[12] Haas, B., Papierfabrikant, **12**, p. 891 et seq.; 1914 (serial).
[13] Hitchins, A. L., "Paper" pp. 11–15, July 24, 1918.
[14] Pulp and Paper Magazine of Canada, **11**, p. 686; 1913.
[15] Paper Trade J., **58**, pp. 18, 38; April 30, 1914.
[16] Papermakers' Monthly J., **56**, p. 40; 1918; also "Paper," **22**, pp. 1, 11; 1918.
[17] "Paper" **30**, pp. 7, 70–72; 1922; also Paper Trade J., **74**, pp. 15, 313–315; 1922.
[18] "Paper," **30**, pp. 7, 70–72; 1922; also, Paper Trade J., **74**, pp. 15, 313–315; 1922.
[19] Paper Trade J., **76**, pp. 11, 50–52; 1922.
[20] Geseboff, L. P., "La Papeterie"; March 23, 1923; also "Paper," **31**, pp. 26, 143; 1923.

between these discolorations and the discoloration of papers, it was thought advisable to study the behavior of rosin, bleached [21] and unbleached, when exposed to the action of light, the samples of rosins to be placed in separate atmospheres, both chemically inert and chemically active with respect to the rosins placed in them. Since the rosins, sizes, chemicals, and papers were and always have been made and stored in air, these artificial atmospheres must represent conditions based upon that fact. The ordinary components of the atmosphere were, therefore, used singly and together.

For the same reason, it was thought advisable to study the behavior of rosin and rosin sizes, when intimately mixed with small quantities of different types of "iron compounds" [22] and placed under the influence of light. The usual commercial process of sizing paper with rosin is, briefly, as follows: The rosin is heated with a solution of "soda ash" (commercial sodium carbonate) to such a degree as to hold the remaining free rosin in colloidal suspension. The size and the pulp are well mixed in the beating machine, and a calculated amount of so-called "paper makers' alum" (aluminum sulphate) is added. This precipitates the rosin upon the paper fibers, which are then run through the machine and formed into sheets. There are many modifications of this general procedure, but, for the most part, they are minor deviations. By reason of the method of manufacture, rosin sizes, as used in a paper mill, contain the resinates of sodium, aluminum, ferrous and ferric iron, in addition to colloidal rosin. The precipitating agent for these rosin sizes, aluminum sulphate, nearly always contains traces of both ferrous and ferric iron, detectable by the ordinary reagents; hence, the presence, in such a size, of ferrous and ferric resinates, is readily accounted for. These facts made it necessary to add known small quantities of "iron compounds" to "iron free" sizes [23] and study the behavior of these under the influence of light. The addition of traces of solutions of iron salts to the liquid "size milk" makes possible a very intimate mixture, similar to that existing on the surface of a commercial rosin sized paper.

The effect of light upon rosin, alone and in combination with other materials, was studied. A study of bleached rosin was included in the program, since it has been claimed [24] that bleached rosin does not darken upon exposure to light. The source of light in these experiments was a carbon-arc lamp, operated with a direct current of 13 amperes at 220 volts, at a distance of 10 cm from the samples, and inclosed in a globe of special glass. These special glass globes are described by their manufacturers as deteriorating at the end of 100 light-hours' service; for this reason they were replaced at the end of each total 75 light-hours' service, as an additional precaution.

[21] Although the use of "bleached" rosin has been strongly advocated by some of the German investigators, it is not known that their recommendations were ever put into practice. So far as is known, no "bleached" rosin has been used in the United States.

[22] To avoid needless repetition "iron compounds" as used in this discussion will be taken to mean "ferrous and ferric compounds singly and together." Details of making such "iron compounds" will be given under the head of "Experiments Performed."

[23] The term "iron free" here and elsewhere in this publication means "tested for both Fe^{++} and Fe^{+++} with negative results." Further details under the head of "Experiments Performed."

[24] Schoeller, V., see footnotes 7 and 8, p. 820; Haas, B., Papierfabrikant, 12, pp. 891 and 919; 1914.

The spectral distribution of radiation from such a glass-inclosed arc as this, as compared with sunlight, is as follows:[25]

Spectral range in $\mu\mu$	Percentage of total radiation	
	Arc	Sun
170 to 320	0.0	2.0
320 to 360	2.0	2.8
360 to 480	18.5	12.6
480 to 600	9.3	21.9
1,400 to 4,200	22.1	21.4
4,200 to 12,000	31.6	.4

II. EXPERIMENTS PERFORMED

1. EFFECT OF LIGHT UPON ROSIN

Four varieties of rosin were used in this phase of the work:

(*a*) Unbleached rosin, grade F, such as is commonly used for sizing paper.

(*b*) Unbleached rosin, grade C, lighter in color than grade F. Used in papers when a lighter color is particularly important.

(*c*) Rosin, grade F, bleached as follows: The rosin was melted on the steam bath, and chlorine gas passed through the melt until the color of the rosin no longer lightened on continued passage of chlorine. The resulting mass was then converted into sodium resinate by the addition of an excess of sodium-hydroxide solution, and the mixture heated on the steam bath until a clear liquid resulted. This sodium-resinate solution was then acidified by adding an excess of strong hydrochloric acid, which precipitated free rosin therefrom. This free rosin was filtered off, washed twice with distilled water, and dried in contact with air. This is Schoeller's method.

(*d*) Rosin, grade F, bleached as follows: The rosin was mixed with a slight excess of sodium carbonate solution, and the mixture heated on the steam bath until a clear liquid was obtained. Chlorine gas was then passed through this liquid until no further lightening of color was observed upon continued passage of the gas. Free rosin was precipitated from this liquid by adding an excess of strong hydrochloric acid, and the free rosin was then filtered off, washed twice with distilled water, and dried in contact with air.

Specimens of each of these rosins were then placed in quartz tubes, one specimen of rosin in each quartz tube, and the tubes connected with gas trains in such a manner that each separate sample of each variety of rosin was surrounded by one of the following gases:[26]

Purified nitrogen, from which the admixed oxygen and carbon dioxide had been removed by passing the gas through a train consisting of gas wash bottles containing a mixed solution of potassium pyrogallate and potassium hydroxide.

Purified oxygen, from which the admixed carbon dioxide had been removed by pasing the gas through a train of gas wash bottles containing potassium hydroxide solution.

Purified carbon dioxide, from which the admixed oxygen had been removed by passing the gas through a train of wash bottles containing cuprous chloride (CuCl) dissolved in hydrochloric acid, to which solution metallic copper had been added. The acid fumes were caught in a saturated solution of sodium bicarbonate, thereby preventing removal of carbon dioxide by the train itself.

[25] Measurements by W. W. Coblentz, Bureau of Standards.

[26] The composition of these artificial atmospheres is based on the composition of the air, as has been previously mentioned, with reasons for choice, in the Introduction.

Purified air, which had been washed free from dust by means of a train of bottles containing water, after which the excess moisture was removed by means of a train of calcium chloride towers.

Air with carbon dioxide removed. This was brought about by passing the air through a train of wash bottles containing a solution of potassium hydroxide.

Before coming into contact with the rosin samples, each gas was dried to such a degree that it contained 0.14 to 0.36 mg of residual water-vapor per liter at 25° C.

Duplicate samples of these rosins were sealed in glass tubes, the air in which had been displaced by each of the purified gases just described. These sealed tubes were preserved in total darkness. In this way there was always on hand a set of reference samples representing the color of the rosin in the dark at the start of the experiment, one sample for every gas used.

The test samples of rosin, bleached and unbleached, each in its separate quartz tube and each surrounded by its own purified and uniformly dried gas—nitrogen, oxygen, carbon dioxide, air, and air less carbon dioxide, as the case might be—were then exposed to the action of the adopted source of light (*q. v.*) for a total period of 288 hours. At the end of that elapsed time the test samples were removed from the source of light and compared with the reference samples. Results are collected and shown in Table 1.

TABLE 1.—*Effect of light upon rosin* [1] [2]

Time of exposure (in hours)	Sample number and description																			
	(a) Unbleached rosin					(b) Unbleached rosin					(c) Bleached rosin					(d) Bleached rosin				
	Atmosphere in which rosin was exposed																			
	N_2	O_2	CO_2	Air	Air $-CO_2$	N_2	O_2	CO_2	Air	Air $-CO_2$	N_2	O_2	CO_2	Air	Air $-CO_2$	N_2	O_2	CO_2	Air	Air $-CO_2$
24	1	2	2	2	2	1	2	2	2	2	2	2	2	1	2	2	3	3	1	4
48	1	1	1	1	1	1	1	2	1	2	2	2	2	1	2	2	2	2	1	2
72	1	1	2	2	2	1	1	2	1	2	2	2	2	1	2	2	3	1	1	3
96	1	1	1	1	2	1	1	2	1	2	2	2	2	1	2	1	2	1	1	2
120	1	1	2	1	1	2	1	3	1	2	3	2	3	1	3	1	2	1	1	2
144	1	1	2	1	1	2	1	3	1	2	3	2	3	1	3	1	2	1	1	2
168	1	1	2	1	1	2	1	3	1	2	3	2	3	1	3	1	2	1	1	2
192	2	1	3	1	1	2	1	3	1	2	2	3	3	1	3	1	2	2	2	3
216	2	1	3	1	1	2	1	3	1	2	2	3	3	1	3	1	2	2	2	3
240	2	1	3	1	1	2	1	3	1	2	2	3	3	1	3	1	3	2	1	2
264	2	1	3	1	1	2	1	2	1	2	2	3	3	1	3	1	3	2	1	3
288	2	1	3	1	2	3	1	2	1	2	1	3	3	1	3	1	3	2	1	2

[1] Color is expressed by a comparative numerical scale: 1, darkest, to 5, lightest. Before exposure to light, the original sample was lighter in color than "5."

[2] At the end of each 24-hour period each set of tubes, (*a*), (*b*), (*c*), and (*d*), were compared with the corresponding original sample and with each other. The numbers in this table represent the results of these comparisons, and are not comparable to preceding or succeeding observations.

2. THE EFFECT OF LIGHT UPON RESINATES OF SODIUM, ALUMINUM, AND IRON

The compounds of rosin which are usually met with in paper-making processes are the "resinates" of sodium, aluminum, ferrous and ferric iron. In order to protect the compounds used in these experiments from the action of light, the whole process of preparing these resinates was conducted in a photographic dark room.

These resinates of aluminum and of ferrous and ferric iron were made by transposing sodium resinate [27] with the sulphates of the metals just mentioned. Aqueous solutions, using triple-distilled water, were used in these reactions. The method of operation was as follows: The sodium resinate and one of the three solutions of metallic sulphates were each placed in separate 250 ml Erlenmeyer flasks, previously swept free of air by a stream of purified nitrogen. The two flasks were connected with each other in the same manner as a train of gas wash bottles, so that the liquid contents of each could be agitated by bubbling, transferred by blowing the contents of one flask into the other, and mixed by bubbling. The gas used for these purposes was the purified nitrogen just described. After blowing this stream of purified nitrogen through the system for five minutes, the metallic sulphate solution was blown over into the sodium resinate solution, and mixed with it by bubbling. The precipitated resinates were washed in this manner with distilled water, filtered by suction, in an atmosphere of purified nitrogen gas, and dried in a desiccator filled with purified nitrogen. All these operations were conducted in a photographic dark room. Samples of these resinates were sealed in pyrex glass tubes, which contained an atmosphere of purified nitrogen, and stored in the dark for use. Two tubes of each resinate were prepared. One set of these tubes was placed in the light of the carbon arc lamp, while the other set was preserved in total darkness as a reference sample. The colors of these compounds before exposure were:

Aluminum resinate: White to pale yellow.
Sodium resinate: White to pale yellow.
Ferrous resinate: Light tan.
Ferric resinate: Yellow-brown to red brown.

Those resinates which were exposed to the adopted source of light for experimental purposes, were exposed for a total period of 25 hours. The results obtained are shown in Table 2.

TABLE 2.—*Effect of light on resinates of sodium, aluminum, and iron*

Substance exposed	Time of exposure (in hours)						
	1	2	7	9	14	19	25
Sodium resinate from unbleached rosin.	(a)	(a)	(a)	(a)	(a)	(a)	(a)
Sodium resinate from bleached rosin.	(a)	(a)	(a)	(a)	(a)	(a)	(a)
Aluminum resinate from unbleached rosin.	(a)	(a)	(a)	(a)	(a)	(a)	(a)
Aluminum resinate from bleached rosin.	(a)	(a)	(a)	(a)	(a)	(a)	(a)
Ferrous resinate from unbleached rosin.	No change	Slight darkening.	Increased darkening.	Distinctly darker.	(b)	(b)	(b)
Ferrous resinate from bleached rosin.	do	Noticeable darkening.	Very dark color.		(b)	(b)	(b)
Ferric resinate from unbleached rosin.	(a)	(a)	(a)	(a)	(a)	(a)	(a)
Ferric resinate from bleached rosin.	(a)	(a)	(a)	(a)	(a)	(a)	(a)

[a] No apparent color changes [b] No further change.

[27] Prepared as per section 1 (*d*)

With the exception of the rosins, the chemicals used—sodium hydroxide, sodium carbonate, and the sulphates of aluminum, ferric and ferrous iron—were of the "C. P." variety. Since iron salts were to be added to various compounds which contained no iron during the course of the experimental work, the first three of these chemicals, as well as the rosins and solvent acids, were tested for and found free from iron.[28]

The water used in making the solutions used in this series of experiments was triple distilled water, which had been boiled for six hours, during which time a stream of purified nitrogen was bubbled through it, for the purpose of sweeping out dissolved oxygen, since ferrous iron was to be put into solution. This water was kept in stoppered flasks until ready for use.

3. THE EFFECT OF LIGHT UPON ROSIN SIZE CONTAMINATED WITH FERROUS AND FERRIC IRON[29]

Since Schoeller[30] and others[31] have claimed that the rosin size used in making papers is responsible for the discoloration of papers, and even their subsequent deterioration, and since it has been claimed[32] that small quantities of iron hastened the discoloration and deterioration of both size and paper, it was thought advisable to study the behavior of rosin sizes contaminated with known small quantities of ferrous and ferric iron. The "size milk" used was obtained from the Bureau of Standards paper mill, and contained 30 per cent of "free" (colloidal) rosin. Samples of this size milk were contaminated with solutions of ferrous and ferric iron in concentrations ranging from 1 part of iron in 100,000 to a concentration of 1 part of iron in 1,000,000,000. These contaminated samples of "size milk" were prepared in duplicate, one set being sealed in quartz tubes in air for exposure to the action of light, and the other set sealed in hard glass tubes in air and preserved in total darkness, as reference samples. The results of a run of 192 light hours are shown in Table 3.

---

[28] For Fe^{++}: Potassium ferricyanide, in presence of HCl. For Fe^{+++}: Potassium ferrocyanide, in presence of HCl. (See Koningh, Z. Angew. Chem., 1898) p. 463.
For Fe^{+++}: Potassium thiocyanate. (See Wagner, Zeit. Anal. Chem., **20**, p. 350; 1881; also Natanson, Ann **130**, p. 246; 1864.
By these means a detection of 1 part of iron per 500,000 to 1,600,000 parts of water is claimed by the above authors. The chemicals were tested in 10g samples, as above, with negative results; the rosins, after decomposition of 40g samples by hot concentrated sulphuric acid, also yielded negative results.

[29] In order to avoid ambiguity of meaning and awkwardness of expression, "ferrous and ferric iron" as used in this discussion means "taken singly and together," and "together" means "equimolar concentrations of each."

[30] See footnote 7, p. 820.

[31] See footnote 3, p. 819, and 13, p. 820.

[32] See footnote 3, p. 819, and 5 and 13, p. 820.

TABLE 3.—*Effect of light on rosin size contaminated with ferrous and ferric iron* [1]

Contaminating agent	Concentration of contaminating agent	Time of exposure (in hours)[1]							
		24	48	72	96	120	144	168	192
Ferrous iron	1:100,000	2	2	2	2	2	2	2	2
	1:1,000,000	1	1	1	1	1	1	1	1
	1:10,000,000	3	3	3	3	3	3	3	3
	1:100,000,000	4	4	4	4	4	4	4	4
	1:1,000,000,000	5	5	5	5	5	5	5	5
Ferric iron	1:100,000	(3)	(3)	(3)	(3)	(3)	(3)	(3)	(3)
	1:1,000,000	(3)	(3)	(3)	(3)	(3)	(3)	(3)	(3)
	1:10,000,000	(3)	(3)	(3)	(3)	(3)	(3)	(3)	(3)
	1:100,000,000	(3)	(3)	(3)	(3)	(3)	(3)	(3)	(3)
	1:1,000,000,000	(3)	(3)	(3)	(3)	(3)	(3)	(3)	(3)
Ferrous and ferric iron [2]	1:100,000	3	3	3	3	3	3	3	3
	1:1,000,000	2	2	2	2	2	2	2	2
	1:10,000,000	(3)	(3)	(3)	(3)	(3)	(3)	(3)	(3)
	1:100,000,000	(3)	(3)	(3)	(3)	(3)	(3)	(3)	(3)
	1:1,000,000,000	(3)	(3)	(3)	(3)	(3)	(3)	(3)	(3)

[1] At the end of each 24-hour period each set of tubes was compared with the corresponding original sample and with each other. The numbers in this table represent the results of these comparisons, and are not comparable to preceding or succeeding observations.

[2] No apparent color change.

[3] In equimolar concentrations.

NOTE.—Color is expressed by a comparative numerical scale: 1 (darkest) to 5 (lightest). Before exposure to light, the original sample was lighter in color than "5."

III. DISCUSSION OF EXPERIMENTAL RESULTS

1. EFFECT OF LIGHT UPON ROSIN

All of the samples of rosin which were exposed to the action of the adopted source of light darkened in color to a considerable degree, regardless of the artificial gas atmosphere used. However, the bleached and unbleached specimens differed as to comparative behavior with respect to light in every artificial atmosphere used, with the exception of air and, in a single instance, carbon dioxide. In the case of the unbleached samples, maximum darkening occurred in those tubes which contained oxygen or air. Some color changes were observed in the absence of oxygen, indicating that the unbleached rosin can be affected by light alone. The increased effect in the presence of oxygen would indicate a photochemical oxidation. On the other hand, the bleached rosins darkened most in those tubes which contained nitrogen or air, which would tend to show that oxygen is not essential to a considerable change in bleached rosins upon exposure to light. Abietic acid, found in ordinary rosins, contains one double carbon bond, and, therefore, may be expected to add two atoms of chlorine when subjected to bleaching as described. Such chlorinated compounds are, in general, unstable to light.[33] These observations are at variance with the recommendations of Schoeller[34] and Haas[35] as to the use of "bleached" rosin for the manufacture of paper size. The fact that rosin, bleached as recommended, was observed to darken in color under the influence of light eliminates it from consideration as a substitute for unbleached rosin on the basis of comparative light sensitivity.

[33] Plotnikow, Lehrbuch der Photochemie, p. 547; 1919.

[34] See footnotes 7 and 8, p. 820.

[35] See footnote 12, p. 820.

2. EFFECT OF LIGHT UPON RESINATES OF SODIUM, ALUMINUM, AND IRON

Ferrous resinate was the only one of these compounds which yielded a visible color change upon an exposure of 25 hours. Regardless of whether bleached or unbleached rosin was used, a distinct change in color was observed after an exposure of two hours. This effect is probably due to a photochemical change in valence of ferrous to ferric iron.

3. EFFECT OF LIGHT UPON ROSIN SIZE, CONTAMINATED WITH FERROUS AND FERRIC IRON, SINGLY AND TOGETHER[36]

The samples of "size milk" containing ferrous iron alone all darkened in color upon exposure to light, exhibiting a maximum darkening in the samples containing 1 part of ferrous iron per 1,000,000 parts of "size milk." Apparently this is a critical concentration. None of the samples to which ferric iron alone had been added exhibited any change in color. The evidence indicates that the ferrous iron catalyzes the action of light upon the rosin size examined. Catalysis of photochemical reactions by traces of ferrous iron is a well-known phenomenon.[37] The color of this intimate mixture of ferrous resinate and rosin after exposure to light is much darker than is the color of rosin similarly exposed.

IV. SUMMARY

As a result of this study of the effect of light upon rosin and rosin size, the following conclusions may be drawn:

1. Rosin is light sensitive, and darkens in color even in an atmosphere of an inert gas.
2. Both bleached and unbleached rosin show approximately the same degree of change in color.
3. Ferrous resinate is light sensitive, and the color change it undergoes upon exposure to light is probably due to photochemical change in valence of ferrous iron to ferric iron. Ferric resinate, aluminum resinate, and sodium resinate are not light sensitive.
4. An intimate mixture of ferrous resinate and rosin, as found in rosin size contaminated with quantities of ferrous iron smaller than those usually found in industrial waters, is light sensitive to a greater degree than rosin alone. The evidence indicates that the ferrous iron catalyzes the action of light upon the rosin size examined.
5. Since rosin-sized paper contains rosin, ferrous resinate, and rosin size contaminated with ferrous iron, and since these substances have been shown to be sensitive to light, some relationship must exist between these facts and the discoloration ("yellowing") of papers upon exposure to light.
6. This article reports the first of a series of investigations as to the deteriorative agencies and their effects upon the components of paper.

WASHINGTON, February 10, 1931.

---

[36] See footnote 22, p. 821.
[37] Plotnikow, Lehrbach der Photochemie, p. 320; 1919.

DIMENSIONAL CHANGES IN THE MANUFACTURE OF ELECTROTYPES

By N. Bekkedahl [1] and W. Blum [2]

ABSTRACT

This investigation was conducted by cooperation between the International Association of Electrotypers and the National Bureau of Standards. Electrotypes made under typical but carefully controlled conditions were measured after each step in the process. The results showed that each operation is likely to produce some change in dimensions. The largest and most variable changes are produced in curving. By controlling all conditions it is possible to produce plates that will register with each other within about 0.05 per cent, though they will usually not have the same dimensions as the originals.

CONTENTS

	Page
I. Introduction	829
II. Outline of the electrotyping process	830
III. Outline of this investigation	831
IV. Results of experiments	833
1. Molding	833
(*a*) Wax molding	833
(*b*) Lead molding	835
2. Deposition	835
3. Casting	837
4. Finishing	839
5. Curving	840
V. Summary	844
1. Molding	844
2. Depositing	844
3. Casting	844
4. Finishing	844
5. Curving	844
VI. Acknowledgments	845

I. INTRODUCTION

Electrotyping is extensively used for the reproduction of printing plates. In this process the details of the original, whether type or half tone, are faithfully reproduced. However, it has long been known that, unless special precautions are observed, the electrotypes are not exactly the same size as the originals. This difference, which in curved plates may be over 1 per cent, is usually not significant if the printing is done in one color, as then only one plate is involved.[3] In multicolor printing, however, two or more plates are employed; that is, one for each color used. For high-grade printing, these plates must have the same corresponding dimensions in order to register

[1] Research associate of the International Association of Electrotypers.
[2] Chemist, National Bureau of Standards.
[3] In printing certain charts, scale diagrams, or cross-section paper, accurate reproduction may be required even for 1-color plates.

properly. Even in this case it is not essential that the different plates should be exactly the same size as the originals, but they must be alike in size. The difficulties sometimes encountered by commercial electrotypers in meeting this latter requirement led the International Association of Electrotypers to select this subject for study by their research associate at the National Bureau of Standards.

This paper is a report of an investigation of this subject, in which the dimensional changes produced in each step of the electrotyping process were measured. In addition, the effects of changes in electrotyping conditions upon the changes in dimension were studied in order to determine how closely such conditions must be controlled to insure any given degree of uniformity in the size of the finished electrotypes.

II. OUTLINE OF THE ELECTROTYPING PROCESS

Electrotypes are made by depositing metal either upon wax molds or lead molds, of which the former are more extensively used. In wax molding, an impression of the original form is made by pressing the latter into a layer of wax that is attached to a flat metal plate. Graphite is then applied to render the wax surface electrically conducting, and metal is deposited on the graphite, forming a thin "shell." Sometimes the graphite surface is treated with a copper sulphate solution and iron filings, which produce a thin film of copper on the graphite. This process, known as "oxidizing," causes the metal to subsequently deposit almost at once over the entire surface, instead of "growing" over from the point where metallic contact is made with the graphite. In copper electrotypes, the shell consists entirely of copper, while in nickel electrotypes the first layer is nickel and the rest of the shell is copper. The nickel is used especially for large editions and for high-grade printing. At present chromium is often applied to finished nickel or copper electrotypes to increase their wear resistance.

A lead mold is made by pressing the original form into a thin sheet of lead. The lead mold is cleaned and treated with a chromate solution to permit separation of the subsequently deposited shell, which is generally of nickel and copper. Lead molds are used especially for half tones. Type-metal forms are not usually reproduced by lead molding, as the high pressure used is likely to deform the type. It is a general practice, however, to make lead molds from specially prepared electrotype patterns of a type subject.

The back of the shell is treated with a solution of zinc chloride which serves as a flux; after which "tin foil," consisting of about 35 per cent tin and 65 per cent lead, is laid on the surface. The shell is then placed face down on a flat cast-iron pan which is heated, usually by floating it upon molten lead or electrotype metal. When the tin foil has melted, molten electrotype metal is poured over the shell to the desired thickness. After the resultant plate is cool it is cleaned, trimmed, shaved on the back to approximately the desired thickness, "finished" to produce a plane printing surface, shaved to the exact thickness, and for flat presses is beveled or mounted on wood. If the plate is to be used on a rotary press, it is curved to fit the cylinder of that press. Any large nonprinting areas on the plate are usually "routed out," in order to prevent them from taking up ink and yielding it to the paper.

III. OUTLINE OF THIS INVESTIGATION

General observations indicated that each of the major steps in the above process might affect the dimensions, namely, the molding, depositing, casting, finishing, and curving. In a preliminary study, plates were made under typical commercial conditions, and the dimensions were measured before and after each of the above operations. These tests indicated the magnitudes of the changes produced in each step. The process was then carried out under more carefully controlled conditions, each of which was varied over definite limits, to determine the corresponding variations in the dimensional changes.

This investigation was facilitated by the active cooperation of the Potomac Electrotype Co., of Washington, D. C., and the Govern-

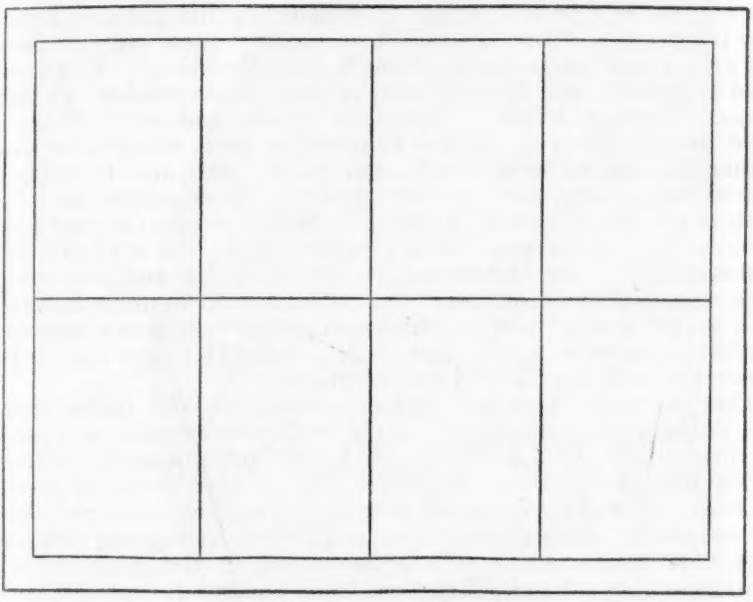

FIGURE 1.—*Design of "plain" pattern plate, showing lines used as gage marks*

The plate was 11 by 14 inches (28 by 26 cm).

ment Printing Office. In general, the molds were made in one of these plants, the shells were deposited at the National Bureau of Standards (in order to measure and control the current used on each plate), and the casting, finishing, and curving were done in the plants. The data, therefore, represent closely the results of actual electrotyping conditions.

In this study two pattern plates were used. The first, designated as the "plain" form, consisted of a polished copper plate about 11 by 14 inches (28 by 36 cm). Upon one side were ruled [4] fine lines, about 0.001 inch (or 0.025 mm) in width which formed a large rectangle divided into eight small ones, as shown in Figure 1. These lines served as gage marks, between which the distances were measured after each step in the process.

[4] Through the courtesy of the United States Coast and Geodetic Survey.

The other pattern, designated as the "type" form, was an electrotype plate, the surface of which consisted mostly of type, with some "rules." This plate was about 9 by 12 inches (23 by 30 cm). Measurements were made between certain well-defined points on this plate and its reproductions.

These two patterns were selected to represent the extremes likely to be encountered in printing plates. Halftone plates are in very low relief, and hence approach the plain form. Commercial plates that include both type and halftone may reasonably be expected to yield results that are intermediate between those obtained with the two patterns used in this investigation.

No difficulty was experienced in measuring the distances between given points on flat plates by means of a graduated steel scale. It is however more difficult to measure accurately the distance between two points on a cylinder, especially if between these points a part of the cylindrical surface has been removed by "routing." If a flexible steel tape were used, it would tend to span the depression as a chord, instead of as an arc of the specified radius, and would hence not yield the true distance on the cylindrical surface, which latter is the actual printing surface. This difficulty was overcome by using the special gage shown in Figure 2, which was designed by one of the authors (W. B.). This gage was made from a polished flat steel plate about 15 by 8 by $\frac{3}{16}$ inches (38 by 20 by 0.5 cm). The arc had a radius of 6.250 ± 0.002 inch (158.8 ± 0.05 mm). This arc and one straight edge were graduated in linear units, the smallest division being 0.01 inch (equal to 0.25 mm). With an optician's lens, readings could readily be made to ± 0.002 inch (0.05 mm). The gage was used for measuring both the flat and curved plates.

This particular gage was designed for the curved plates used in this investigation, which were made to fit the cylinder of a 3-color Sterling press. In order to make similar measurements on plates curved for different size cylinders, a separate gage would be required for each radius of curvature of the printing surface, which is one-half the so-called "bearer diameter." In a large electrotyping plant, this might necessitate the use of a large number of such gages if the dimensions of the curved plates were to be measured.

The dimensional changes are expressed in terms of (*a*) changes produced by a given step in the process, and (*b*) the net change from the original, produced by all operations performed up to and including that step. The latter values, or more strictly the final dimensions, are significant in the use of the plates; while the former show how variations in the latter may arise.

The register of two or more printing plates depends upon the actual differences in distance between corresponding points on the plates. Experience indicates that for fine printing; for example, of color process half tones, the extreme difference of corresponding points in the final impressions should be not more than about 0.003 inch (0.08 mm). To secure this accuracy of register, it is necessary that the dimensions of the plates should correspond only within about 0.005 inch (0.13 mm); as the effort is always made to have the plates register exactly at their centers, which causes half of the error to appear on each end. For practical purposes we may then consider that the object of this investigation was to define conditions that would insure an equality of length within ± 0.005 inch (0.13 mm).

FIGURE 2.—*Gage used for measuring dimensions of curved electrotypes*

Both the arc and the straightedge were graduated in intervals of 0.01 inch.

Such a variation in length would, however, represent entirely different percentage discrepancies, according to the dimensions of the particular plate; for example, 0.1 per cent on a 5-inch (12.7 cm) plate, or 0.02 per cent on a 25-inch (63.5 cm) plate. Evidently, therefore, a measurement of the percentage variation is not in itself a criterion of the accuracy of register. As printing plates, including those made in this study, vary in dimensions, the only practicable way to express general conclusions is in terms of percentage changes. For any given size of plate the corresponding actual differences may then be calculated. Thus for a 10-inch (25 cm) plate, which is probably about the average length used commercially, each one-hundredth of 1 per cent is equal to 0.001 inch (or 0.025 mm). The general conclusions of this paper are based on a plate of about that length.

All the measurements reported in this paper were the averages of at least two plates, and in some cases of 10 or more. Except in a few cases that will be mentioned, the individual results were concordant to within about ± 0.03 per cent. The changes were generally about equal in both directions, except in curving, when the significant changes occur only in the direction of curvature. In lead molding, changes in the two directions may be slightly different if the lead overlaps the pattern in one direction and not in the other. In the measurements here recorded, the lead projected beyond the pattern on all four sides, which is the common commercial practice. A positive sign attached to a change, for example, +0.03 per cent, indicates an increase in length ("stretch") and a negative sign a decrease ("shrinkage"). All measurements were made at room temperature, which was approximately 75° F. (24° C.).

IV. RESULTS OF EXPERIMENTS

The conditions used in each operation and the dimensional changes thereby produced, may conveniently be considered under each of the principal steps involved.

1. MOLDING

(a) WAX MOLDING

The cases used for wax molding were prepared by pouring molten wax consisting largely of ozokerite, to a depth of about 0.15 inch (4 mm) on a flat plate made of electrotype metal (containing about 93 per cent lead, 4 per cent antimony, and 3 per cent tin). The surface of the wax was shaved to make it plane, and brushed lightly with molding graphite to prevent the form from sticking. Molding was done in a hydraulic press at the slightly elevated temperature that is commonly used, and also at room temperature. The results in Table 1 show that in neither case was there any measurable difference in the dimensions of the original form and the wax mold.

TABLE 1.—*Dimensional changes in molding*

Experiment No.	Pattern	Mold	Molding temperature		Per cent change in molding
			°F.	°C.	
1	Plain	Wax	120	49	0.00
2	do	do	75	24	.00
3	do	Lead	75	24	+.05
4	Type	do	75	24	+.05

This result is somewhat surprising in view of the fact that the molding wax has a much higher coefficient of expansion than that of copper. If the wax were free to expand and contract laterally the wax mold made at a high temperature would become smaller than the copper pattern when both were again at room temperature. The expansion coefficients of some of the materials used in electrotyping are shown in Table 2.

TABLE 2.—*Approximate linear coefficients of thermal expansion*

Material	Parts per million per degree C.
Aluminum	23
Antimony	11
Copper	(0 to 50° C.) 16 (0 to 300° C.) 18
Nickel	13
Lead	31
Tin	23
Electrotype metal (93 per cent Pb, 4 per cent Sn, 3 per cent Sb)	28
Zinc	30
Molding wax (ozokerite base)	250

The values in this table for the metals are derived from those values in the literature that represent approximately the temperature ranges involved in this investigation. Aluminum is included because it or its alloys are sometimes used in the case on which the wax is poured. Zinc is included because zinc plates often serve as patterns for electrotyping. No values were found for electrotype metal. The value found [5] for a type metal containing 85 per cent lead, 12 per cent antimony, and 3 per cent tin is 25 parts per million per degree centigrade. The available data indicate that the expansion coefficient of ordinary electrotype metal, which contains 93 per cent of lead, is intermediate between this value and that of pure lead, or about 28 parts per million per degree centigrade. The expansion coefficient of electrotypers' wax varies with its composition. The value given in the table is the approximate average of a few samples on which purely preliminary measurements were made in connection with this investigation.

If then the wax expanded freely when heated from about 75° to 120° F. (24° to 49° C.), its length would increase by about $25 \times 0.000250 = 0.00625$, or 0.63 per cent. The copper form would expand in this same temperature range, by about $25 \times 0.000016 = 0.000400$, or 0.04 per cent. Hence, we would expect that on cooling, the wax mold would contract more than the copper and at 75° F. (24° C.) would be smaller than the original copper by the difference in these two expansions (or contractions); that is, by 0.63 minus 0.04 per cent, or practically 0.6 per cent. As no such difference was observed, it is evident that the layer of wax that is attached to the metal base, in this case type metal, is not free to contract or expand laterally, and that it retains very closely the size of the underlying plate. If this is true, the only change that would be measured after molding would be that due to the difference in expansion of the copper pattern and the type metal case. This would be equal to about 25 (0.000028−

[5] Geo. F. Taylor, Phys. Review, **26**, p. 841; 1925.

0.000016) = 25 (0.000012) = 0.000300, or 0.03 per cent. This difference, which would result in −0.03 per cent change, is just about at the limit of observation, especially on wax molds. If, however, the copper pattern is expanded slightly by pressure, even at the moderate pressure used in wax molding, this will tend to compensate for the tendency of the mold to contract. At least the results show clearly that expansion of the molding wax does not lead to an appreciable change in lateral dimensions, and that differences in the composition or expansivity of the wax are not likely to affect the dimensions of the mold.

(b) LEAD MOLDING

As lead molding is done at ordinary temperature, there is no opportunity for dimensional changes to be caused by differences in thermal expansivity. Nevertheless it was found, as shown in Table 1, that the lead molds are slightly larger than the originals. This difference is undoubtedly due to the fact that at the higher pressures used in lead molding, the pattern expands slightly. If this expansion is within the elastic limit of the pattern metal, in this case copper, the pattern returns to its original length when the pressure is removed, while the lead, which has a very low elastic limit, retains the slightly larger dimension.

That the pattern plates do expand slightly in lead molding, even in extreme cases to the extent of a permanent change, is indicated by the fact that the plain pattern was 0.02 per cent larger in both length and width after about 100 impressions had been made from it. The type pattern was about 0.07 per cent longer and 0.02 per cent wider after about 50 impressions had been made. The greater expansion in length of the type plate was probably due to the fact that the type lines ran across the plate. Hence, the lateral pressure perpendicular to these lines was greater than that parallel with them. These very small changes in the size of pattern plates as a result of repeated molding have been reported by electrotypers.

2. DEPOSITION

It is well known that all electrodeposited metals are in a state of strain and tend to contract during their deposition. This contraction is most marked with the harder metals, and with those, such as nickel, that absorb much hydrogen. For a given metal the tendency to contract is greatest at a low temperature and a high current density, and increases with the thickness of deposit.

These well-known principles are illustrated by the data shown in Table 3. In these experiments the copper was deposited from a solution containing 250 g/l (33 oz./gal.) of copper sulphate ($CuSO_4.5H_2O$), 75 g/l (10 avoir. oz./gal.) of sulphuric acid (H_2SO_4) and 1.0 g/l (0.13 oz./gal.) of phenol, added as phenolsulphonic acid. Preliminary observations showed that the use of phenol as an addition agent produced no measurable change in the dimensions of the shells. (As will be noted later, it may affect the changes that occur in curving.) The nickel was deposited from a solution containing 70 g/l (9 oz./gal.) of nickel sulphate ($NiSO_4.7H_2O$) and 5 g/l (0.7 oz./gal.) of ammonium chloride (NH_4Cl) at a pH of about 6.4 (with brom cresol purple, uncorrected for salt error).[6]

[6] W. Blum and N. Bekkedahl, Trans. Am. Electrochem. Soc., **56**, p. 291; 1929.

TABLE 3.—*Dimensional changes in deposition*

Experiment No.	Pattern	Mold	Temperature of deposition				Current density				Thickness of shell				Change—	
			Nickel		Copper		Nickel		Copper		Nickel		Copper		In deposition	From original
			°F.	°C.	°F.	°C.	Amp./ft.²	Amp./dm²	Amp./ft.²	Amp./dm²	Inch	mm	Inch	mm	Per cent	Per cent
5	Plain	Wax			70	20			75	8			0.006	0.15	−0.07	−0.07
6	do	do			105	40			75	8			.006	.15	.00	.00
7	do	do			105	40			150	16			.006	.15	.00	.00
8	do	do			105	40			150	16			.012	.30	.00	.00
9	do	do			105	40			75	8			.012	.30	.00	.00
10	do	Lead			70	20			75	8			.006	.15	−.04	+.01
11	do	do	85	30	105	40	20	2	150	16	0.002	0.05	.012	.30	−.14	−.09
12	do	do			105	40			75	8			.006	.15	−.02	+.03
13	do	do			105	40			150	16			.006	.15	−.02	+.03
14	do	do	85	30	105	40	20	2	150	16	.001	.025	.006	.15	−.12	−.07
15	Type	do	85	30	105	40	20	2	150	16	.001	.025	.006	.15	−.12	−.07
16	do	do	85	30	105	40	20	2	150	16	.002	.05	.012	.30	−.15	−.10
17	do	do			105	40			150	16			.006	.15	−.05	.00

In most experiments the shells were smaller than the molds, and the contraction of the nickel-copper shells was always greater than of the copper alone. With the latter, the contraction was significant only with shells deposited at a relatively low temperature (experiment 5). The absence of a measurable change when the copper was deposited at a high temperature, even at a high-current density, was propably due to the fact that, as previously explained, the wax mold on a type-metal base was slightly larger (about 0.03 per cent) at the elevated temperature. Hence, the small contraction produced by deposition may have just compensated for this tendency to expand. Strictly speaking, the contraction caused by the deposition itself on either the wax or lead molds at the higher temperature was, therefore, about 0.03 per cent greater than that shown in Table 3. Practically, however, the actual changes in dimensions of the shells are significant.

The shrinkage produced in depositing nickel-copper shells was relatively large (from 0.12 to 0.15 per cent) but fairly uniform, regardless of whether a plain or type form was used, or whether the shells varied in thickness by as much as 100 per cent. In the latter case, the contraction was slightly greater, but not sufficiently different to affect the register.

The last column in Table 3 shows that the changes in molding and in depositing tend to compensate each other. Hence, the dimensions of the shells are not much different from those of the patterns. As will be seen, the changes in casting and curving are relatively large. If these operations could be eliminated, there would be little difficulty in obtaining plates of uniform dimensions. This elimination is not practicable in regular electrotyping as now practiced, but it has been accomplished by making the entire printing plate of deposited metal; for example, of iron, at the Bureau of Engraving and Printing,[7] or of copper as is being done for special purposes in a few electrotyping plants.

[7] C. T. Thomas and W. Blum, Trans. Am. Electrochem. Soc., 57, p. 59; 1930.

TABLE 4.—*Dimensional changes in casting*

Experiment No.	Pattern	Electrotype metal composition			Shell thickness				Casting temperature		Rate of cooling	Change—	
		Pb	Sn	Sb	Nickel		Copper					In casting	From original[1]
		P. ct.	*P. ct.*	*P. ct.*	*Inch*	*mm*	*Inch*	*mm*	*°F.*	*°C.*		*P. ct.*	*P. ct.*
18	Plain	93	4	3	------	------	0.006	0.15	635	335	Fast	−0.18	−0.15
19	do	93	4	3	0.001	0.025	.006	.15	635	335	do	− .15	− .22
20	do	93	4	3	.001	.025	.006	.15	790	420	do	− .14	− .21
21	do	93	4	3	.001	.025	.006	.15	635	335	Slow	− .16	− .23
22	do	93	4	3	.002	.05	.012	.30	635	335	do	− .09	− .18
23	do	88	9	3	.001	.025	.006	.15	635	335	do	− .11	− .18
24	Type	93	4	3	------	------	.006	.15	635	335	Fast	− .15	− .15
25	do	93	4	3	.001	.025	.006	.15	635	335	do	− .17	− .24
26	do	93	4	3	.001	.025	.006	.15	790	420	do	− .15	− .22
27	do	93	4	3	.001	.025	.006	.15	635	335	Slow	− .16	− .23
28	do	93	4	3	.002	.05	.012	.30	635	335	do	− .14	− .24
29	do	88	9	3	.001	.025	.006	.15	635	335	do	− .16	− .23

[1] These values were obtained by assuming lead molding, copper deposition at 105° F. (40° C.), and nickel deposition at 85° F. (30° C.).

3. CASTING

The data in Table 4 show clearly that the casting process always causes shrinkage of the plates. The most reasonable explanation is that the solid electrotype metal has a higher expansivity than the copper shell. Hence, when the cast plate cools, the type metal tends to contract the copper. This effect can not start until the electrotype metal has solidified, as above the melting point of the type metal the latter and the copper are free to expand and contract independently. As the electrotype metal freezes at about 527° F. (275° C.) (see fig. 3) we may assume that the differential contraction of the type metal and copper is significant from about 275° C. to 25° C.; that is, for about 250 centigrade degrees or 450 Fahrenheit degrees. The independent contractions in this range would be about as follows:

$$\text{Copper} = 250 \times 0.000018 = 0.0045 = 0.45 \text{ per cent}$$
$$\text{Type metal} = 250 \times 0.000028 = 0.007 \ = 0.7 \ \text{ per cent}$$

From these figures we might expect that the cast plate would be about 0.25 per cent shorter than the shell, instead of only about 0.15 per cent as shown in Table 4. The difference is no doubt due to the fact that the copper (or copper-nickel) shell has too high a compressive strength to be fully contracted by the electrotype metal. Hence, the latter must either slip or be stretched beyond its elastic limit during the cooling. The net result is a shortening of the plate by an amount that is less than the difference between the two coefficients.

If the above explanation is correct, the casting temperature should have no effect on the shrinkage, as the latter can not start until the metal solidifies. This prediction is borne out by the data in Table 4. (Compare experiment 18 with 20 and 25 with 26.)

Differences in the rate of cooling produce no marked differences in the dimensions. In the "slow" process, the cast plates were allowed to stand on the pans without any artificial cooling. In the "fast" cooling, cold air was blown against the bottom of the pans. The different rates of cooling are shown by the "cooling curves" in Figure 3. These were made by imbedding "chromel-alumel"

thermocouples in the type metal as the latter was poured on the pans, and reading the temperatures at regular time intervals by means of a millivoltmeter. In all cases it was observed that the "break" in the curve; that is, the freezing point, occurred at about 527° F. (275° C.), even with type metals of different compositions. It is recognized that an accurate measurement of the melting or freezing point was not obtained under these conditions, as the metal was not stirred while cooling. The results represent, however, the approximate cooling rates of the type metal under the conditions used.

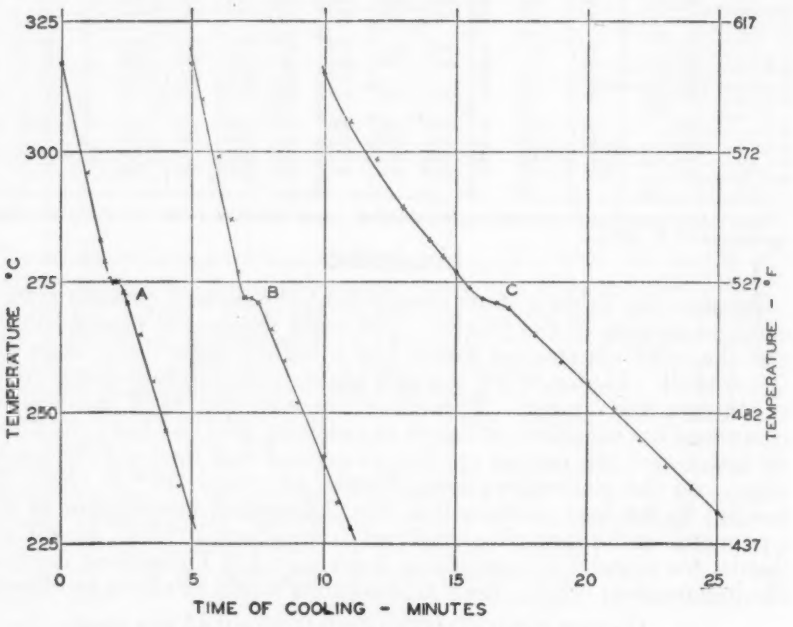

FIG. 3.—*Cooling curves for electrotype metal in the casting pans*

The "break" in each curve represents the freezing or solidification of the metal.
A, 88 per cent lead, 9 per cent tin, and 3 per cent antimony. Cooled rapidly.
B, 93 per cent lead, 4 per cent tin, and 3 per cent antimony. Cooled rapidly.
C, 93 per cent lead, 4 per cent tin, and 3 per cent antimony. Cooled slowly.
(For convenience the initial readings are spaced at 5-minute intervals. To compare *B* or *C* with *A*, 5 minutes should be deducted from the values on *B*, and 10 minutes from those on *C*.)

An increase in the tin content of the type metal produced a somewhat smaller contraction of the plain plates (compare experiment 21 with 23), but no similar difference with the type pattern (compare experiment 27 with 29). The higher tin content presumably reduces slightly the expansivity of the electrotype metal, which would result in a smaller contraction of the cast plate. The larger contraction with the type pattern may be due to the fact that the latter presents a rough surface and, therefore, retards any slippage, and also that the corrugated surface of the shell is more easily contracted than is a plain surface. Any warping of the plates is likely to make their measured dimensions less than those when the plate is plane.

The other factor that caused a variation in the contraction was the thickness of the shell. The smaller contraction of a thick shell (compare experiment 21 with 22) is to be expected since the thicker copper and nickel would offer more resistance to shrinkage. Here again the effect is negligible with the type pattern, probably for the reasons stated above.

In general, it may be concluded that the casting process produces a contraction of about 0.15 per cent, which value is not appreciably affected by differences in the temperature of casting or rate of cooling; but it may be changed slightly, especially on plain plates, by a change in the composition of the type metal or in the shell thickness. As the deposited shells have nearly the same dimensions as the originals, the contraction in casting always results in a cast plate that is smaller than the originals.

4. FINISHING

The cast plates are not likely to have a plane printing surface, as both the deposition and the casting tend to produce distortions. The purpose of the finishing process is to straighten the plate so that the entire printing surface is in one plane. This operation generally tends to cause an increase in the dimensions of the plate. The extent of this stretch depends upon the amount of finishing required and the method used to eliminate defects that may have been present in the original patterns or produced in the electrotyping process. It is therefore difficult to obtain data that represent "average" conditions. The results in Table 5 are simply typical values that show the probable magnitudes of the changes.

TABLE 5.—*Dimensional changes in finishing*

Experiment No.	Pattern	Shell metal	Method of finishing	Change—	
				In finishing	From original [1]
				Per cent	*Per cent*
30	Plain	Copper	Hand hammering	+0.14	−0.01
31	do	Nickel-copper	do	+.09	−.21
32	do	Copper	Cold press	+.03	−.12
33	do	Nickel-copper	do	+.03	−.17
34	do	Copper	Hot press	−.11	−.26
35	do	Nickel-copper	do	−.08	−.28
36	Type	Copper	do	−.09	−.24
37	do	Nickel-copper	do	−.06	−.29
38	do	Copper	Cold press	+.10	−.05
39	do	Nickel-copper	do	+.08	−.15

[1] These values were obtained by assuming lead molding, copper deposition at 105° F. (40° C.), and nickel deposition at 85° F. (30° C.).

In the common practice of hammering the back of the plates at the points that are too low on the printing surface, the amount of stretch is variable. In some cases at least the expansion thereby produced is just sufficient to bring the dimensions back to the original. At best, however, hand finishing is troublesome and expensive, and in recent years many efforts have been made to perform this process mechanically.

Straightening in a press at ordinary temperature also causes expansion, the extent of which depends largely on the pressure applied. This expansion by pressure is similar to but greater than that produced by molding, in which lower pressures are generally used. The results obtained indicate that for similar plates and designs and at a controlled pressure, the expansion is fairly uniform. Type plates expand more readily than plain plates. In all cases the net result is to make the plate dimensions approach the originals.

When the plates are straightened in a press at a temperature of approximately 500° F. (260° C.); that is, just below the melting point of the type metal, there is a tendency to contract. Apparently in this second cooling of the electrotype metal, its high coefficient of expansion (or contraction) causes it to produce additional shrinkage of the copper. Plates straightened by this method are likely to be appreciably shorter than the originals.

Tests not recorded in the tables showed that increasing the thickness of the shells had no appreciable effect upon the changes produced by finishing with any of the above processes.

5. CURVING

If a flat homogeneous plate is bent around a cylindrical mandrel, the outer or convex surface tends to expand from tension, and the inner or concave surface tends to contract from compression. If we assume in the ideal case that the effect of the tension is exactly equal to that of compression, the proportional stretch of the outer surface is equal to the thickness of the plate divided by the outside diameter of curvature. This assumption implies that there is in the middle of the plate a "neutral plane" which neither expands nor contracts.

The plates used in this investigation, had a thickness of 0.183 inch (4.65 mm), and were curved to yield an outside diameter of 12.500 inches (317.5 mm).[8] According to the above formula, the percentage stretch would be

$$\text{Per cent stretch} = \frac{\text{Thickness} \times 100}{\text{Diameter}} = \frac{0.183 \times 100}{12.5} = 1.46 \text{ per cent}$$

Actually the average stretch for all the plates included in Table 6 is 1.42 per cent. This close average agreement is, however, largely a coincidence, as under different conditions the stretch varied from 1.02 to 1.65 per cent, for reasons that will be discussed. Even under specified conditions the results were not as reproducible as those obtained in other operations. Small differences in the tabulated results are, therefore, not significant.

[8] As these plates were made for use on a cylinder with a diameter of 12.125 inches (308 mm), the desired outside diameter would correspond to a plate thickness of 0.1875 inch (4.76 mm). A smaller plate thickness, in this case 0.183 inch (4.65 mm), is generally used in order to allow for an "under lay" of paper in the "make-ready"; that is, the process of bringing all parts of the printing surface into the position needed to give it the desired "printing value."

TABLE 6.—*Dimensional changes in curving*

Experiment No.	Pattern	Electrotype metal			Shell thickness				Rate of cooling	Hours till curved	Method of curving	Change—	
		Pb	Sn	Sb	Nickel		Copper					In curving	From original [1]
		P. ct.	*P. ct.*	*P. ct.*	*Inch*	*mm*	*Inch*	*mm*				*P. ct.*	*P. ct.*
40	Plain	93	4	3	------	------	0.006	0.15	Slow	24+	Cold	+1.41	+1.29
41	do	93	4	3	0.002	0.05	.012	.30	do	24+	do	+1.02	+.85
42	do	93	4	3	.001	.025	.006	.15	do	24+	do	+1.30	+1.13
43	do	93	4	3	.001	.025	.006	.15	do	24+	Hot	+1.33	+1.16
44	do	93	4	3	.001	.025	.006	.15	do	2	Cold	+1.29	+1.12
45	do	88	9	3	.001	.025	.006	.15	do	24+	Hot	+1.22	+1.05
46	Type	88	9	3	.001	.025	.006	.15	do	24+	do	+1.58	+1.43
47	do	93	4	3	.002	.05	.012	.30	do	24+	do	+1.41	+1.26
48	do	93	4	3	.002	.05	.012	.30	do	24+	Cold	+1.35	+1.20
49	do	93	4	3	.001	.025	.006	.15	Fast	24+	do	+1.53	+1.38
50	do	93	4	3	.001	.025	.006	.15	do	24+	Hot	+1.65	+1.50
51	do	93	4	3	.001	.025	.006	.15	Slow	24+	Cold	+1.51	+1.36
52	do	93	4	3	.001	.025	.006	.15	do	24+	Hot	+1.60	+1.45
53	do	93	4	3	.001	.025	.006	.15	do	2	Cold	+1.49	+1.34
54	do	93	4	3	------	------	.006	.15	do	24+	do	+1.56	+1.51

[1] These values were obtained from assuming lead molding, copper deposition at 105° F. (40° C.), nickel deposition at 85° F. (30° C.), and cold-press method of finishing.

An electrotype plate is not homogeneous, and the outer shell is much stronger than the electrotype metal that constitutes over 90 per cent of the plate. Hence, the neutral plane as above defined is nearer to the printing surface, and on curving, the plate stretches like a thinner plate; that is, the expansion is less than that calculated as above. This is illustrated by the data in Table 6 for plain plates, for which the average stretch is only 1.26 per cent.

On the other hand, the type pattern represents a surface corrugated in the direction perpendicular to that of curvature. When such plates are bent, the average increase in length is 1.52 per cent; that is, slightly greater than that calculated. In bending a type plate the increase in length of the printing surface is caused not only by stretching the shell, but also by bending the latter where the vertical portions meet the depressed horizontal portions. This is illustrated in Figure 4. The depressions in the face have the same effect as if the diameter of the plate were decreased, while the thickness (as defined by the printing surface) remains constant.

This same effect is observed to an even greater degree if certain areas of the plate are routed out before the plate is curved. Experiments not recorded in the table showed that the stretch of a routed plate is much greater than of an unrouted plate. This difference is due partly to a decrease in the effective diameter as above noted, and also to the reduction in the strength of the shell by removing portions of it. It is therefore preferable to rout the plates after curving. It was found in these tests that this subsequent routing does not change the dimensions of the curved plate. When it is practicable to reduce or eliminate the routing by "building up" the wax mold, the shell is continuous, and the stretch is more nearly uniform than that of a plate routed before curvature.

With either kind of plate, the stretch was decreased by any increase in strength of the shell such as may be produced by using both nickel and copper, by increasing the thickness, or by increasing the strength

of the copper; for example, by the use of addition agents. A few tests not recorded in the table showed that plates made from shells deposited in a copper solution that contained no phenolsulphonic acid stretched slightly more than those here recorded. The smallest stretch (1.02 per cent) was obtained with a nickel-copper shell, plain form and of double thickness.

A slight decrease in the stretch of plain plates was caused by increasing the tin content of the electrotype metal (compare experiment 43 with 45), but any such effect with the type pattern was very small (compare experiment 46 with 52). As the addition of tin hardens the type metal, a decreased stretch would be expected.

No appreciable difference was observed in the stretch whether the cast plates were cooled rapidly or slowly (compare experiments 51

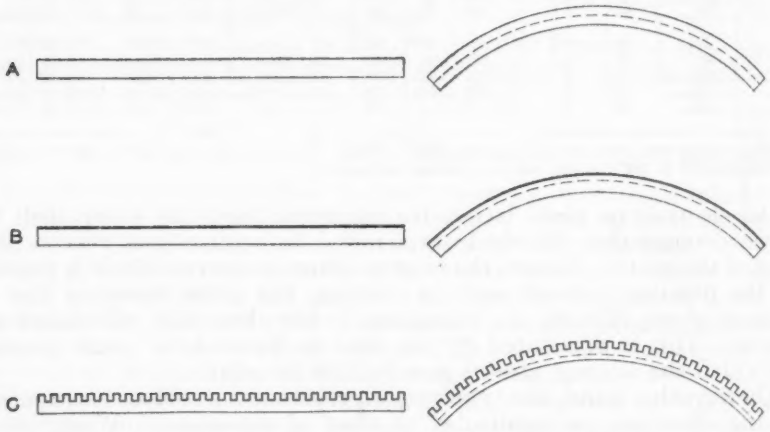

FIGURE 4.—*Diagram showing types of curved plates*

A. A homogeneous plate. When curved the convex surface stretches approximately in accordance with the equation

$$\text{Per cent stretch} = \frac{\text{Plate thickness} \times 100}{\text{Diameter of curvature}}$$

The neutral plane is in the center.

B. A plain electrotype plate, with a shell of copper or nickel, backed-up with electrotype metal. The stretch is less than that calculated in *A*. The neutral plane is closer to the outer surface.

C. An electrotype of a type pattern. This stretches slightly more than that calculated in *A*. The neutral plane is closer to the inner surface.

with 49, and 52 with 50). Similarly it made no difference whether the plates were curved soon after casting (within about two hours), or after 24 hours or more.

The cold curving was done at room temperature with the ordinary 3-roll bender. In this method the plates are rolled to fit the mandrel, a hemicylinder which is known in electrotyping as the "turtle." In hot curving the plate is heated to about 480° F. (249° C.) and is then bent directly to fit the appropriate cylinder. In general, the hot curving produced a slightly greater stretch than cold curving. The difference was not significant with the plain plates (compare experiment 42 with 43), but was appreciable with the type plates (compare experiments 51 with 52, and 49 with 50). The greater stretch in hot curving is probably caused by the fact that at the higher temperature the electrotype metal softens relatively more than does

the shell. The results with hot curving were somewhat more uniform than with cold, and the hot-curved plates retained their curvature better than did the cold-curved plates.

At best it is difficult to produce curved plates of equal dimensions. When a given method of curving is used, the results are fairly reproducible if the shells are of the same thickness, strength, and type of pattern and if the type metal is of uniform composition. This conclusion agrees with the common experience that it is much easier to make several plates of a series with accurate register if they are produced simultaneously than at different times. For example, when a single plate is required to replace a spoiled one of a set, it is often difficult to make it register, because then the conditions may not be the same as when the first plates were made.

As previously noted, it is occasionally desirable to produce electrotype plates that have exactly the same dimensions as the originals. The results described above show that it may be possible, though difficult, to produce flat plates that meet this requirement. Inspection of the data in Table 5 shows that the stretch produced by cold finishing tends to compensate for the contraction in casting. In special cases the finishing operation may be deliberately extended in order to restore the original dimensions.

In the ordinary methods of curving, however, the stretch is usually 1 per cent or more. If uniform, this stretch is not objectionable for regular printing. For "dimensional" printing, however, such plates are useless. One way to overcome this difficulty is to make the pattern plates shorter in the direction in which they are to be curved. This involves a preliminary measurement of the stretch. In another ingeneous method, commonly known as the "nonstretch" process, electrotype metal is poured upon the face of a finished flat electrotype which has been treated with chalk or graphite to prevent the metal from sticking permanently. As a first approximation it might be assumed that when such a plate is cast so as to have the printing face practically in the middle, and is then curved by the usual methods, the printing surface would become the "neutral plane"; that is, it would neither stretch nor contract during the curving.

In order to determine the effectiveness of this procedure a few experiments were made with the same patterns used above. The results showed clearly that if the printing surface is in the center of the plate there is still an appreciable stretch. This can be reduced by making the added type metal layer thicker than the layer on the under side of the shell. For example it was found that if the plate (including the shell) had a thickness of 0.094 inch (2.35 mm) and type metal was cast on the face to a thickness of 0.166 inch (4.2 mm), thus making the total thickness 0.260 inch (6.6 mm) and the plate was subsequently curved on the 3-roll bender, the stretch of either a plain or type plate was only about 0.15 per cent. When, however, the thickness of the added type metal was increased to make the total thickness 0.354 inch (9.0 mm) and the plate was then curved, there was an actual contraction in length of the printing surface.

To eliminate the stretch the shell must evidently be closer to the inside than to the outside surface. It is necessary to determine by experiment what thickness of type metal must be applied to the surface to reduce the stretch to approximately zero. When this is

once determined for a plate and shell of specified thickness and curvature, fairly uniform results can be obtained. It is readily possible thereby to reduce the stretch to about 0.2 per cent, which tends to counteract the shrinkage caused in casting. (This compensation occurs only in the direction of curving, and not in the other direction.) At best it is very difficult to produce finished curved plates that reproduce the originals within about 0.2 per cent in both directions.

V. SUMMARY

The different operations in the electrotyping process produce the following changes in dimension and must be controlled accordingly to produce plates with uniform dimensions.

1. MOLDING

Wax molds are almost exactly the same size as the originals. Lead molds are slightly larger (about 0.05 per cent) than the originals. No special precautions are required to produce uniform plates by either method of molding, but plates made by the two methods are not likely to match each other exactly.

2. DEPOSITING

When copper shells are deposited from cold solutions there is a slight contraction (about 0.05 per cent). The use of warm solutions at a high-current density produces the desired hardness with no appreciable change in dimensions. Nickel-copper shells always contract by about 0.15 per cent. This value is not affected by increasing the thickness of copper and nickel. Such a change in thickness does, however, materially affect the stretch in curving. It is therefore important to keep the conditions for nickel and copper deposition constant, and to produce shells of uniform thickness and strength.

3. CASTING

Casting always causes a shrinkage of about 0.15 per cent, which is not much affected by the temperature of casting or the rate of cooling. Any large change in composition of the electrotype metal will affect the shrinkage. Shrinkage is decreased by increasing the thickness of the shells.

4. FINISHING

Hand finishing always stretches the plates, by amounts that vary with the extent of the finishing operation. Straightening under pressure at ordinary temperature also stretches the plate, but more uniformly than does hand finishing. Straightening in a hot press causes a contraction of about 0.10 per cent.

5. CURVING

The stretch of plain plates in curving is usually less than that calculated from the formula for a homogeneous plate; and a type form stretches more than calculated. Hot curving may produce a slightly greater stretch than cold curving. With a given method, most uniform results are obtained when the shells are of the same

thickness and strength and have the same type of pattern, and when the electrotype metal is of the same composition. The temperature of casting and rate of cooling of the electrotype metal have little, if any, effect on the stretch in curving.

In curving by the "nonstretch" method, it is possible by adjusting the thickness of metal cast upon the face of the plate to reduce the stretch to approximately zero. If too much metal is applied, shrinkage may be produced in curving.

VI. ACKNOWLEDGMENTS

The authors desire to express their appreciation for the cooperation received from the officers and research committee of the International Association of Electrotypers, and for the assistance received from the Potomac Electrotype Co. and the Government Printing Office.

WASHINGTON, March 11, 1931.

THE HEAT OF IONIZATION OF WATER

By Frederick D. Rossini

ABSTRACT

The heat of ionization of water has been calculated by combining the data on heats of neutralization given by Richards and Rowe and the data on heats of dilution recently compiled by the present author. The value so obtained is corroborated by using the data on heats of neutralization reported by Gillespie, Lambert, and Gibson. For the reaction, $H_2O = H^+ + OH^-$, at infinite dilution in water and for the temperature range 10 to 35° C., the heat absorbed is given by the equation: $\Delta H = 13{,}721 - 57.9\ (t-18) + 0.15(t-18)^2$ g-cal$_{18}$ per mole. The uncertainty is estimated to be ± 16 calories per mole. Using the factor 4.181 for coverting g-cal$_{18}$ to absolute joules gives $\Delta H = 57{,}370$ absolute joules per mole at 18° C.

CONTENTS

		Page
I.	Introduction	847
II.	Available data	848
	1. Heats of neutralization	848
	2. Heats of dilution	851
III.	Calculated results	851
IV.	Temperature coefficient	853
V.	Discussion	854
VI.	Conclusion	855

I. INTRODUCTION

The ionization of water may be expressed by the equation

$$H_2O = H^+ + OH^- \qquad (1)$$

Although the heat absorbed in this reaction is not susceptible of direct measurement, its value can be determined in several ways.

Data on the change with temperature of the equilibrium constant for reaction (1) permits calculation of the change in heat content by means of the thermodynamic formula:[1]

$$\frac{d\ ln\ K}{d\left(\frac{1}{T}\right)} = -\frac{\Delta H}{R} \qquad (2)$$

This method was employed by Noyes, Kato and Sosman,[2] who measured at various temperatures the hydrolysis of ammonium acetate and calculated the ionization constant for water.

A summation of the heat changes associated with appropriate other reactions may lead to the desired heat value. The following reactions compose such a series:

$$HCl \cdot 100H_2O + NaOH \cdot 100H_2O = NaCl \cdot 201H_2O \qquad (3)$$

$$HCl \cdot \infty H_2O = HCl \cdot 100H_2O + (\infty - 100)H_2O \qquad (4)$$

[1] The nomenclature of Lewis and Randall ("Thermodynamics," McGraw-Hill Co., New York, 1923) will be used throughout this discussion.

[2] Noyes, Kato, and Sosman, J. Am. Chem. Soc., **32**, p. 159; 1910.

$$NaOH\cdot\infty H_2O = NaOH\cdot 100H_2O + (\infty - 100)H_2O \quad (5)$$

$$NaCl\cdot 201H_2O + (\infty - 201)H_2O = NaCl\cdot\infty H_2O \quad (6)$$

$$HCl\cdot\infty H_2O + NaOH\cdot\infty H_2O + \infty H_2O = NaCl\cdot\infty H_2O + (2\infty + 1)H_2O \quad (7)$$

$$(H^+ + Cl^- + Na^+ + OH^-)\cdot 3\infty H_2O = (Na^+ + Cl^- + H_2O)\cdot 3\infty H_2O \quad (8)$$

or

$$H^+ + OH^- = H_2O \quad (9)$$

The reaction expressed by equation (7) is obtained by summing equations (3), (4), (5), and (6). Neglecting the somewhat philosophical question as to the heat of mixing $NaCl\cdot\infty H_2O$ with $2\infty H_2O$, etc., which is negligibly small, equation (8) is equivalent to (7) and leads directly to the desired reaction (9). In other words, the heat of neutralization at infinite dilution may be taken as equivalent to the heat evolved when H^+ combines with OH^- to form H_2O, which reaction is the reverse of the ionization of water.

Utilizing the then best available data for the heat changes associated with reactions (3), (4), (5), and (6), Richards and Hall [3] calculated a value for the heat of ionization of water in the above manner. Richards and Rowe[4] obtained values for the heat of ionization of water by plotting heats of neutralization against the concentration and extrapolating the curves to infinite dilution. Richards and Mair[5] employed a like procedure.

In their calculation of the heat of ionization of water, Richards and Hall were limited to the use of one series of reactions because of the lack of suitable data on heats of dilution for electrolytes other than HCl, NaOH, and NaCl. Since that time, however, additional data on the heats of dilution of electrolytes in aqueous solution have been published, which permits the use of six different series of reactions.

It is the purpose of this paper to combine the data on heats of neutralization obtained by Richards and Rowe,[6] and incidentally the data of Gillespie, Lambert, and Gibson,[7] with the values for heats of dilution recently calculated by the present author,[8] and obtain a value for the heat of ionization of water by utilizing six different series of reactions similar to the one employed by Richards and Hall.

II. THE AVAILABLE DATA

1. HEATS OF NEUTRALIZATION

A review of the data on the heats of neutralization of uni-univalent strong electrolytes indicates that the only reliable measurements—especially with regard to purity of materials, proper statement of concentrations, and recognition of the proper temperature of the reaction—are those of Richards and Rowe,[9] and some few by Gillespie, Lambert, and Gibson.[10]

[3] Richards and Hall, J. Am. Chem. Soc., **51,** p. 736; 1929.
[4] Richards and Rowe, J. Am. Chem. Soc., **44,** p. 703; 1922.
[5] Richards and Mair, J. Am. Chem. Soc., **51,** p. 739; 1929.
[6] Richards and Rowe, J. Am. Chem. Soc., **44,** p. 684; 1922.
[7] Gillespie, Lambert, and Gibson, J. Am. Chem. Soc., **52,** p. 3806; 1930.
[8] Rossini, B. S. Jour. Research, **6,** p. 791; 1931.
[9] See footnote 6.
[10] See footnote 7.

Richards and Rowe measured the heats of neutralization of HCl, HBr, HI, and HNO_3 with LiOH, NaOH, and KOH, respectively. Lack of suitable data on heats of dilution precludes the use of their data on HBr and HI in the present calculations. For each salt formed, Richards and Rowe performed 6 to 11 experiments, some having an initial temperature of about 15.5° C. and the remainder 16.5° C. The temperature rise in each experiment was about 4° C. These authors used the heat capacities of the factors in calculating the heat capacity of their calorimeter system, and, consequently, obtained the heat of the reaction at the final temperature. The heats of neutralization given by Richards and Rowe were reduced to 20° C. from the average values for the experiments having final temperatures of about 19.5° and 20.5° C., respectively. The concentration of each acid and base was 1 mole in 100 moles of H_2O, and the salt solution formed was $MX \cdot 201H_2O$.

The heats of neutralization calculated by Richards and Rowe depend directly upon the accuracy of the values chosen by them for the heat capacities of aqueous solutions of HCl, HNO_3, LiOH, NaOH, and KOH. Because of the fact that in most cases the heat capacities of aqueous solutions of acids and bases are not known as accurately as are those of the corresponding salt solutions, the present author has recalculated the heats of neutralization from the experimental data of Richards and Rowe, using the heat capacities of the formed salt solutions and thus obtaining the heat of neutralization at the initial temperature. Inasmuch as the amount of excess alkali solutions used by Richards and Rowe was only about 1/1000 of the resulting salt solution this latter can be assumed to be the pure salt solution in computing the heat capacity, without an error greater than 1 or 2 in 100,000. An example of the method of calculation employed for the data of Richards and Rowe is given in Table 1.

TABLE 1.—*Sample calculation*

Data given by Richards and Rowe for experiment No. 13:
610.22 g $HCl \cdot 100.06H_2O$ and 615.42 g $NaOH \cdot 100.19H_2O$.
Heat capacity of calorimeter = 18.98 g-cal_{18} per °C.
Initial temperature = 15.66° C.
Final temperature = 19.50° C.
Average temperature = 17.58° C.
Corrected temperature rise = 3.841° C.
Calculations by the present author:
Heat capacity of formed solution (1,225.64 g $NaCl \cdot 201H_2O$) at the average temperature, 17.58° C. = (1,225.64) (0.97908) = 1, 200.00 g-cal_{18} per °C.
Total heat capacity = 1,218.98 g-cal_{18} per °C.
Total heat evolved = (1,218.98) (3.841) = 4,682.1 g-cal_{18}.
Number of moles of HCl = 0.33180.
Heat evolved per mole of HCl = 14,111 g-cal_{18}.
This gives the heat of reaction at the initial temperature, 15.66° C.

In the case of NaCl, Richards and Rowe performed five experiments at an average initial temperature of 16.79° C. and four at an average initial temperature of 15.66° C. A value for 16.00° C. was interpolated from the two average values, and the small correction for differences in concentration was made. In like manner, the data for the other five salts were calculated. A summary of the data of Richards and Rowe for 52 experiments is given in Table 2.

The values used by the present author for the specific heats of the various salt solutions at 18° C. were computed from values for the

apparent molal heat capacities of these solutes in water at 18° C.[11] These values, given in Table 3, are slightly different from those of Richards and Rowe.[12]

TABLE 2.—*Data on heats of neutralization*

[From the data of Richards and Rowe]

Reaction	Number of experiments performed	Temperature of reaction	ΔH, heat absorbed
		° C.	$g\text{-}cal_{18}$ per mole
$HCl \cdot 100\ H_2O + LiOH \cdot 100\ H_2O = LiCl \cdot 201\ H_2O$	6	16.00	−14,173
$HCl \cdot 100\ H_2O + NaOH \cdot 100\ H_2O = NaCl \cdot 201\ H_2O$	9	16.00	−14,099
$HCl \cdot 100\ H_2O + KOH \cdot 100\ H_2O = KCl \cdot 201\ H_2O$	7	16.00	−14,189
$HNO_3 \cdot 100\ H_2O + LiOH \cdot 100\ H_2O = LiNO_3 \cdot 201\ H_2O$	10	16.00	−14,024
$HNO_3 \cdot 100\ H_2O + NaOH \cdot 100\ H_2O = NaNO_3 \cdot 201\ H_2O$	11	16.00	−14,031
$HNO_3 \cdot 100\ H_2O + KOH \cdot 100\ H_2O = KNO_3 \cdot 201\ H_2O$	9	16.00	−14,272

TABLE 3.—*Heat capacities of salt solutions at 18° C.*

Solution	Heat capacity of solution
	$g\text{-}cal_{18}\ g^{-1}\ ^\circ C.^{-1}$
$LiCl \cdot 201\ H_2O$	0.9842
$NaCl \cdot 201\ H_2O$	.9792
$KCl \cdot 201\ H_2O$	.9730
$LiNO \cdot 201\ H_2O$	.9807
$NaNO_3 \cdot 201\ H_2O$	.9760
$KNO_3 \cdot 201\ H_2O$	.9702

Gillespie, Lambert, and Gibson reported the results of eight experiments on the heat of neutralization of NaOH and HCl, and one for KOH and HCl. Their data, excluding two experiments at 50° C., are given in Table 4. The next to the last column gives the heat capacities of the salt solutions as computed from the values for the apparent molal heat capacities of these aqueous salt solutions.[11] These can be compared with the values actually used by Gillespie, Lambert, and Gibson. The last column gives the heat of neutralization for the given temperature and concentration as corrected by these new values for heat capacity.

TABLE 4.—*Data on heats of neutralization*

[From the data of Gillespie, Lambert, and Gibson]

Experiment No.	Solution formed	Temperature of reaction = initial temperature	Average temperature	Heat capacity of salt solution at average temperature	ΔH, heat absorbed	Calculations by present author	
						Heat capacity of salt solution at average temperature	ΔH, heat absorbed
		° C.	° C.	$g\text{-}cal_{20}\ g^{-1}\ ^\circ C^{-1}$	$g\text{-}cal_{20}$ per mole	$g\text{-}cal_{18}\ g^{-1}\ ^\circ C^{-1}$	$g\text{-}cal_{18}$ per mole
1	$NaCl \cdot 1080.7\ H_2O$	20.00	20.35	0.9961	−13,784	0.9954	−13,774
2	$NaCl \cdot 566.5\ H_2O$	20.00	20.68	.9924	−13,803	.9917	−13,793
3	$NaCl \cdot 1101.4\ H_2O$	24.99	25.33	.9957	−13,582	.9948	−13,570
4	$NaCl \cdot 568.8\ H_2O$	32.27	32.92	.9922	−13,211	.9909	−13,194
5	$NaCl \cdot 566.0\ H_2O$	32.27	32.95	.9922	−13,274	.9909	−13,257
6	$NaCl \cdot 520.5\ H_2O$	32.30	33.01	.9916	−13,284	.9902	−13,265
9	$KCl \cdot 547.8\ H_2O$	20.00	20.71	.9896	−13,864	.9893	−13,859

[11] Rossini, B. S. Jour. Research; 1931.

[12] Richards and Rowe, J. Am. Chem. Soc., **41**, p. 770; 1921.

2. HEATS OF DILUTION

The changes in heat content associated with reactions (4), (5), and (6) can be obtained from the values of $\Phi_h - \Phi_h^\circ$, the relative apparent molal heat content of the solute, given for aqueous solutions of HCl, HNO_3, LiOH, NaOH, KOH, LiCl, NaCl, KCl, $LiNO_3$, $NaNO_3$, and KNO_3, at 18° C., by the present author in a previous publication.[13]

For example, in reaction (4)

$$HCl \cdot \infty H_2O = HCl \cdot 100\ H_2O + (\infty - 100)\ H_2O \qquad (4)$$

$$\Delta H = \Phi_h - \Phi_h^\circ \qquad (10)$$

where Φ_h is the apparent molal heat content of HCl in the solution $HCl \cdot 100\ H_2O$, and Φ_h° is the apparent molal heat content of HCl at infinite dilution in water.

III. THE CALCULATED RESULTS

The values cited above for heats of dilution are given for 18° C.; the data of Richards and Rowe on heats of neutralization, shown in Table 2, are for 16° C.; and those of Gillespie, Lambert, and Gibson on heats of neutralization are given at temperatures of 20°, 25°, and 32.3° C. (Table 4.)

Because the changes in heat content for these reactions have large temperature coefficients, it is necessary that these latter be known accurately for the proper conversion of the various data to 18° C. Once the values for the heats of neutralization are calculated to 18° C., it becomes a relatively simple matter to sum the changes in heat content for reactions (3), (4), (5), and (6), and obtain thereby values for the change in heat content for reaction (9)

$$H^+ + OH^- = H_2O \qquad (9)$$

For reaction (3)

$$HCl \cdot 100\ H_2O + NaOH \cdot 100\ H_2O = NaCl \cdot 201\ H_2O \qquad (3)$$

the temperature coefficient of the change in heat content is given by

$$\Delta C_p = 201\ \overline{C}_{p1}^\circ + \Phi_{c(NaCl)} - (100\overline{C}_{p1}^\circ + \Phi_{c(HCl)} + 100\overline{C}_{p1}^\circ + \Phi_{c(NaOH)}) \qquad (11)$$

or

$$\Delta C_p = \overline{C}_{p1}^\circ + \Phi_{c(NaCl)} - \Phi_{c(HCl)} - \Phi_{c(NaOH)} \qquad (12)$$

where $\Phi_{c(NaCl)}$, $\Phi_{c(HCl)}$ and $\Phi_{c(NaOH)}$ are the apparent molal heat capacities of NaCl, HCl, and NaOH in their respective solutions and $\overline{C}_{p1}^\circ$ is the molal heat capacity of pure H_2O. In correcting a heat of

[13] See footnote 8, p. 848.

neutralization from $t°$ C. to 18° C., values of Φ_c for the average temperature, $\frac{t+18}{2}$ °C., are needed. For converting the data of Richards and Rowe from 16° to 18° C., values of Φ_c for 17° C. were used; and for converting the data of Gillespie, Lambert, and Gibson from 32.3°, 25°, and 20° to 18° C., values of Φ_c for 25°, 21.5°, and 19° C., respectively, were used.[14]

A comparison of the temperature coefficients given by Richards and Rowe[15] for the six different heats of neutralization with those calculated by the present author is given in Table 5.

The data of Richards and Rowe on heats of neutralization at 16° C., as given in Table 3, can now be converted to 18° C., and combined with the appropriate heats of dilution, to give values for the heat of ionization of water. The results of these calculations are summarized in Table 6.

The calculations from the data of Gillespie, Lambert, and Gibson are summarized in Table 7.

TABLE 5.—*Temperature coefficient of heat of neutralization, at 18° C.*

[For the reaction: $HX \cdot 100\ H_2O + MOH \cdot 100\ H_2O = MX \cdot 201\ H_2O$]

Solution formed	ΔC_p, in cal. mole^{-1}°C.$^{-1}$	
	Richards and Rowe	Present author
$LiCl \cdot 201\ H_2O$	55.4	42.3
$NaCl \cdot 201\ H_2O$	52.7	46.0
$KCl \cdot 201\ H_2O$	48.4	46.4
$LiNO_3 \cdot 201\ H_2O$	53.6	40.8
$NaNO_3 \cdot 201\ H_2O$	50.5	45.7
$KNO_3 \cdot 201\ H_2O$	45.1	47.3

TABLE 6.—*The heat of neutralization at infinite dilution*

[Combining data of Richards and Rowe with data on heats of dilution.]

Solution formed	$HX \cdot 100\ H_2O + MOH \cdot 100\ H_2O = MX \cdot 201\ H_2O$			Heats of dilution at 18° C., g-cal.$_{18}$ per mole			$H^+ + OH^- = H_2O$	Deviation from mean
	ΔH at 16° C. g-cal.$_{18}$ per mole	ΔC_p at 17° C. g-cal.$_{18}$ mole^{-1}° C^{-1}	ΔH at 18° C. g-cal.$_{18}$ per mole	Acid $\Phi_A - \Phi_A°$	Base $\Phi_A - \Phi_A°$	Salt $\Phi_A° - \Phi_A$	ΔH at 18°C. g-cal.$_{18}$ per mole	
$LiCl \cdot 201\ H_2O$	−14,173	42.6	−14,088	+305	+243	−174	−13,714	+7
$NaCl \cdot 201\ H_2O$	−14,099	46.3	−14,006	+305	+39	−48	−13,710	+11
$KCl \cdot 201\ H_2O$	−14,189	46.7	−14,096	+305	+137	−46	−13,700	+21
$LiNO_3 \cdot 201\ H_2O$	−14,024	41.1	−13,942	+86	+243	−132	−13,745	−24
$NaNO_3 \cdot 201\ H_2O$	−14,031	46.0	−13,939	+86	+39	+83	−13,731	−10
$KNO_3 \cdot 201\ H_2O$	−14,271	47.6	−14,176	+86	+137	+229	−13,724	−3
Mean							−13,721	±13

[14] See footnote 11, p. 850.

[15] Richards and Rowe, J. Am. Chem. Soc., **44**, p. 699; 1922.

TABLE 7.—*The heat of neutralization at infinite dilution*

[Combining data of Gillespie, Lambert, and Gibson with data on heats of dilution]

Solution formed	$HX \cdot nH_2O + MOH \cdot nH_2O = MX \cdot (2n+1)\ H_2O$				Heats of dilution at 18° C., g-cal.$_{18}$ per mole			$H^+ + OH^- = H_2O$	Deviation from mean
	The reaction temperature. ° C.	ΔH at reaction temperature. g-cal.$_{18}$ per mole	ΔC_p at $\left(\frac{t+18}{2}\right)°$ C. g-cal.$_{18}$ mole^{-1} °C.$^{-1}$	ΔH at 18° C. g-cal.$_{18}$ per mole	Acid $\Phi_A - \Phi_A°$	Base $\Phi_A - \Phi_A°$	Salt $\Phi_A° - \Phi_A$	ΔH at 18° C. g-cal.$_{18}$ per mole	
NaCl·1080.7H_2O	20.00	−13,774	52.6	−13,879	+140	+84	−59	−13,714	+4
NaCl·566.5H_2O	20.00	−13,794	50.5	−13,895	+190	+85	−63	−13,683	+35
NaCl·1101.4H_2O	24.99	−13,568	51.8	−13,931	+139	+83	−58	−13,767	−49
NaCl·568.8H_2O	32.27	−13,192	48.8	−13,890	+190	+85	−63	−13,678	+40
NaCl·566.0H_2O	32.27	−13,253	48.8	−13,951	+190	+85	−63	−13,739	−21
NaCl·521.0H_2O	32.30	−13,263	48.6	−13,958	+197	+84	−63	−13,740	−22
KCl·547.8H_2O	20.00	−13,858	50.7	−13,959	+193	+123	−60	−13,703	+15
Mean								−13,718	±27

IV. THE TEMPERATURE COEFFICIENT

The temperature coefficient of the heat of reaction (9)

$$H^+ + OH^- = H_2O \tag{9}$$

can be calculated from the values of the heat capacities of the substances involved. That is

$$\Delta C_p = \overline{C}_r{}^\circ_{(H_2O)} - \left(\overline{C}_p{}^\circ_{(H^+)} + \overline{C}_p{}^\circ_{(OH^-)}\right) \tag{13}$$

The heat capacity of H_2O is known, and the sum of the partial molal heat capacities[16] for H^+ and OH^- at infinite dilution can be determined as follows:

$\overline{C}_{p2}{}^\circ$, the partial molal heat capacity of the solute at infinite dilution, is known for NaCl, HCl, and NaOH. Now

$$\overline{C}_p{}^\circ_{(HCl)} + \overline{C}_p{}^\circ_{(NaOH)} = \overline{C}_p{}^\circ_{(H^+)} + \overline{C}_p{}^\circ_{(Cl^-)} + \overline{C}_p{}^\circ_{(Na^+)} + \overline{C}_p{}^\circ_{(OH^-)} \tag{14}$$

and

$$\overline{C}_p{}^\circ_{(NaCl)} = \overline{C}_p{}^\circ_{(Na^+)} + \overline{C}_p{}^\circ_{(Cl^-)} \tag{15}$$

Subtracting equation (15) from equation (14) gives

$$\overline{C}_p{}^\circ_{(HCl)} + \overline{C}_p{}^\circ_{(NaOH)} - \overline{C}_p{}^\circ_{(NaCl)} = \overline{C}_p{}^\circ_{(H^+)} + \overline{C}_p{}^\circ_{(OH^-)} \tag{16}$$

From the values for $\Phi°_c$ (which is equal to $\overline{C}_{p2}{}^\circ$) compiled by the present author,[17] one finds, for 18° C.,

[16] For an extended discussion of apparent and partial molal heat capacities in aqueous solution see (a) Randall and Rossini, J. Am. Chem. Soc., **51**, p. 323; 1929; and (*b*) Rossini, B. S. Jour. Research, **4**, p. 313; 1930.

[17] See footnote 11, p. 850.

$$\bar{C}_p^\circ{}_{(H^+)} + \bar{C}_p^\circ{}_{OH^-} = -39.9 \text{ g-cal. mole}^{-1} \circ C.^{-1} \quad (17)$$

And for reaction (1)

$$H_2O = H^+ + OH^- \quad (1)$$

$$\Delta C_p = -39.9 - 18.0 = -57.9 \text{ g-cal. mole}^{-1} \circ C.^{-1} \quad (18)$$

The temperature coefficient[17] of $\bar{C}_p^\circ{}_{(H^+)} + \bar{C}_p^\circ{}_{(OH^-)}$ can be taken as 0.3 g-cal. mole^{-1} °C.$^{-2}$. For any temperature t, near 18° C., the temperature coefficient of the heat change associated with reaction (1) is

$$\Delta C_p = -57.9 + 0.3(t - 18) \text{ g-cal. mole}^{-1} \circ C.^{-1} \quad (19)$$

V. DISCUSSION

The value for the change in heat content for reaction (9), as obtained from the data of Richards and Rowe on heats of neutralization, is

$$\Delta H = -13{,}721 \quad \text{g-cal.}_{18} \text{ per mole at } 18° \text{ C.} \quad (20)$$

or for the ionization reaction

$$\Delta H = 13{,}721 \quad \text{g-cal.}_{18} \text{ per mole at } 18° \text{ C.} \quad (21)$$

The average deviation of the six individual results from this value is ± 13 calories per mole.

Using the data of Gillespie, Lambert, and Gibson on heats of neutralization, one obtains for the ionization of water

$$\Delta H = 13{,}718 \quad \text{g-cal.}_{18} \text{ per mole at } 18° \text{ C.} \quad (22)$$

Here the average deviation is ±27 calories per mole. Inasmuch as the experiments of Gillespie, Lambert, and Gibson consist of 3 at 20° C., 1 at 25° C., and 3 at 32.3° C., as compared with the 52 experiments of Richards and Rowe at 16° C., the value given by equation (21) will be selected as the "best" value for the change in heat content which accompanies the ionization of water at infinite dilution. The value obtained from the Gillespie, Lambert, and Gibson data serves as an excellent verification of the selected value. The agreement also serves to establish the reliability of the heat content values[18] as well as the apparent molal heat capacity values[19] which were used to convert the data of Gillespie, Lambert, and Gibson to infinite dilution and to 18° C., respectively.

The error in the value calculated for the heat of ionization of water by the present method depends upon the accuracy of the determination of the various heats of neutralization and of the heats of dilution. The absolute accuracy of the final values for heats of neutralization calculated from the data of Richards and Rowe, using the new heat

[18] See footnote 8, p. 848.
[19] See footnote 11, p. 850.

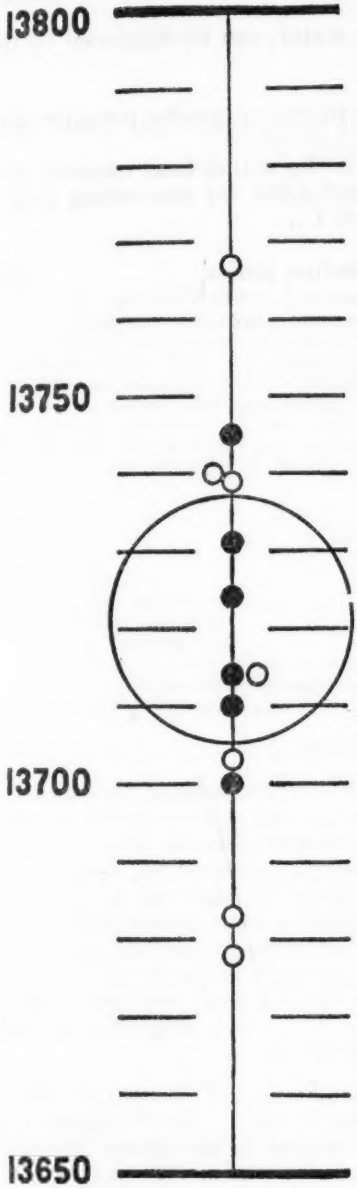

FIGURE 1.—*Plot of the data on the heat of ionization of water*

The ordinate scale, in g-cal.$_{18}$ per mole, gives the heat absorbed in the reaction, $H_2O = H^+ + OH^-$, at 18° C. and infinite dilution. The circle shows the estimated error in the selected "best" value, 13,721. The values obtained from the data of Richards and Rowe on heats of neutralization are indicated by ●; and those from the data of Gillespie, Lambert, and Gibson by ○. The latter values are from single experiments on the heat of neutralization, while the values of Richards and Rowe for heats of neutralization are each the average of 6 to 11 experimental values.

capacity values, can be placed at ±8 calories per mole. If the uncertainty in the heats of dilution for reactions (4), (5), and (6) is estimated to be in each case ±8 calories, the error in the final selected value for ΔH may be taken as $\pm\sqrt{8^2+8^2+8^2+8^2} = \pm 16$ calories per mole.

A graphical representation of the results obtained for the heat of ionization of water from the data of Richards and Rowe, and of Gillespie, Lambert, and Gibson, on heats of neutralization is shown in Figure 1.

It is interesting to note the values obtained for the heat of ionization of water by the investigators cited at the beginning of this paper.

For the ionization reaction

$$H_2O = H^+ + OH^- \qquad (1)$$

the values, converted by means of the proper temperature coefficient to 18° C., from whatever temperature they were given are:

	ΔH, at 18° C., in g-cal.$_{18}$ per mole
Noyes, Kato, and Sosman	14,070.
Richards and Rowe	Between 13,730 and 13,790.
Richards and Hall	13,760.
Richards and Mair	13,760.
This paper	13,721.

VI. CONCLUSION

By combining the data on heats of neutralization obtained by Richards and Rowe with appropriate heats of dilution, there has been found for the reaction

$$H_2O = H^+ + OH^- \qquad (1)$$

$$\Delta H = 13{,}721 \pm 16 \text{ g-cal.}_{18} \text{ per mole at } 18° \text{ C.} \qquad (23)$$

and

$$\Delta C_P = -57.9 + 0.3(t-18) \text{ g-cal.}_{18} \text{ per mole per degree} \qquad (24)$$

For the temperature range of about 10° to 35° C., the heat absorbed

in reaction (1), at infinite dilution in water, can be expressed by the equation

$$\Delta H = 13{,}721 - 57.9\ (t-18) + 0.15\ (t-18)^2 \quad \text{g-cal.}_{18} \text{ per mole} \tag{25}$$

Here t is in °C. and the unit calorie is the actual heat capacity of 1 g of water at 18° C. Using the factor 4.181 for converting g-cal.$_{18}$ to absolute joules, gives, per mole at 18° C.,

$$\Delta H = 57{,}370 \text{ absolute joules} \tag{26}$$

WASHINGTON, February 14, 1931.

FACTORS AFFECTING THE STRENGTH OF MASONRY OF HOLLOW UNITS

By Douglas E. Parsons

ABSTRACT

A study was made of the data reported in University of Illinois Bulletin No. 27 and Bureau of Standards Technologic Papers Nos. 238 and 311 in order to determine the importance of some of the factors affecting the strength of masonry of hollow units. For end-construction walls a simple empirical equation was found to express fairly well the relation between the strength of the walls and certain easily determined properties. For both end and side construction, the geometrical properties of the units appeared to have an important effect, and the strength of the units was not a close measure of the effect of their characteristics on the strength of the walls.

CONTENTS

	Page
I. Introduction	857
II. The test data	857
III. Studies of the data	860
1. General	860
2. End-construction masonry	861
3. Side-construction masonry	865
IV. Concluding remarks	866

I. INTRODUCTION

Allowable working stresses for walls of hollow units for buildings usually are the same for units having equal compressive strengths. These stresses are different with different mortars, but appear to be based upon the assumption that the compressive strength is the only property of the unit affecting the strength of walls. The strength values obtained in tests of large masonry specimens indicate strongly that there are other properties of the units which have an important effect on the strength of masonry, and it seemed worth while to study further the test data and to find, if possible, a better measure of masonry strength.

II. THE TEST DATA

The reports of Talbot and Abrams[1], Whittemore and Hathcock[2], and Stang, Parsons, and Foster[3] give the results of tests on large masonry specimens of hollow clay units in which the arrangement (bonding) of the units was similar to that used in ordinary building construction. Moreover, these reports contain rather complete data on physical tests of the materials and descriptions of the method of construction and the workmanship. A summary of the data pertaining to compressive tests under concentric loading of end-construction masonry (cells vertical) with broken joints is given in Table 1. A similar summary of the data pertaining to side-construction walls (cells horizontal) is given in Table 2.

[1] Tests of Brick Columns and Terra Cotta Block Columns, Univ. of Illinois Bul. No. 27; 1908.
[2] Some Compressive Tests of Hollow-Tile Walls, B. S. Tech. Paper No. 238, 1923.
[3] Compressive and Transverse Strength of Hollow Tile Walls, B. S. Tech. Paper No. 311; 1926.

TABLE 1.—*Compressive strength of end-construction masonry of hollow units*

Designation	Source of data	Author's specimen Nos.	Type of units and size (in inches)	Mortar mixture by volume [1]	Mortar		Estimated ratio of bearing area to gross area *b*	Compressive strength of units		Compressive strength of masonry (gross area) *M*
					Specimens	Compressive strength *m*		Gross area *u*	Net area	
						Lbs./in.²		*Lbs./in.²*	*Lbs./in.²*	*Lbs./in.²*
1	Bulletin 27	1, 2	3-cell 4 by 8.5 by 8 (thick shells).	1C:2S			0.85	3,470	4,100	2,880
2	do	3, 4	do	do			.85	3,470	4,100	3,070
3	do	5, 6	do	do			.74	3,470	4,100	2,950
4	do	8, 15	do	1C:3S	6-inch cubes	3,400	.74	5,170	6,110	4,300
5	do	12	do	do	do	3,130	.74	5,170	6,110	3,300
6	do	17	do	do	do	3,370	.74	5,170	6,110	3,050
7	do	18, 19	do	1C:5S			.74	5,170	6,110	3,350
8	Technologic Paper 238	1, 2, 3	XXX, 12 by 12 by 12	1C:1/4L:3S	2-inch cubes	2,150	.41	2,850	6,930	933
9	do	4, 5, 6	XXX, 6 by 12 by 12	do	do	2,150	.47	4,020	8,520	1,020
10	do	7, 8, 9	XXX, 8 by 12 by 12	do	do	2,150	.46	2,320	5,010	1,040
11	do	25, 26	XXX, 12 by 12 by 12	do	do	2,150	.45	1,680	3,770	930
12	do	27, 28	XXX, 6 by 12 by 12	do	do	2,150	.53	1,900	3,610	690
13	Technologic Paper 311	1–E–1	6-cell, 8 by 12 by 12	1–1/4L:3S	2 by 4-inch cylinders	85	.19	1,830	4,470	90
14	do	1–E–2	do	1C:1–1/4L:6S	do	760	.19	1,830	4,470	275
15	do	4–E–2	do	do	do	760	.23	1,270	2,740	295
16	do	6–E–2	XXX, 8 by 12 by 12	do	do	760	.34	2,100	4,260	370
17	do	2–E–2	6-cell, 12 by 12 by 12	do	do	760	.25	1,860	4,940	335
18	do	1–E–3	6-cell, 8 by 12 by 12	1C:1–1/4L:4S	do	1,190	.26	1,830	4,470	460
19	do	5–E–3	do	do	do	1,190	.28	2,840	6,470	550
20	do	6–E–3	XXX, 8 by 12 by 12	do	do	1,190	.49	2,100	4,260	650
21	do	7–E–3	do	do	do	1,190	.39	2,030	5,280	610
22	do	9–E–3	Double shell, 8 by 12 by 5	do	do	1,190	.30	3,320	6,900	555
23	do	1–E–4	6-cell, 8 by 12 by 12	1C:3S	do	1,990	.19	1,830	4,470	355

[1] C=cement, L=lime and S=sand.

TABLE 2.—*Compressive strength of side construction masonry of hollow units*

Designation	Source of data	Author's specimen Nos.	Type of unit and size (in inches)	Mortar			Compressive strength of units		Compressive strength of masonry (gross area)
				Mixture by volume [1]	Specimens	Compressive strength	Gross area	Net area	
						m	*u*		*M*
						Lbs./in.[2]	*Lbs./in.*[2]	*Lbs./in.*[2]	*Lbs./in.*[2]
24	Technologic Paper 238	10, 11, 12	XXX, 12 by 12 by 12	1C:1/4L:3S	2-inch cubes	2,150	810	3,780	375
25	do	13, 14, 15	XXX, 8 by 12 by 12	do	do	2,150	1,240	5,460	395
26	do	16, 17, 18	XXX, 6 by 12 by 12	do	do	2,150	1,665	5,930	700
27	do	29, 30	do	do	do	2,150	585	1,870	380
28	Technologic Paper 311	1-S-1	6-cell, 8 by 12 by 12	1-1/4L:3S	2 by 4 inch cylinders	85	500	2,210	165
29	do	1-S-2	do	1C:1-1/4L:6S	do	760	500	2,210	285
30	do	8-S-2	H-shaped, 8 by 10¼ by 12	do	do	760	1,040	3,350	455
31	do	2-S-2	6-cell, 12 by 12 by 12	do	do	760	580	2,620	385
32	do	1-S-3	6-cell, 8 by 12 by 12	1C:1-1/4L:4S	do	1,190	500	2,210	405
33	do	4-S-3	do	do	do	1,190	330	1,290	230
34	do	5-S-3	do	do	do	1,190	1,740	7,080	500
35	do	6-S-3	XXX, 8 by 12 by 12	do	do	1,190	430	1,500	240
36	do	10-S-3	2-cell, 8 by 5 by 12	do	do	1,190	820	3,740	335
37	do	13-S-3	3-cell, 8 by 5 by 12	do	do	1,190	900	3,540	440
38	do	14-S-3	T-shaped, 8 by 6¼ by 12	do	do	1,190	340	1,150	305
39	do	15-S-3	do	do	do	1,190	630	1,870	430
40	do	14-S-3	do	do	do	1,190	340	1,150	340
41	[2]	16-S-3	Cube, 8 by 8 by 8	do	do	1,190	780	3,060	430
42	Technologic Paper 311	1-S-4	6-cell, 8 by 12 by 12	1C:3S	do	1,990	500	2,210	360

[1] C=cement, L=lime and S=sand.

[2] Unpublished data.

No other data[4] on tests of large masonry specimens of either hollow clay or hollow concrete units with as complete information on materials and workmanship have come to my attention. Indeed, there appears to be no published information of this character on the strength of masonry of hollow concrete units.

Values of the strength of the mortar specimens are lacking in a few cases as indicated in Table 1. And the strength (2,150 lbs./in.^{2}) given for the 1C:1/4L:3S mortar at the age for testing the masonry was estimated from the values of strengths at the ages of 7 days and 6 months.

The ratios b in Table 1 of bearing area to gross area of masonry are estimates based upon the dimensions of the units and descriptions (and observations in the case of the tests reported in Bureau of Standards Technologic Paper No. 311) of the workmanship and method of laying the units.

III. STUDIES OF THE DATA

1. GENERAL

It is expected that the compressive strength M of a masonry specimen would depend chiefly on the compressive strength of the units u, the compressive strength of the mortar m, other strength properties and the elastic properties of the materials of the units and of the mortar and on the various dimensions describing the shapes and sizes of the masonry and its component parts. If these quantities are the only ones having a significant influence, the relations between them may be expressed according to the principle of dimensional homogeneity[5] by the following equation:

$$M = KuF\left(\frac{m}{u}, R_1, R_2 \cdots R_m, r_1, r_2 \cdots r_n\right) \tag{1}$$

K = an unknown numerical constant.

F = an unknown function of the dimensionless ratios within the brackets.

$R_1, R_2 \cdots R_m$ = ratios of other strength properties and of the moduli of elasticity of the materials to u.

$r_1, r_2 \cdots r_n$ = ratios of other linear dimensions of the masonry to a chosen linear dimension L, or ratios of areas to a chosen area. In any case, geometrical ratios describing the shape and size of the masonry and its component parts.

It is, of course, optional which of the strength properties or elastic moduli of the materials is chosen in the place of u, provided the R's contain all of the quantities of the same dimensions that have an influence on M. The form of the function F and the value of the constant K can be determined only from test data.

The obvious direct way to determine the form of the function F by a set of new experiments would be to vary the dimensionless ratios

[4] Data on the strength of walls 3 feet long and 3 feet high are reported by Ingberg and Foster in the paper "Fire Resistance of Hollow Load-Bearing Wall Tile," B. S. Jour. Research, 2 (RP37); 1928.

[5] Also known as the principle of similitude or when applied to mechanical problems as the law or principle of dynamic similarity. Those not already familiar with the subject will enjoy reading Dr. Edgar Buckingham's excellent presentation in the paper "Model Experiments and the Forms of Empirical Equations," Trans. Am. Soc. Mech. Engrs., 37, p. 263; 1915.

of F, one at a time, holding all the others constant. Then writing the equation (1) in the form

$$\frac{M}{u}=KF\left(\frac{m}{u}, R_1, R_2 \cdots R_m, r_1, r_2 \cdots r_n\right) \tag{1a}$$

the relation between $\frac{M}{u}$ and each of the ratios could be determined. When using the common materials for hollow walls, however, it is sometimes impracticable to vary one ratio over a wide range without affecting the values of some of the others. For example, mortars having a wide range in compressive strengths also will vary in other strength properties and in elastic properties. The present purpose, however, is to find what useful information may be derived from existing data.

It is apparent from the outset that, with so few data and so many variable factors, the form of the presumably complete equation (1) or (1a) can not be determined at present. In order to obtain useful results it becomes necessary to simplify the expression by omitting some of the ratios. In doing this it is necessary to omit none that has a large influence if the resulting equation is to be a fair approximation, and, if the results are to be useful, to include only those terms based on values that may be readily determined in practice.

2. END-CONSTRUCTION MASONRY

The test results do not provide sufficient data of the right sort to determine the manner in which the ratios (r_1, $r_2 \cdots r_n$) describing the sizes and shapes of the masonry, masonry units, and mortar joints enter into the equation. If as a first approximation one ratio were to be selected, which by itself would serve to indicate roughly the effects of all of the geometrical ratios, it seems likely that the one best suited would be the ratio b of the bearing area to the gross area of the masonry. Numerically the value of b is equal to the ratio of the total area, at the plane of a joint, of the material of the units given a bearing by the mortar, to the gross area of the masonry at the same plane. If as a further approximation all the R's are omitted, equation (1) may be written

$$M=kuf\left(\frac{m}{u}, b\right)$$

or (2)

$$\frac{M}{u}=kf\left(\frac{m}{u}, b\right)$$

where f is some unknown function of the ratios within the brackets and k is an unknown numerical constant.

By comparing the distributions of the values in Figures 1 and 2,[6] it appears that the value of b has an important effect on the strength

[6] The proportions for and the properties of the 1C:3S and the 1C:1/4L:3S mortars were so near alike that one symbol was used in the figures to represent values relating to both.

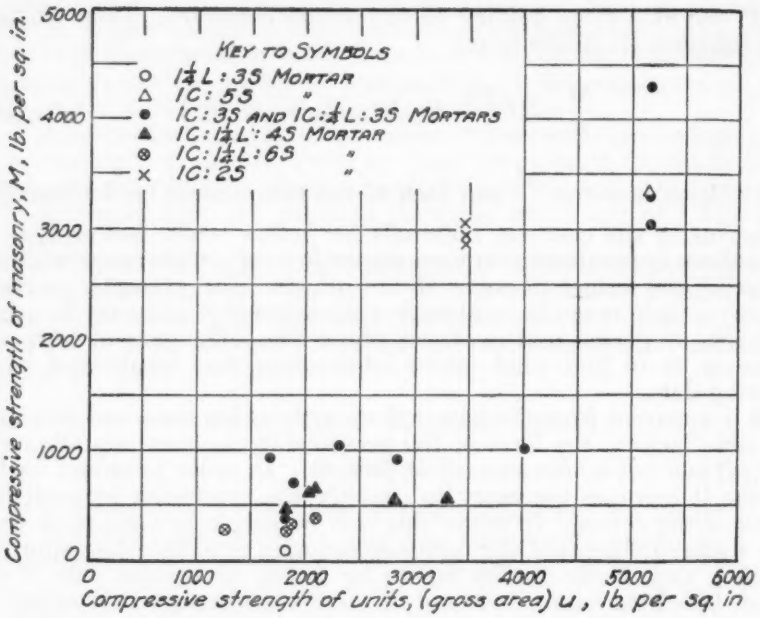

FIGURE 1.—*Relation between compressive strength (gross area) of end-construction masonry and compressive strength of units*

The proportions for the mortars are by volumes, with the abbreviations C for cement, L for lime, and S for sand.

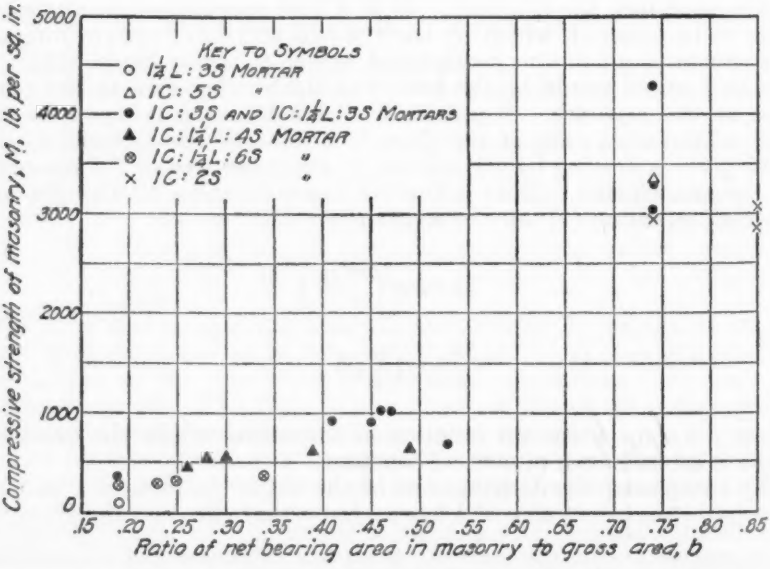

FIGURE 2.—*Relation between compressive strength (gross area) of end-construction masonry and the ratio of net bearing area in masonry to gross area*

The proportions for the mortars are by volumes, with the abbreviations C for cement, L for lime, and S for sand.

of the masonry M. Since the data are inadequate for determining the relation between $\frac{M}{u}$ and b while $\frac{m}{u}$ remains constant, all of the values are plotted in Figure 3. By considering, one at a time, the values for which $\frac{m}{u}$ varied only over a small range there seemed to be a rough relation between $\frac{M}{u}$ and b. Such meager data do not justify any refinements in the selection of a cumbersome form for representing the relationship. A linear relation probably is close enough for the purpose and on that basis the approximation becomes

$$\frac{M}{bu} = K_1 f\left(\frac{m}{u}\right) \tag{3}$$

where f is an unknown function of $\frac{m}{u}$ and K_1 is an undetermined numerical constant.

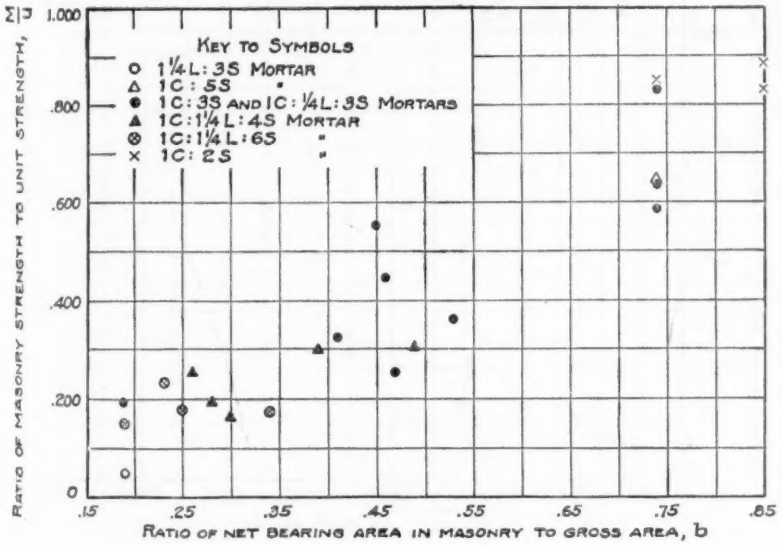

FIGURE 3.—*Relation between* $\frac{M}{u}$ *and* b, *where*

M = *compressive strength of masonry (gross area) lbs./in.*^{2}
u = *compressive strength of units (gross area) lbs./in.*^{2}
b = *ratio of bearing area in masonry to gross area*

The proportions for the mortars are by volume, with the abbreviations C for cement, L for lime, and S for sand.

Without burdening the reader further with the details of developing the approximate equation, it was found that the following relation fits the data for end construction masonry as well as any other equally simple form investigated:[7]

or
$$\frac{M}{bu} = K_1\left(\frac{m}{u}\right)^{\frac{1}{2}} \tag{4}$$
$$M = K_1 b\sqrt{mu}$$

[7] Other forms of equations were investigated, but the main point to be emphasized is the necessity for considering other factors than u and m, and this is done equally well by the more simple form (4).

The value of K_1 is approximately unity. A comparison between values of masonry strength calculated by means of equation (4) with test results is shown in Figure 4. Different empirical equations for expressing the relations between the quantities of equation (2) may be found readily, but with so many factors (quantities) left out of consideration it is useless to begin splitting hairs here.

The scattering of the plotted points of Figure 4 gives an indication of the incompleteness of equation (4). A part of the scattering may be attributed rather definitely to known causes. For example, the two values for which the ratio of test to estimated strength are lowest pertain to specimens 12 feet high and only 6 inches thick. It seems likely that the large ratio of height to thickness of the walls accounts in part for the unusually low strengths of these specimens. Of the

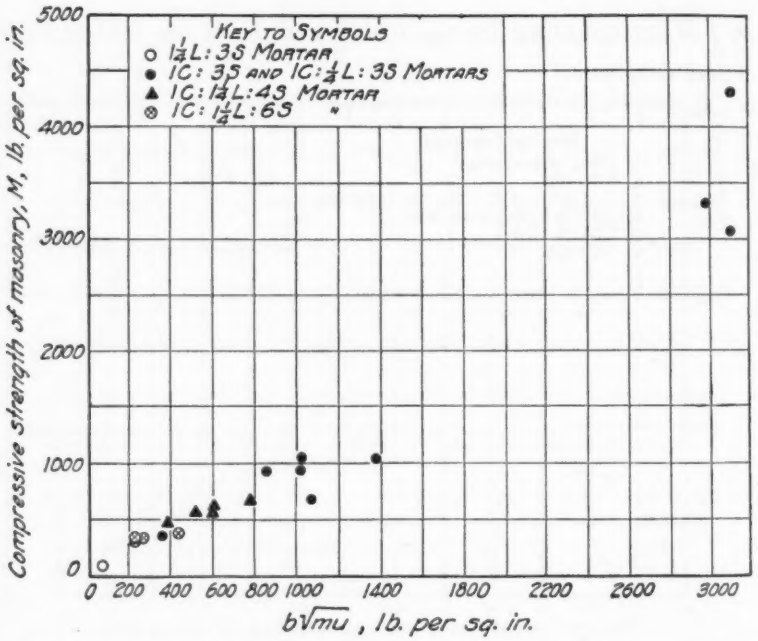

FIGURE 4.—*Relation between compressive strength (gross area) of end-construction masonry and* $b\sqrt{mu}$, *where*
b=ratio of bearing area in masonry to gross area
m=compressive strength of mortar specimens, lbs./in.²
u=compressive strength (gross area) of units, lbs./in.²

three values from the data of Talbot and Abrams, one pertains to masonry specimens built with units specially selected because of their uniformity of size and shape, another to units having warped bearing surfaces and the third to a "poorly laid" masonry specimen. Obviously, such factors as these are not taken into account by equation (4).

Among the several other possible causes of the scattering, one difficult to evaluate is that the properties of the mortar in the joints probably are different than those of the mortar specimens. Water absorbed from the mortar by the units and differences in curing conditions would be likely to affect the relations between the properties

of the joints and specimen mortars. Another possible cause for deviations is the fact that the size and shape of the mortar specimens were not the same in the three investigations. Such variables also suggest reasons why it would be quite useless to attempt a great refinement in selecting a form of equation to represent the available data.

3. SIDE-CONSTRUCTION MASONRY

The relation between the comprehensive strengths (gross area) of side-construction masonry and of the units is shown in Figure 5. Here the relation seems to be somewhat more regular than that for end construction masonry illustrated in Figure 1.

A part of the lack of regularity in the distribution of the plotted points in Figure 5 is assignable to known causes. The masonry specimens designated Nos. 33 and 35 in Table 2 were built with units

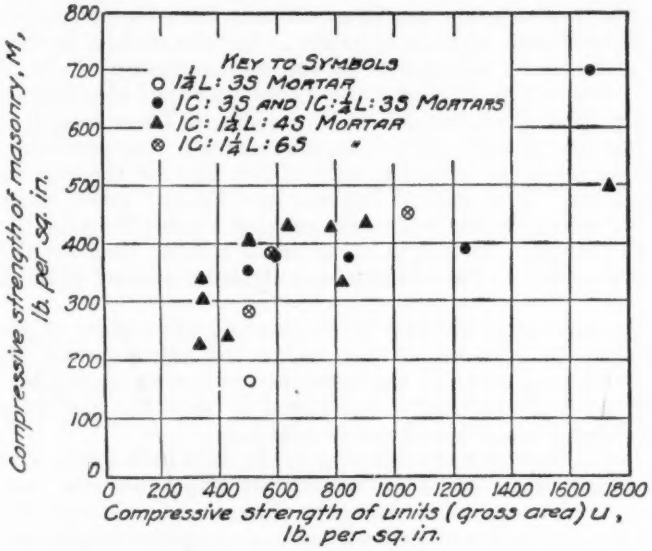

FIGURE 5.—*Relation between comprehensive strength (gross area) of side-construction masonry and compressive strength of units*

The proportions for the mortars are by volume with the abbreviations C for cement, L for lime, and S for sand.

having irregular bearing surfaces. A portion of the bearing shells near the vertical mid plane of the walls was concave toward the mortar joint. It is understood that these tiles were formed in this manner purposely in order to lessen the likelihood of there being a continuous mortar joint through walls. The recesses in the bearing shells resulted in there being a continuous bearing only for the outer shells; for ordinary tile of this design about 70 per cent of the net sectional area would be given a direct bearing.

Differences in the ratios between the thickness of the bearing (horizontal) shells and the horizontal distances between the supports provided by the vertical shells and webs probably is another major cause for the lack of a closer relationship between the variables shown in Figure 5. Comparing No. 36 with No. 37 in Table 2, it is seen that

the masonry with 3-cell tiles was stronger than that with the 2-cell units. In fact, all of those having relatively closely spaced vertical shells and webs (Nos. 30, 37, 38, 39, and 40) lie above an average line through the points of Figure 5. It has been observed [8] that in many cases the cracking of the horizontal shell in contact with the mortar was the first sign of the failure of side-construction walls in compressive tests. It seems apparent, therefore, that the bending strength of the shells is important with some unit designs.

However, the available data relating to side construction masonry are inadequate for a determination of the form of equation (1). In fact the two important factors mentioned in the preceding paragraphs can not be well evaluated at present.

For the end-construction walls account was taken of the workmanship by the ratio b, this ratio being a function of the design of the units and the proportion of the shells and webs given mortar bearing by the mason. No such simple way of evaluating the effect of workmanship in side-construction walls is apparent. It is probable, however, that there were marked differences in the workmanship of the different masons. Walls Nos. 32 and 42 of Table 2 were of identical construction except for the mortar and workmanship. The strength ($M = 405$ lbs./in.^{2}) of No. 32 with 1C:1–1/4L:4S mortar was appreciably greater than the strength ($M = 360$ lbs./in.^{2}) of No. 42 with the much stronger 1C:3S mortar. The tests of Ingberg and Foster [9] gave, on the average, higher strengths for walls with cement mortar than for those with 1C:1L:4S mortar. Hence, it is logical to assume that with the same workmanship No. 42 would have been stronger instead of weaker than No. 32.

Without having some way for evaluating the effects of workmanship, direct comparisons to determine the relations between wall strength and properties of the mortars are not easily made. About the only general statement warranted is that the use of stronger mortars usually results in stronger masonry.

In so far as the units are concerned, the data indicate that the three following properties have an important effect on the strength of masonry: (1) Compressive strength, (2) ratio of thickness of bearing shells to maximum span between vertical supports (shells and webs), and (3) features of design affecting the proportion of area given a bearing at bed joints.

IV. CONCLUDING REMARKS

Equation (4) must be considered as only a rough approximation. It is obvious that no such simple expression could be correct since it does not take account of many factors, such as the elastic properties of the materials and the size and shape of the masonry and its parts. In addition to the cause mentioned previously, the methods of testing masonry, the units and the mortar would affect the values derived from the tests and, hence, the agreement between any predicted and determined values.

In addition to the general size and shape of the masonry and the units, two other geometrical properties, namely, the thickness of the

[8] B. S. Tech. Paper No. 311, p. 339.

[9] See Table 2, B. S. Research Paper No. 37.

mortar joints and the regularity of the bearing surfaces of the units are of importance. A discussion of the effect of the latter is given by Talbot and Abrams, but the effect of neither of them has been considered here.

Nevertheless the test data indicate that properties of the units other than the compressive strength must be considered for even rough estimates of the compressive strength of masonry. The values shown in Figures 2, 3, and 4 indicate that the ratio b of the net bearing area to the gross sectional area of the masonry is an important property with end-construction masonry. For side-construction masonry it appears that the two factors (1) the ratio of thickness of bearing shells to maximum span between supports and (2) the proportion of area given a bearing, should be considered.

WASHINGTON, February 24, 1931.

DETERMINATION OF THE BENZENE AND THE NORMAL HEXANE CONTENT IN A MID-CONTINENT PETROLEUM [1]

By Johannes H. Bruun [2] and Mildred M. Hicks-Bruun

ABSTRACT

The benzene content of fractions of a mid-continent petroleum has been determined by converting the benzene to *m*-dinitrobenzene. All of the benzene was found as a constant boiling mixture with the hexanes in the fractions boiling below the boiling point of pure benzene. The large fraction boiling between 69° and 70° C. contained the greatest amount of benzene. The greatest concentration (6.5 per cent of benzene) was found in the 68° to 69° fraction. Based upon the crude petroleum the benzene content was found to be 0.08 per cent. A sample of pure benzene was isolated from its constant boiling mixture by extracting with aniline and successive equilibrium melting.

The *n*-hexane content of the crude petroleum has been estimated to be about one-third per cent. This is more than the combined amounts of the other isomers of hexane. A sample of pure *n*-hexane has been isolated by treatment with chlorosulphonic acid.

Time-temperature cooling curves, as well as the following physical constants, have been determined for the isolated hydrocarbons: Freezing point, boiling point, density, and refractive index. All of these constants agree well with those of the synthetic hydrocarbons.

The benzene-hexane ratio of a petroleum oil is the determining factor with respect to the temperature at which the benzene distills.

The boiling ranges have been accurately determined by means of a continuous boiling-point apparatus which has been placed in the distillation system between the top of the column and the condenser. The advantages of this method are discussed.

CONTENTS

	Page
I. Introduction	870
II. Experimental procedure	870
1. Distillation	870
2. Nitration of benzene	872
3. Extraction of benzene	873
4. Isolation of *n*-hexane	875
III. Discussion of the results	876
1. Benzene	876
2. *n*-Hexane	877
IV. Acknowledgment	879

[1] This paper described some of the results obtained in an investigation on the separation, identification, and determination of the chemical constituents of commercial petroleum fractions listed as project No. 6 of the American Petroleum Institute Research. Financial assistance in this work has been received from a research fund of the American Petroleum Institute donated by John D. Rockefeller. This fund is being administered by the institute with the cooperation of the central petroleum committee of the national research council.

[2] American Petroleum Institute research associate.

I. INTRODUCTION

The presence of benzene in American petroleum was established as early as 1863 by Schorlemmer[3], who found that some nitrobenzene was formed, when a fraction from Pennsylvania petroleum was boiled with nitric acid. Mabery,[4] in his pioneer work on American petroleum, found that, in the distillation of an Ohio crude oil, benzene concentrated in the fractions boiling between 75° and 86° C. The greatest concentration of benzene (15 per cent) was found in the fraction boiling between 79° and 81° C., or, in other words, around the boiling point of pure benzene (80.2° C.). Based upon the crude oil, Mabery estimated that the Ohio petroleum contained 0.017 per cent of benzene. Mabery's method consisted of nitrating the benzene to mononitrobenzene and weighing it as such. Mabery and Hudson[5] found that the bulk of the benzene from a California petroleum also collected in the fractions distilling between 79° and 81° C.

On the other hand, Young,[6] in his work on Pennsylvania petroleum, found that all of the benzene distilled over far below its normal boiling point and that it concentrated largely in the fractions boiling at about 65° to 66° C. The reason for this is that constant-boiling mixtures (with minimum boiling point) are formed between benzene and the hexanes. Young determined the benzene by nitrating it to its dinitro derivative.

The isolation of the isomers of hexane has been discussed in a previous paper.[7] In the present investigation some additional information has been obtained concerning the approximate amounts in which these isomers of hexane are present in the petroleum.

II. EXPERIMENTAL PROCEDURE

1. DISTILLATION[8]

The material for this investigation was obtained from an Oklahoma oil field. 600 gallons of crude oil from a single well[9] was subjected to a preliminary distillation in an oil refinery. The fractions thus obtained were first redistilled twice in a rectifying still[10] (20-liter capacity) with 20 bubbling-cap plates of steel.[11] The lower boiling fractions from these distillations were then subjected to a final distillation through a 30-plate rectifying column[11] of Pyrex laboratory glass. This distillation was carried out at a rate of about 2 ml per minute with a reflux ratio of about 10:1. The final distribution of the fractions with respect to their boiling range is shown by Graph I, in Figure 2.

Instead of the usual method of reading the condensation temperature at the top of the column the following method has been developed, in accordance with a suggestion by E. W. Washburn. The

[3] C. Schorlemmer, Ann., **127**, p. 311; 1863.
[4] C. F. Mabery, Proc. Am. Ac., **31**, p. 34; 1894.
[5] C. F. Mabery and E. J. Hudson, Proc. Am. Ac., **36**,, p. 259; 1901.
[6] S. Young, J. Chem. Soc., **73**, p. 914; 1898.
[7] J. H. Bruun and M. M. Hicks-Bruun, B. S. Jour. Research, **5**, pp. 933–42; 1930.
[8] The final distillation fractionation was carried out by S. T. Schicktanz and a staff of still operators.
[9] Well No. 6 of the South Ponca Field, Kay County, Okla. For properties, see E. W. Washburn, J. H. Bruun, and M. M. Hicks, B. S. Jour. Research, **2**, p. 469, Table 1; 1929.
[10] E. W. Washburn, J. H. Bruun, M. M. Hicks, B. S. Jour. Research, **2**, pp. 470–3; 1929.
[11] J. H. Bruun, Ind. Eng. Chem., Anal. ed., **1**, p. 212; 1929.

distillate, after leaving the top of the column, is allowed to pass down into a Cottrell[12] boiler as shown in Figure 1. The hot liquid from the top of the retifying column enters the boiler at *A*, and by means of an electric heating coil, *H*, in the bell, *B*, is kept boiling continuously. A mixture of vapor and boiling liquid ascends from the

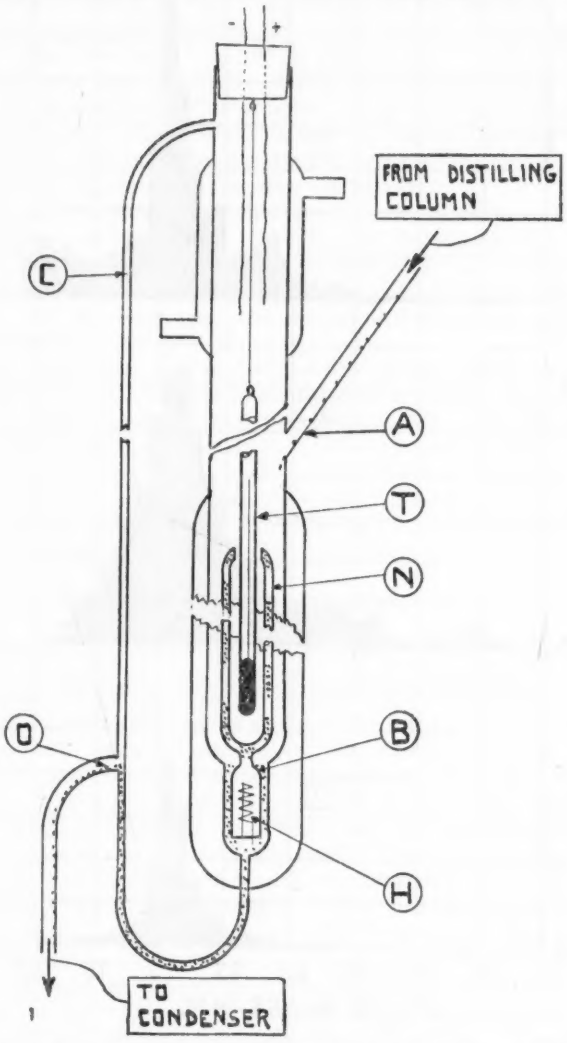

FIGURE 1.—*A continuous boiling point apparatus*

The lower part of the apparatus in Figure 1 is insulated by a vacuum jacket, as shown.

bell, *B*, through the narrow tubes, *N*, and is discharged against the thermometer, *T*. The liquid overflows continuously through *O* into the condenser and receiver unit of the still. The main advantages of this method of reading the distillation temperatures are: (1) The method gives the true boiling point rather than the "condensa-

[12] F. G. Cottrell, J. Am. Chem. Soc., **41**, p. 721; 1919

tion" point, which is the usual one obtained at the top of a rectifying column; and (2) greater precision as well as convenience in reading the thermometer, because the Cottrell boiler may be placed at any convenient level in the laboratory.

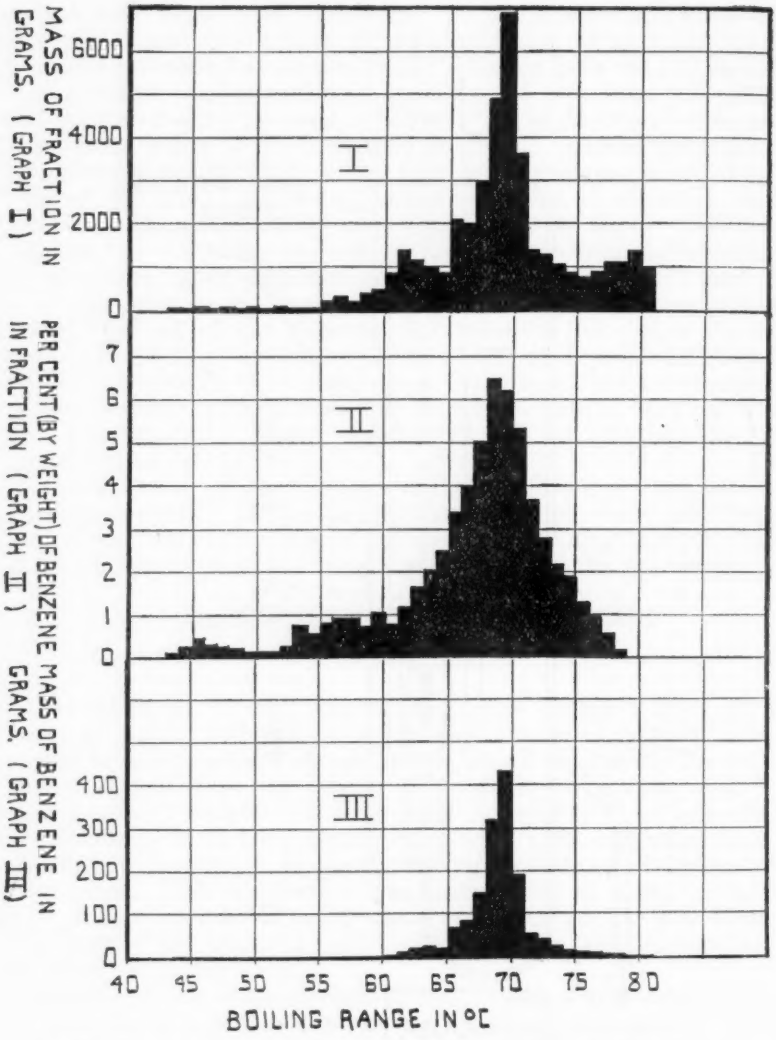

FIGURE 2.—*Mass data plotted against boiling range of fraction*

2. NITRATION OF BENZENE

As a result of the distillation, 37 one-degree cuts were obtained between 44° and 81° C., as shown in Graph I, Figure 2. The benzene in each of these cuts was then converted into *m*-dinitrobenzene by a nitrating method similar to that previously used [13] for the determin-

[13] J. H. Bruun, R. T. Leslie, S. T. Schicktanz, B. S. Jour. Research, 6, pp. 363-367; 1931.

ation of toluene. However, as it is well known that the reactivity of benzene toward nitric acid is less than that of its homologues, it was necessary to use a large excess of nitrating acid and very vigorous agitation for a long time in order to obtain quantitative conversion. During the nitration the temperature was kept below 10° C. by means of a continuous stream of tap water through the cooling bath.

Before nitration, the absence of olefine hydrocarbons was proved by testing with bromine. A check run on an unnitrated benzene-free fraction indicated that the nitrating treatment did not remove or attack the aliphatic hydrocarbons. A nitration was also carried out on a synthetic mixture of olefin and aromatic-free petroleum ether to which known amounts of benzene were added. A quantitative yield of dinitrobenzene was obtained.

Because small amounts of dinitrobenzene remain in solution in the petroleum fraction after nitration, a corresponding correction was made in calculating the benzene content. The correction was found by determining the solubility of *m*-dinitrobenzene in the fraction. This was in every case less than 0.2 g dinitrobenzene per 100 g of hydrocarbons.

After each nitration the melting point of the dried nitro product was determined. All of the melting points were close to that of *m*-dinitrobenzene and by recrystallization of the material they could easily be raised to the accepted melting point of this compound (89.7° C.).

From the weight of the nitro products the amount of benzene in each fraction was calculated. The results of the nitration are shown in Figure 2, Graphs II and III.

3. EXTRACTION OF BENZENE

From some of the fractions benzene was removed by extraction with aniline at about 0° C. This was done as illustrated in Figure 3.[14] The apparatus consists of a narrow brass box, *A*, (80 cm long 8 cm high and 4 cm wide) divided into 20 sections by means of 19 brass plates, *B*. A shaft, *C*, with 17 propellers, *D*, passes through the entire length of the apparatus. The shaft is rotated by means of a motor, *M*. The plates are provided with narrow vertical slits (not shown in the figure) to allow liquid to pass from one section into another.

The apparatus is operated on the counter-current principle, aniline entering at *F* and leaving at *G*. The hydrocarbon to be extracted enters at *H* and overflows through *I*. The two liquid layers are thoroughly mixed by the propellers (about 300 r. p. m.) so that equilibrium is established between the phases. The apparatus is covered with a glass plate, *J*, and is placed in a cooling bath as shown. A sight glass in each end of the apparatus (not shown in the figure) indicates the height of the interface between the two layers. The right-hand side of the apparatus may be lowered or raised by means of the leveling screw, *K*. This permits regulation of the overflow ratio of the two liquids. As indicated by the broken line, the hydrocarbon phase may be recirculated for futher extraction. This can be done either continuously by means of a circulation pump or intermittently by pouring.

[14] Acknowledgment is made to F. W. Rose, jr., for the drawing of Fig. 3.

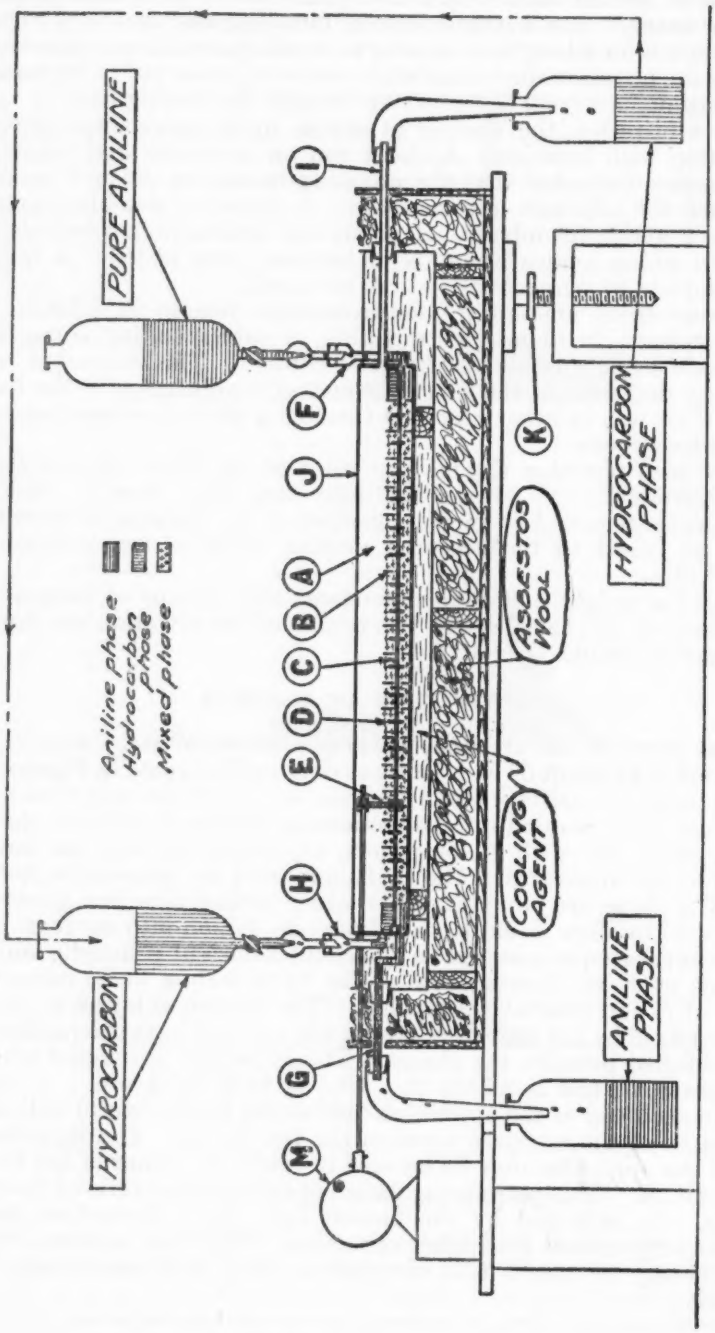

FIGURE 3.—*Apparatus for extraction with aniline*

After extraction the hydrocarbon phase is washed with hydrochloric acid and with water until it is free from aniline. The aniline phase is distilled and the first distillates, containing the extracted hydrocarbons, are freed from remaining aniline in the same way.

The extraction method was applied to the constant boiling mixture of benzene and *n*-hexane. In this experiment 1,600 ml of the 68° to 69° C. cut ($n_D^{20}=1.395$) was extracted once as described. As a result 2 fractions were obtained, 1 of 200 ml with $n_D^{20}=1.419$ and 1 about 1,300 ml of material with a refractive index $n_D^{20}=1.391$.

By subjecting the 200 ml fraction to equilibrium melting [15] a small purified sample of benzene ($n_D^{20}=1.501$) was obtained (See p. 877.)

Removal of the benzene by extraction with liquid SO_2 was also tried. The apparatus and technic developed by R. T. Leslie, of this bureau were used. A 500 ml portion of the 68° to 69° ($n_D^{20}=1.395$) cut was split up as follows: 7 ml with $n_D^{20}=1.492$, 20 ml with $n_D^{20}=1.427$, and 425 ml with $n_D^{20}=1.392$.

4. ISOLATION OF *N*-HEXANE

In order to isolate the *n*-hexane, the fraction boiling at about 69° C. was treated with chlorosulphonic acid.[16] [17] This acid reacts comparatively slowly with the normal hydrocarbons, while the isomers and cyclic compounds are attacked vigorously and destroyed. A 1,000 ml sample of the 69° to 70° C. cut was agitated with an equal volume of chlorosulphonic acid (technical) at 40° to 60° C. for about 12 hours. The acid sludge was then replaced with fresh acid and the agitation continued for another 12 hours at about 60° C. After separation from the heavier acid sludge, the hydrocarbon layer was washed in a separatory funnel with 5 per cent NaOH solution and with water finally dried over $CaCl_2$. After this treatment the material consisted of almost pure hexane which was distilled over sodium in a 10-plate column.[18] The result of this distillation is shown in Table 1.

TABLE 1.—*Distillation of n-hexane*

Fraction No.	Volume of fraction	Boiling point corrected	Refractive index n_D^{β}
	ml	°*C.*	
1	3	68.6	
2	60	68.7	1.3749
3	60	68.7	1.3751
4	60	68.7	1.3750
5	60	68.7	1.3750
6	60	68.7	1.3751
7	60	68.7	1.3752
8	70	68.7	1.3759
Residue	90		

Fractions Nos. 4 and 5 were mixed, after which the freezing behavior and the physical constants of the sample were determined. As shown later, these constants agree well with those of the best samples of synthetic *n*-hexane prepared by other investigators.

[15] M. M. Hicks, B. S. Jour. Research **2**, p. 484; 1929.
[16] O. Aschan, Ber., **31**, p. 1801; 1898.
[17] A. F. Shepherd and E. L. Henne, Ind. Eng. Chem., **22**, p. 356; 1930.
[18] See footnote 11, p. 870.

III. DISCUSSION OF THE RESULTS

1. BENZENE

Graph II in Figure 2 represents the concentration of benzene (in per cent) in the different cuts. The fraction boiling between 68° and 69° C. has the highest concentration of benzene, 6.5 per cent.

Graph III in Figure 2, representing the distribution of the benzene in the different fractions, shows that the greatest amount of benzene (433 g) is present in the large fraction boiling between 69° and 70° C. Practically all of the benzene of this petroleum is found in the fractions boiling between 65° and 75° C.

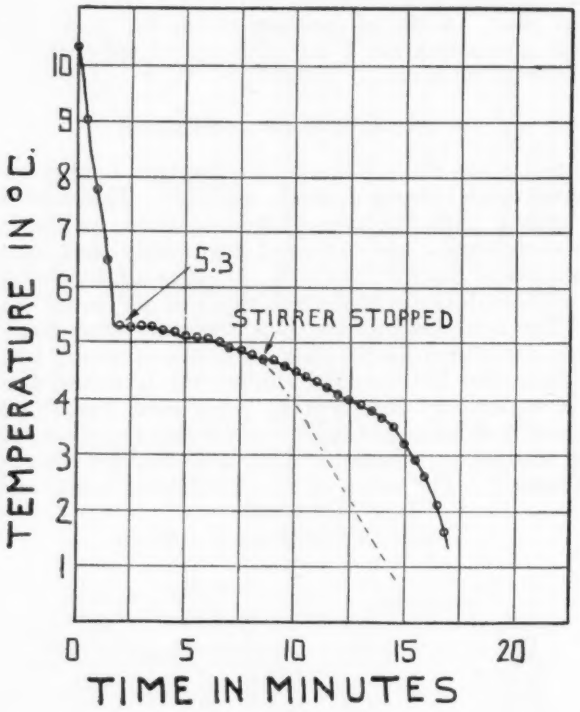

FIGURE 4.—*Freezing curve for benzene*

It is interesting to note that while the peak for Graph III (mass of benzene in fraction) is exhibited by the fraction boiling between 69° and 70° C., Graph II (concentration of benzene in the fraction) reaches its maximum for the fraction distilling between 68° and 69° C. This is to be expected in view of the fact that the fraction 69° to 70° consists mainly of *n*-hexane and the fact that the constant-boiling mixture of *n*-hexane and benzene has a minimum boiling point. Had this been a maximum boiling point, the peak of Graph II would have fallen to the right of the peak for Graph III.

Another interesting feature of Graph II is the fact that while the right branch rapidly falls toward the abscissa, the left branch falls off at first rapidly and then exhibits a rather irregular behavior. For

concentrations of benzene below 1 per cent the slope of this left side is nonuniform and only slowly approaches the abscissa. The explanation of this may be found in the fact that the isomers of *n*-hexane[19] also form constant-boiling mixtures with benzene.

A total yield of 1,530 g of benzene was obtained. Based upon the original material, 600 gallons of crude oil (specific gravity 0.9), it can be concluded that the crude oil contains not less than 0.08 per cent of benzene.

TABLE 2.—*Physical constants of benzene*

Benzene	Normal boiling point	Freezing point (in air)	Refractive index ^{20}nD	Density $^{20}d4$
	°C.	°C.		
Isolated from petroleum	80.1	5.3	1.501	0.878
Pure benzene	[1] 80.2	[1] 5.5	[2] 1.5014	[2] .878

[1] J. Timmermans and F. Martin, J. chim. phys., **23**, p. 751; 1926.
[2] Int. Crit. Tables, **1**, p. 198.

The physical constants of the purified sample of this benzene are compared with those of pure benzene in Table 2. The time-temperature freezing curve of the sample of benzene isolated is shown in Figure 4. As indicated by an arrow, the benzene froze solid after eight minutes, at which time the stirrer had to be stopped. The benzene near the thermometer bulb then cooled more slowly than that near the walls of the tube, and this caused the curve to fall gradually at first, then to drop suddenly. The dotted curve indicates the approximate slope, which would have been expected, if the stirrer could have been kept in operation. The initial freezing point of 5.3° corresponds to an estimated purity of 99.8 mole per cent.

2. *n*-HEXANE

The physical constants of the *n*-hexane isolated from petroleum are shown below.

TABLE 3.—*Physical constants of n-hexane*

n-Hexane	Boiling point 760 mm	Freezing point (in air)	Refractive index n_D^{20}	Density d_4^{20}	Aniline point
	°C.	°C.			
n-Hexane isolated from petroleum	68.7	−95.67	1.3750	0.6599	68.6
Synthetic:					
B. J. Mair [1] (99.94 mole per cent)	68.7	−95.34	1.3750		
Timmermans [2]	68.80	−95.0	1.375	.659	[3] 68.9

[1] B. J. Mair, unpublished work.
[2] J. Timmermans, J. chim. Phys., **24**, p. 411; 1928.
[3] G. Chavanne, Bull. soc. chim. Belg., **31**, p. 331; 1922.

A sensitive criterion for purity of a hydrocarbon is its behavior during freezing.[20] A comparison was made by B. J. Mair [21] between the freezing behavior of a sample of very pure synthetic *n*-hexane

[19] J. H. Bruun and M. M. Hicks-Bruun, B. S. Jour. Research, **5**, pp. 933–42; 1930.
[20] E. W. Washburn, Ind. Eng. Chem., **22**, p. 985; 1930.
[21] See footnote 1, Table 3.

prepared by him, and that of the *n*-hexane obtained by us. The comparison was made in the same apparatus, on the same day, and by using exactly the same technic in both cases. The time-temperature freezing curve of the *n*-hexane from petroleum is shown in Figure 5. The initial freezing point of the sample (−95.67° C.) is 0.33° C. lower than that of the synthetic hexane (−95.34° C.). If the value 34.8 cal./g.[22] is used as the heat of fusion of hexane, a depression of the freezing point of 0.33° C. corresponds to a purity of 98.3 mole per cent. As it is not within the scope of this project to prepare hydrocarbons of the very highest purity, further treatment with chlorosulphonic acid of the hexane sample was omitted. However, the *n*-heptane fraction [23] from petroleum, which has been treated for a longer time with chlorosulphonic acid, has freezing behavior (F. P. −90.68° C.),[24] which indicates a high degree of purity.

Graph I in Figure 2 shows that normal hexane is present to a much greater extent than any of its isomers. All of the fractions boiling

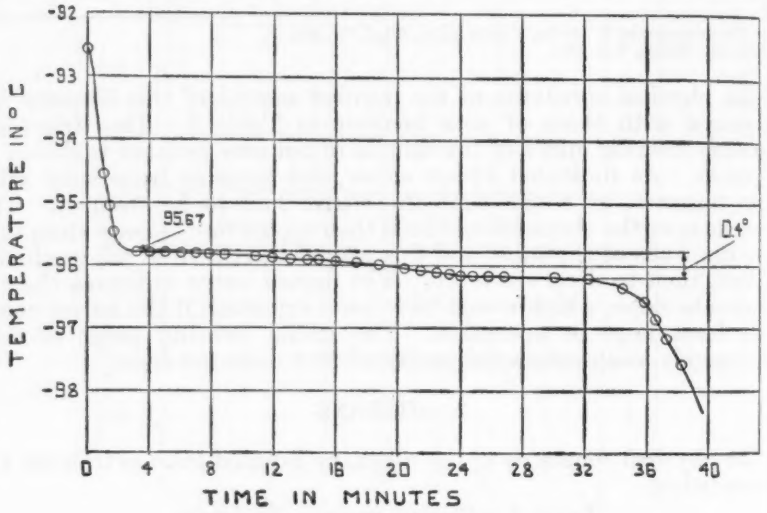

FIGURE 5.—*Freezing curve for n-hexane*

between 67° and 72° consist mainly of *n*-hexane. The minor constituents of these fractions are probably 3-methylpentane,[25] benzene,[26] and methylcyclopentane.[27] From a conservative estimate of the fractions distilling between 67° and 72° C., we may conclude that at least 10 kg of normal hexane, or one-third of 1 per cent, is present in the crude petroleum.

Graph I in Figure 2 gives us the following information as to the quantities of material distilling at the respective boiling points of the isomers of *n*-hexane:

Mass of fraction (g)	Boiling range (°C.)
900	44 to 55 (boiling point of 2.2-dimethylbutane is about 50° C.).
800	55 to 58 (boiling point of 2.3-dimethylbutane is about 58° C.).
1,900	58 to 61 (boiling point of 2-methylpentane is about 60° C.).
3,700	61 to 64 (boiling point of 3-methylpentane is about 63° C.).

[22] Parks and Todd, Ind. Eng. Chem., **21**, p. 1236; 1929.
[23] To be discussed in a later paper.
[24] See footnote 20, p. 877.
[25] See footnote 7, p. 870.
[26] See p. 873.
[27] To be discussed in a later paper.

Without further investigation these data do not justify any statement concerning the relative amounts in which the isomers of hexane are present. In a previous investigation on the same petroleum by the authors,[28] however, it was found that all the isomers of *n*-hexane (except the 2.2-dimethylbutane which was not found) were found in the fractions boiling between 54° and 75° C. Based upon this fact as well as the Graph I in Figure 2, we might draw the conclusion that the isomers of *n*-hexane are present in the following approximate quantities:

3-methylpentane 0.18 (or less) per cent of the crude oil.
2-methylpentane 0.09 (or less) per cent of the crude oil.
2.3-dimethylbutane 0.04 (or less) per cent of the crude oil.

The relation between the content of hexanes and the percentage of benzene in a given petroleum is important in that it determines the temperature at which the bulk of the benzene will distil. In the absence of the hexanes, the benzene will normally be present in the fractions which boil around 80° C. When relatively small amounts of the hexanes are present some of the benzene will distil (as a constant boiling mixture) with the hexanes below 70° C. after which the bulk of the benzene will come over at about 80° C. If the hexane-benzene ratio is large most of the benzene will be found (as an azeotropic mixture) in the distillates boiling at about 70° C.

IV. ACKNOWLEDGMENT

The authors wish to express their thanks to E. W. Washburn, chief, chemistry division, Bureau of Standards, and director of American Petroleum Institute research project No. 6, under whose direction this investigation has been conducted.

WASHINGTON, February 27, 1931.

[28] See footnote 7, p. 870.

CALORIMETRIC DETERMINATIONS OF THERMAL PROPERTIES OF METHYL ALCOHOL, ETHYL ALCOHOL, AND BENZENE

By E. F. Fiock, D. C. Ginnings, and W. B. Holton

ABSTRACT

The method and calorimetric equipment previously used in the determination of thermal properties of saturated water and steam were applied, without essential modification, in an investigation of corresponding properties of methyl alcohol, ethyl alcohol, and benzene. Precautions were taken to obtain these liquids in a very pure state. Determinations were made in the range from 40° to 110° C., yielding values of latent heats of vaporization and changes in heat content. Empirical equations fitted to these properties aid in the interpolation, extropolation, and application of the data. An estimate is made of the precision of the final results. A skeleton table of the more commonly used thermal properties of the saturated liquids and vapors has been prepared. Comparisons with the values of previous investigators are included.

CONTENTS

		Page
I.	Introduction	881
II.	Method, apparatus, and procedure	882
III.	Notation	884
IV.	Preparation and physical properties of compounds	885
	1. Methyl alcohol	885
	2. Ethyl alcohol	886
	3. Benzene	887
V.	Results of measurements	888
VI.	Discussion of accuracy	896
VII.	Comparison with previous work	896
	1. Heat capacity	896
	2. Latent heat	898
VIII.	Summary	900
IX.	Acknowledgment	900

I. INTRODUCTION

The calorimetric equipment which was designed and used at the National Bureau of Standards [1] for the measurement of thermal properties of saturated water and steam became available for a limited survey of similar properties of other liquids upon completion of the initial steam program. Reliable thermal data on methyl alcohol, ethyl alcohol, and benzene were needed to supplement calorimetric measurements on heats of combustion which are now in progress at this bureau. On account of the physical and chemical properties of these liquids, the apparatus could be used without essential modification. They can be obtained in comparatively pure form, and their purity can be estimated by rather simple physical measurements.

[1] B. S. Jour. Research, 5, p. 411; 1930.

II. METHOD, APPARATUS, AND PROCEDURE

Each of the three organic liquids already mentioned was subjected to two distinct calorimetric processes. The first of these consisted in heating a known mass of the fluid from one saturation temperature to another, observing the total energy added and the temperature rise. Such measurements yield essentially the change in heat content or enthalpy of the calorimeter and its contents over the observed temperature interval. The second process consisted in removing saturated vapor from the calorimeter at practically constant temperature. These measurements yield essentially the value of the latent heat of vaporization at the temperature of the experiments.

To obtain values of heat content and of latent heat from the measurements as they were performed, a correction is necessary to take into account the change in the ratio of the masses of liquid and vapor in the calorimeter from the beginning to the end of an experiment. This correction has been shown in the published theory of the method [2] to be the same for both types of experiment, and, where desirable, can be determined by a third type of experiment in the same apparatus. For temperatures near the normal boiling points this correction is small compared to the quantities with which it must be combined, and its value can be calculated from specific volume and vapor pressure data more accurately than it can be measured calorimetrically.

The present series of experiments was undertaken primarily for obtaining values of latent heats, but, since it is not possible to start and finish each latent-heat experiment at identically the same temperature, the heat-capacity experiments were necessary for the evaluation of end corrections. The values of heat content obtained from the present work are probably as precise as any now available, but are not as well established as would have been desirable had more time been available for this work and had there been a specific need for more precise values.

The theory of the method, the apparatus, and the procedure were essentially the same as those developed in the work on steam. The two reports to which reference has already been made are given in considerable detail, and it is deemed unnecessary to include a lengthy repetition here.

The apparatus is built to provide for accurately controlling, observing, and accounting for the amount, change in state, and change in energy of a sample of fluid. A single calorimetric equipment yields results which establish values of latent heat and changes in heat content of the saturated fluids in the range covered by the experiments. A schematic representation of the calorimeter is given in Figure 1.

A quantity of fluid, part liquid and part vapor, is contained in a metal calorimeter shell (C). The liquid is circulated rapidly over an electric heater (H) and about the interior of the shell by a small centrifugal pump (P), to distribute heat and promote close approximation to thermal equilibrium. The sample at some chosen saturation state is heated to some other chosen saturation state, or else is withdrawn as saturated vapor. Energy is added and measured electrically.

Outlets with valves provide for the introduction and withdrawal of both liquid and vapor. The line at the top (L') is for removing vapor, and is provided with a throttle valve (T) for controlling the rate of

[2] B. S. Jour. Research, 4, p. 609; 1930.

vapor flow. Following the throttle valve in this line are three other valves (*S*) for diverting the flow into any one of three receivers. These detachable receivers, suitable for weighing, are connected to the outlets to hold the samples of fluid transferred.

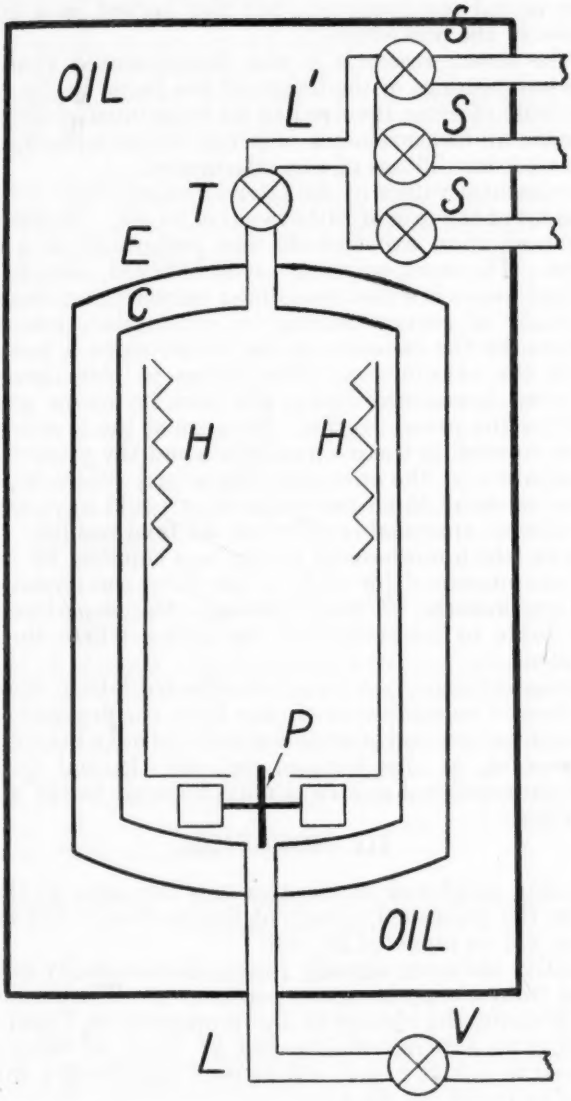

FIGURE 1.—*Schematic representation of the calorimeter*

The calorimeter is surrounded by an envelope (*E*) and the intervening space is filled with nitrogen. The envelope temperature is controlled and regulated by an oil bath which surrounds the entire apparatus.

Absolute temperatures are measured by means of a platinum resistance thermometer and small temperature differences by means of thermoelements.

In the present series of experiments the operators had the advantage of previous experience with the calorimeter. This proved useful not only in the actual manipulation, but also served as a guide in the simplification of the procedure.

During the steam research it was demonstrated that the pump energy was independent of the height of the liquid in the calorimeter, within the limit of error involved in its experimental determination. For this reason all measurements of pump energy with organic liquids were made with low fillings of the calorimeter.

The experimental values of the latent heat of water were shown to be independent of the rate of withdrawal of vapor. Hence the present series of vaporization experiments was performed at a single convenient rate. The work on steam, it is believed, demonstrates that only saturated vapor is withdrawn under normal operating conditions.

The quantity of energy passing by conduction, convection, and radiation between the calorimeter and its envelope is independent of the fluid in the calorimeter. The values of this thermal-leakage coefficient were determined during the work on steam, and were not remeasured for the present series. Because of the favorable range of temperature covered in these experiments and the greater skill which had been acquired by the operators, the actual values of the thermal leakage were so small in all cases that they could have been entirely neglected without appreciable effect on the final results.

The rate at which mechanical energy was supplied by the circulating pump was measured for each of the three compounds at several different temperatures. Curves through the experimental points made it possible to interpolate at the places where there were no determinations.

The resistance thermometer was recalibrated late in the steam program and showed no significant change from the previous calibration.

The potentiometers and electrical standards have been calibrated at frequent intervals at this bureau, and the thermal quantities are reported in international electrical units referred to the standards as maintained here.

III. NOTATION

The notation employed in this report is the same as that used by Osborne [3] in the published theory of the method. For convenience his notation will be repeated in part.

The quantity obtained directly from a heat-capacity experiment is called α and from a vaporization experiment γ. The correction which takes into account the change in the proportion of liquid and vapor masses during an experiment is called β. Each of these quantities, when referred to in this paper, will be used specifically; that is, referring always to 1 g of the fluid.

Other quantities may be defined as follows:

H = heat content or enthalpy per unit mass of saturated liquid $(\epsilon + \pi u)$.

H' = heat content or enthalpy per unit mass of saturated vapor $(\epsilon' + \pi u')$.

[3] See footnote 2, p. 882.

ϵ = internal energy per unit mass of saturated liquid.
ϵ' = internal energy per unit mass of saturated vapor.
L = latent heat of vaporization per unit mass.
θ = temperature on the international scale.
Θ = temperature on the Kelvin scale.
π = saturation vapor pressure.
u = specific volume of saturated liquid.
u' = specific volume of saturated vapor.
Q = total energy added to the calorimeter in any experiment.
Z = a constant of the calorimeter depending on its temperature and the liquid it contains.
M = total mass of fluid in the calorimeter.

As shown in the published theory, the following thermodynamic relations may be used to reduce the quantities actually observed to those more commonly employed.

$$H=\alpha+\beta \tag{1}$$
$$L=\gamma-\beta \tag{2}$$
$$\gamma=L\frac{u'}{u'-u}=\Theta u'\frac{d\pi}{d\Theta} \tag{3}$$
$$\beta=L\frac{u}{u'-u}=\Theta u\frac{d\pi}{d\Theta} \tag{4}$$
$$H'=H+L \tag{5}$$
$$Q=Z+M\alpha \tag{6}$$
$$\gamma_1=\frac{1}{\Delta M}\left\{Q-[Z+M_2\alpha]_1^2+\int_1^2(H-H_1)dM\right\} \tag{7}$$

The values of H and L were obtained from the experimental values of α and γ and the values of β calculated from other data with the aid of the second form of equation (4).

The absolute value of H can not be determined, but any arbitrary datum may be chosen within the temperature range covered by the experiments, and values of H at other temperatures in the range can be established relative to the datum. Adoption of a datum for H simultaneously fixes a reference value for α.

IV. PREPARATION AND PHYSICAL PROPERTIES OF COMPOUNDS

1. METHYL ALCOHOL

Mallinckrodt's methyl alcohol, specially ordered as chloroform free, was distilled by Dr. J. H. Bruun, of the chemistry division of this bureau, in a nonsiphoning, 30-plate, bubbling-cap still [4] to remove water and other impurities which can be separated by fractional distillation. The middle fraction of 1,000 cm^3 was used from a charge of 2,500 cm^3 which was introduced into the still pot. The distillation was performed in an atmosphere of dry carbon dioxide at approximately atmospheric pressure. The distillate was collected in a bottle filled initially with dry air and was stored in a dessicator. Provision was made for transferring the liquid without further contact with the

[4] Ind. Eng. Chem., Anal. ed., **1**, p. 212; October, 1929.

air to a second still, which could be used both for refluxing and distilling. Here the sample was freed from dissolved gases by repeated refluxing, cooling, and evacuation. After thus pumping off the dissolved gas, the sample was distilled under its own vapor pressure at a temperature of about 50° C., and collected in evacuated silver containers. From these it was transferred to the calorimeter.

The specific gravity of the gas-free product, before its use in the calorimeter, was measured by the volumetric section of this bureau. To avoid contact with the atmosphere the alcohol was introduced into an evacuated picnometer through an evacuated line. The volume of the picnometer was about 87 cm^3, and the samples used therein were always discarded. The observed specific gravity at 20° C. compared to water at 4° C. was $D_4^{20}=0.79133$. According to the International Critical Tables, vol. 3, p. 27, Klason and Norlin give as their value for absolute methyl alcohol $D_4^{20}=0.79134$.

An accurate combustion analysis of the original material was made by Dr. F. D. Rossini, of the chemistry division of this bureau. This analysis showed that the carbon-hydrogen ratio was that required by the formula CH_3OH, within the limit of error of the analysis, which was ± 0.03 per cent.

After the completion of a vaporization experiment the sample was in four containers, and had to be reassembled before being weighed into the calorimeter again. This was accomplished by transfer under its own vapor pressure through an evacuated line, without any contact with the atmosphere. Such a procedure made possible the performance of the whole series of calorimetric experiments on an original sample of about 350 g.

At one stage in the experiments with methyl alcohol a leak developed in the lower tube leading to the calorimeter. This permitted contact of a portion of the sample with the atmosphere. This portion was again freed from dissolved gas, but contained a small amount of water. For the remainder of the experiments the entire sample of alcohol was reunited, since the amount of water which could have been taken from the air was known to be small.

After the completion of the calorimetric experiments the specific gravity of the assembled sample was again measured and the value obtained was $D_4^{20}=0.79142$.

The increase in specific gravity was thus 0.00009, corresponding, if the impurity was all water, to about 0.026 per cent of water by weight. This fraction of water would produce no measurable effect on the values of α and would correspond to an increase in γ of only about 3 parts in 10,000. Since this is well within the experimental uncertainty involved, it was deemed unnecessary to repeat the experiments with another sample of alcohol.

2. ETHYL ALCOHOL

Through the courtesy of Dr. F. M. Hildebrandt, the United States Industrial Alcohol Co. furnished an especially selected sample of ethyl alcohol (192 volume proof) having a very low aldehyde content.

Most of the water present was removed by refluxing and distilling from an excess of freshly ignited lime at atmospheric pressure. About 2,500 cm^3 of alcohol, whose specific gravity indicated a water content of 0.15 per cent by weight, were prepared by this method.

This 2,500 cm³ sample, together with 40 cm³ of Timmermans' benzene, which will be described later, was introduced into a still similar to that used for fractionating the methyl alcohol.

The remainder of the water was removed from this mixture by fractional distillation. The first fraction to distil consists of a constant boiling mixture of benzene, alcohol, and water. When all the water has been removed, a constant boiling binary mixture of benzene and alcohol continues to distil as long as any benzene remains. Since the indices of refraction of benezne and alcohol are so widely different, this property was used as a criterion for the complete removal of the benzene. About 250 cm³ were rejected after the index of the distillate became constant. The next 900 cm³ which distilled were used as the best product of the fractionation.

The method of collecting the sample and of removing dissolved gases from it was the same as that described for methyl alcohol. The specific gravity of the gas-free product was found to be $D_4^{20} = 0.78946$. According to the International Critical Tables, vol. 3, p. 27, Osborne, McKelvy, and Bearce give as their best value for absolute ethyl alcohol $D_4^{20} = 0.78934$. If water was the only impurity the initial sample contained 0.038 per cent by weight. The specific gravity of the alcohol which had been used in the entire series of observations was $D_4^{20} = 0.78949$, indicating 0.047 per cent of water by weight. The effect of this quantity of water on the measured values of latent heat could not have been greater than 0.6 joule per gram, or 1 part in 1,400 of the total.

3. BENZENE

About 1,000 cm³ of benzene prepared by Timmermans and Martin[5] at the International Bureau of Physico-Chemical Standards at Brussels were refluxed for three hours with about 15 g of a 50–50 mol per cent sodium-potassium alloy. This alloy was furnished by Dr. O. C. Bridgeman, of this bureau, who had prepared it in very pure form for use in determining quantitatively the water content of gasolines.

The benzene was introduced into an apparatus which could be used both for refluxing and distilling. After it had been frozen and the permanent gas present removed by pumping, the alloy was introduced. After refluxing for a time the benzene was again frozen, and the gas evolved on boiling was pumped off. This process was repeated four times, the amount of noncondensible gas coming off the last time being practically nil.

After three hours of refluxing, during which numerous droplets of liquid alloy were in vigorous circulation within the liquid benzene, the benzene was distilled under its own vapor pressure at a temperature of about 50° C., and collected in evacuated silver containers.

The specific gravity of the air-free product was not measured before the calorimetric experiments because a sufficient quantity could not be spared. After the measurements were completed, specific gravities were measured on two samples which had been distilled from the

[5] J. chim. phys., **23**, p. 18; 1926.

calorimeter, and on the residue left in it after a series of vaporization experiments. The values of $D\,\frac{20}{4}$ obtained were 0.87906 and 0.87907 for the distillate and 0.87906 for the residue.

The recorded determinations of the specific gravity of benzene at 20° C. vary from 0.8787 to 0.8795, with those which seem more reliable averaging about 0.8790. From specific-gravity measurements alone it is difficult to estimate the purity of benzene for want of a well-established reference value.

The product used in these experiments was prepared from the source which, according to our advices, was the best available. The water content was probably reduced to well below 0.01 per cent. The presence of homologs of benezene in minute quantities would have produced no measurable effects on the thermal properties observed.

V. RESULTS OF MEASUREMENTS

In the following record of these measurements the results have been assembled in the form of tables. An explanation of the mechanism of the reduction of the quantities observed to the properties desired is given in the report on the work on steam.[6]

Three complete sets of α experiments were performed with a large mass and three with a small mass of fluid in the calorimeter. The experiments did not start and stop at exactly the even 10° temperatures so the measured values of Q were corrected to the even intervals for convenience. From curves of $\frac{\Delta Q}{\Delta \theta}$ plotted against temperature, the small corrections to the even 10° points were determined, and these corrections, applied to the measured values of Q, yielded the values of $Q]_1^2$ corrected to the even temperature intervals.

Choosing for example the interval 40° to 50°, the value of the change in α for the liquid was computed for this interval as follows. For each observed value of $Q]_{40}^{50}$ there is an observed mass M of fluid in the calorimeter system. To determine the values of the two constants Z and α in the equation.

$$Q]_{40}^{50} = Z]_{40}^{50} + M\alpha]_{40}^{50}$$

the method of least squares was employed. As an indication of the consistency of the results, the value of $Z]_{40}^{50}$ so obtained was used for the computation of the value of α indicated by each individual experiment. The tabulated values of α_m are the values obtained by the method of least squares, and the other values of α were computed for the separate determinations as just described. The results of the α experiments are shown in Table 1.

[6] See footnote 1, p. 881.

TABLE 1.—*Results of α experiments*

$$\alpha\Big]_1^2-\Big[H-L\frac{u}{u'-u}\Big]_1^2$$

Temperature interval (°C.)	Methyl alcohol		Ethyl alcohol		Benzene	
	$\alpha\Big]_1^2$	$\alpha\Big]_1^2-\alpha_m$	$\alpha\Big]_1^2$	$\alpha\Big]_1^2-\alpha_m$	$\alpha\Big]_1^2$	$\alpha\Big]_1^2-\alpha_m$
	Int. J./g	*Int. J./g*	*Int. J./g*	*Int. J./g*	*Int. J./g*	*Int. J./g*
40-50	26.075	−0.005	26.025	−0.012		
	26.075	−.005	26.030	−.007		
	26.089	.009	26.057	.020		
	26.087	.007	26.023	−.014		
	26.068	−.012	26.061	.024		
	26.084	.004	26.028	−.009		
α_m=	26.080		26.037			
50-60	26.799	−.019	26.906	−.016	18.340	0.037
	26.847	.029	26.918	−.004	18.290	−.013
	26.808	−.010	26.944	.022	18.279	−.024
	26.807	−.011	26.908	−.014	18.280	−.023
	26.816	−.002	26.920	−.002	18.319	.016
	26.829	.011	26.940	.018	18.310	.007
α_m=	26.818		26.922		18.303	
60-70	27.567	.021	27.986	.004	18.546	.010
	27.512	−.034	27.967	−.015	18.554	.000
	27.557	.011	27.992	.010	18.546	−.008
	27.520	−.026	27.990	.008	18.582	.028
	27.553	.007	27.960	−.022	18.513	−.041
	27.564	.018	27.995	.013	18.568	.014
α_m=	27.546		27.982		18.554	
70-80	28.208	−.004	29.045	.006	18.782	.014
	28.223	.011	29.033	−.006	18.764	−.004
	28.204	−.008	29.026	−.013	18.757	−.011
	28.262	.050	29.017	−.022	18.726	−.042
	28.176	−.036	29.073	.034	18.792	.024
	28.197	−.015	29.041	.002	18.785	.017
α_m=	28.212		29.039		18.768	
80-90	28.866	−.003	30.026	.005	19.012	.009
	28.874	.005	29.996	−.025	18.998	−.005
	28.868	−.001	30.042	.021	18.999	−.004
	28.892	.023	29.999	−.022	18.968	−.035
	28.854	−.015	30.058	.037	19.022	.019
	28.862	−.007	30.007	−.014	19.019	.016
α_m=	28.869		30.021		19.003	
90-100	29.704	.034	31.316	.021	19.284	.024
	29.651	−.019	31.309	.014	19.262	.002
	29.656	−.014	31.259	−.036	19.235	−.025
	29.693	.023	31.327	.032	19.295	.035
	29.667	−.003	31.288	−.007	19.239	−.021
	29.650	−.020	31.269	−.026	19.247	−.013
α_m=	29.670		31.295		19.260	
100-110	30.338	.020	32.208	−.021	19.501	.004
	30.313	−.005	32.220	−.009	19.501	.004
	30.302	−.016	32.258	.029	19.488	−.009
	30.340	.022	32.209	−.020	19.504	.007
	30.302	−.016	32.231	.002	19.490	−.067
	30.311	−.007	32.246	.017	19.496	−.001
α_m=	30.318		32.229		19.497	

Before continuing further with the reduction of the data from the heat-capacity determinations, the results of the γ experiments will be tabulated. The values of γ were calculated from equation (7), in which γ_1 is the value of γ at the initial temperature and ΔM represents the mass of vapor removed. The quantity $[Z+M_2\alpha]_1^2$ is that energy quantity involved in a change in calorimeter temperature from the initial to a different final value. The values of Z and α are available

from the results of the α experiments, and that of M_2, the mass remaining in the calorimeter at the completion of a γ experiment, is known from the weighings. The quantity $\int_1^2(H-H_1)dM$ represents the energy involved in a change in the temperature of the vapor leaving the calorimeter during an experiment. It is negligibly small under the steady temperature conditions which prevailed during the present work. It is mentioned only for consistency with the exact theory.

The results of the γ experiments are assembled in Table 2. The corrections of the observed values of γ_1 to the desired temperatures involved graphical determinations of $\frac{d\gamma}{d\theta}$. The corrections are very small because the values of θ_1 were so near to the temperatures recorded.

TABLE 2.—*Results of γ experiments*

$$\gamma=\frac{Lu'}{u'-u}$$

Methyl alcohol			Ethyl aclohol			Benzene		
Temperature (° C.)	γ	$\gamma-\gamma_m$	Temperature, (° C.)	γ	$\gamma-\gamma_m$	Temperature, (° C.)	γ	$\gamma-\gamma_m$
	Int. J./g	*Int. J./g*		*Int. J./g*	*Int. J./g*		*Int. J./g*	*Int. J./g*
	1129.2	−0.1		886.5	−0.4		415.6	−0.1
	1129.0	−.3		885.6	−1.3		415.9	.2
	1128.8	−.5		886.7	−.2		415.8	−.1
	1129.4	.1		887.7	.8	50	416.2	.3
	1129.2	−.1		887.3	.4		416.3	.4
50			50				415.9	.0
	1129.6	.3		887.5	.6			
	1129.7	.4		887.2	.3	γ_m=	415.9	
	1129.6	.3		887.0	.1			
	1129.6	.3		887.0	.1		395.0	−.2
							395.7	.5
γ_m=	1129.3		γ_m=	886.9			394.8	−.4
							395.1	−.1
	1101.6	−.9		856.8	.3		395.7	.5
	1102.2	−.3		856.0	−.5	80	395.1	−.1
	1102.2	−.3		856.5	.0		395.2	.0
	1101.5	−1.0		856.8	.3		395.4	.2
			70				394.9	−.3
	1102.2	−.3		856.4	−.1			
	1102.9	.4		856.5	.0	γ_m=	395.2	
64.7	1102.7	.2		856.6	.1			
	1102.9	.4		856.5	.0		373.1	−.1
							373.0	−.2
	1102.7	.2	γ_m=	856.5			373.2	.0
	1102.8	.3				110	373.6	.4
	1103.0	.5		820.9	−.4		373.3	.1
	1103.0	.5		820.5	−.8		373.4	.2
				821.3	.0		373.0	−.2
γ_m=	1102.5			821.8	.5			
			90			γ_m=	373.2	
	1049.2	−.3		821.5	.2			
	1048.8	−.7		821.5	.2			
	1049.4	−.1		821.9	.6			
90	1050.0	.5		821.3	.0			
	1049.9	.4						
	1048.6	−.9	γ_m=	821.3				
	1050.7	1.2						
				782.5	−.2			
γ_m=	1049.5			781.7	−1.0			
				783.2	.5			
	1001.7	.1	110	782.7	.0			
	1000.8	−.8		783.1	.4			
	1001.9	.3		783.2	.5			
	1001.2	−.4						
110			γ_m=	782.7				
	1002.1	.5						
	1000.8	−.8						
	1002.0	.4						
	1002.3	.7						
γ_m=	1001.6							

To reduce the values of α and γ to the desired quantities H and L, it is necessary to evaluate the correction term β throughout the range of the experiments. Since β is small in this range, it is believed that its values can be calculated more accurately from vapor pressure and specific volume data than they could be measured calorimetrically.

All terms in the right-hand member of the equation $\beta=\Theta u\frac{d\pi}{d\Theta}$ were evaluated for each of the substances concerned from the results of measurements made by Young.[7] Values of $\frac{d\pi}{d\Theta}$ were calculated by differentiation of his vapor pressure equations. Table 3 shows the quantities taken from the work of Young and the values of β computed therefrom at those temperatures where they are needed in the further reduction of the data.

TABLE 3.—*Calculation of values of* β

$$\beta=\Theta u\frac{d\pi}{d\Theta}$$

[1 liter-atmosphere=101.29 international joules]

Temperature		Methyl alcohol			Ethyl alcohol			Benzene		
t	Θ	$u\times10^3$	$\frac{d\pi}{d\Theta}$	β	$u\times10^3$	$\frac{d\pi}{d\Theta}$	β	$u\times10^3$	$\frac{d\pi}{d\Theta}$	β
°C.	°K.	*Liters/g*	*Atm./deg.*	*Int. J./g*	*Liters/g*	*Atm./deg.*	*Int. J./g*	*Liters/g*	*Atm./deg.*	*Int. J./g*
0	273.1	1.2345	0.00245	0.08	1.2403	0.00111	0.04	(1.1110)	(0.0020)	(0.06)
10	283.1	1.2489	.00416	.15	1.2534	.00200	.07	1.1243	.00309	.10
20	293.1	1.2637	.00677	.25	1.2669	.00344	.13	1.1380	.00469	.16
25	298.1	1.2713	.00852	.33	1.2738	.00443	.17	1.1449	.00568	.20
30	303.1	1.2790	.01061	.41	1.2808	.00570	.22	1.1520	.00688	.24
40	313.1	1.2948	.01606	.65	1.2953	.00907	.37	1.1664	.00978	.36
50	323.1	1.3111	.02353	1.00	1.3104	.01394	.59	1.1813	.01350	.52
60	333.1	1.3240	.03355	1.48	1.3261	.02073	.92	1.1967	.01814	.72
64.7	337.8	1.3362	.03917	1.77						
70	343.1	1.3405	.04651	2.14	1.3430	.02989	1.38	1.2126	.02383	.99
80	353.1	1.3600	.06302	3.03	1.3609	.04192	2.01	1.2278	.03064	1.33
90	363.1	1.3790	.08359	4.19	1.3791	.05729	2.87	1.2436	.03865	1.75
100	373.1	1.401	.1088	5.69	1.397	.07648	3.99	1.262	.04794	2.26
110	383.1	1.424	.1391	7.59	1.417	.0999	5.42	1.281	.05857	2.87
120	393.1	1.449	.1751	9.97	1.444	.1280	7.27	1.300	.07059	3.61
130	403.1	1.477	.2174	13.11	1.473	.1612	9.69	1.321	.08407	4.53

Table 4 gives the values of L computed from the mean experimental values, γ_m, by the relation $L=\gamma-\beta$.

TABLE 4.—*Computation of latent heats*

$$L=\gamma-\beta$$

Temperature t	Methyl alcohol			Ethyl alcohol			Benzene		
	γ	β	L	γ	β	L	γ	β	L
°C.	*Int. J./g*	*Int. J./g*	*Int. J./g*	*Int. J./g*	*Int. J./g*	*Int. J./g*	*Int. J./g*	*Int. J./g*	*Int. J./g*
50	1,129.3	1.0	1,128.3	886.9	0.6	886.3	415.9	0.5	415.4
64.7	1,102.5	1.8	1,100.7						
70				856.5	1.4	855.1			
80							395.2	1.8	393.9
90	1,049.5	4.2	1,045.3	821.3	2.9	818.4			
110	1,001.6	7.6	994.0	782.7	5.4	777.3	373.2	2.9	370.3

[7] Proc. Roy. Dublin Soc., 12, p. 374; 1910.

To facilitate the interpolation and extrapolation of the values of latent heat, an empirical equation expressing L as a function of θ was fitted to the observed values for each of the substances. The type chosen for these equations was the same as that which proved adequate to represent the experimental values for water. Each equation requires that the latent heat approach zero at the critical temperature θ_c at a negatively infinite rate, and that no real values exist above this temperature. Table 5 gives the values of L calculated from the equations which appear below the columns of figures.

TABLE 5.—*Formulation of latent heat values*

Temperature θ	Methyl alcohol		Ethyl alcohol		Benzene	
	Latent heat of vaporization					
	Observed	Equation	Observed	Equation	Observed	Equation
°C.	*Int. J./g*	*Int. J./g*	*Int. J./g*	*Int. J./g*	*Int. J./g*	*Int. J./g*
0	.....	[1] (1, 200. 1)	.....	(946. 0)	.....	(447. 2)
10	.....	(1, 188. 5)	.....	(936. 2)	.....	(441. 2)
20	.....	(1, 175. 4)	.....	(925. 4)	.....	(435. 0)
25	.....	(1, 168. 4)	.....	(919. 6)	.....	(431. 9)
30	.....	(1, 161. 0)	.....	(913. 5)	.....	(428. 7)
40	.....	(1, 145. 3)	.....	(900. 5)	.....	(422. 1)
50	1, 128. 3	1, 128. 2	886. 3	886. 5	415. 4	415. 4
60	.....	1, 109. 7	.....	871. 3	.....	408. 4
64. 7	1, 100. 7	1, 100. 5	.....	.....	.....	.....
70	.....	1, 089. 8	855. 1	854. 9	.....	401. 3
80	.....	1, 068. 3	.....	837. 3	393. 9	393. 9
90	1, 045. 3	1, 045. 2	818. 4	818. 5	.....	386. 3
100	.....	1, 020. 5	.....	798. 4	.....	378. 4
110	994. 0	994. 1	777. 3	777. 0	370. 3	370. 3
120	.....	(965. 9)	.....	(754. 0)	.....	(361. 9)
130	.....	(935. 7)	.....	(729. 6)	.....	(353. 2)

[1] Values in parentheses are outside the range of the experiments.

For methyl alcohol

$$L=-0.005\ (240-\theta)^2+2.60875\ (240-\theta)+219\ (240-\theta)^{1/4}$$

For ethyl alcohol

$$L=-0.004067\ (240-\theta)^2+2.198\ (240-\theta)+165.83\ (240-\theta)^{1/4}$$

For benzene

$$L=-0.00056185\ (290-\theta)^2+0.65028\ (290-\theta)+74.11\ (290-\theta)^{1/4}$$

The values of the changes in heat content as shown in Table 6 follow directly from the data of Tables 1 and 3, through the equation

$$H\Big]_1^2=\alpha\Big]_1^2+\beta\Big]_1^2.$$

TABLE 6.—*Computation of changes in heat content*

$$H\Big]_1^2=\alpha\Big]_1^2+\beta\Big]_1^2$$

Temperature θ	Methyl alcohol			Ethyl alcohol			Benzene		
	$\alpha\Big]_{40}^{\theta}$	$\beta\Big]_{40}^{\theta}$	$H\Big]_{40}^{\theta}$	$\alpha\Big]_{40}^{\theta}$	$\beta\Big]_{40}^{\theta}$	$H\Big]_{40}^{\theta}$	$\alpha\Big]_{50}^{\theta}$	$\beta\Big]_{50}^{\theta}$	$H\Big]_{50}^{\theta}$
°C.	*Int. J./g*	*Int. J./g*	*Int. J./g*	*Int. J./g*	*Int. J./g*	*Int. J./g*	*Int. J./g*	*Int. J./g*	*Int. J./g*
40	0. 00	0. 00	0. 00	0. 00	0. 00	0. 00	.....	.....	.....
50	26. 08	. 35	26. 43	26. 04	. 22	26. 26	0. 00	0. 00	0. 00
60	52. 90	. 83	53. 73	52. 96	. 55	53. 51	18. 30	. 20	18. 50
70	80. 44	1. 49	81. 93	80. 94	1. 01	81. 95	36. 86	. 47	37. 33
80	108. 66	2. 38	111. 04	109. 98	1. 64	111. 62	55. 62	. 81	56. 43
90	137. 52	3. 54	141. 06	140. 00	2. 50	142. 50	74. 63	1. 23	75. 86
100	167. 20	5. 04	172. 24	171. 30	3. 62	174. 92	93. 89	1. 74	95. 63
110	197. 51	6. 94	204. 55	203. 52	5. 05	208. 57	113. 38	2. 35	115. 73

Empirical equations in the form of power series have been fitted to these values of $H]_1^2$. These equations are shown in Table 7, together with a comparison of the experimental values with those calculated from the equations.

TABLE 7.—*Formulation of heat content values*

Temperature θ	Methyl alcohol $H]_{40}^{\theta}$		Ethyl alcohol $H]_{40}^{\theta}$		Benzene $H]_{50}^{\theta}$	
	Observed	Equation	Observed	Equation	Observed	Equation
°C.	*Int. J./g*	*Int. J./g*	*Int. J./g*	*Int. J./g*	*Int. J./g*	*Int. J./g*
40	0.00	0.00	0.00	0.00		
50	26.43	26.47	26.26	26.26	0.00	0.00
60	53.73	53.75	53.51	53.57	18.50	18.51
70	81.93	81.91	81.95	81.99	37.33	37.32
80	111.04	111.01	111.62	111.62	56.43	56.43
90	141.06	141.11	142.50	142.55	75.86	75.87
100	172.24	172.26	174.92	174.86	95.63	95.63
110	204.55	204.54	208.57	208.63	115.73	115.75

For methyl alcohol

$$H]_{\theta_1}^{\theta_2} = \left[23.529\left(\frac{\theta}{10}\right) + 0.2583\left(\frac{\theta}{10}\right)^2 + 0.010036\left(\frac{\theta}{10}\right)^3\right]_{\theta_1}^{\theta_2}$$

For ethyl alcohol

$$H]_{\theta_1}^{\theta_2} = \left[22.648\left(\frac{\theta}{10}\right) + 0.3053\left(\frac{\theta}{10}\right)^2 + 0.014233\left(\frac{\theta}{10}\right)^3\right]_{\theta_1}^{\theta_2}$$

For benzene

$$H]_{\theta_1}^{\theta_2} = \left[17.184\left(\frac{\theta}{10}\right) + 0.1008\left(\frac{\theta}{10}\right)^2 + 0.002462\left(\frac{\theta}{10}\right)^3\right]_{\theta_1}^{\theta_2}$$

From the equations for $H]_1^2$ there were obtained values of a quantity $C_\pi = \frac{dH}{d\theta}$, defined as the rate of change of the heat content with temperature under saturation conditions. Since the values of $H]_1^2$ as recorded in Table 6 were measured under such conditions, equations for C_π were obtained by differentiation of the equations already given for $H]_1^2$. The derived equations and the values of C_π calculated at several temperatures are given in Table 8.

TABLE 8.—*Computation of specific heat values*

$$C_\pi = \frac{dH}{d\theta} = C_p \text{ (approximately)}$$

Temperature θ	Methyl alcohol C_π	Ethyl alcohol C_π	Benzene C_π
°C.	*Int. J./g.* °C.	*Int. J./g.* °C.	*Int. J./g.* °C.
40	2.608	2.577	
50	2.686	2.677	1.838
60	2.771	2.785	1.866
70	2.862	2.901	1.896
80	2.959	3.027	1.927
90	3.062	3.160	1.960
100	3.171	3.302	1.994
110	3.286	3.453	2.030

For methyl alcohol

$$C_\pi = 2.3529 + 0.5166\left(\frac{\theta}{10}\right) + 0.003011\left(\frac{\theta}{10}\right)^2$$

For ethyl alcohol

$$C_\pi = 2.2643 + 0.06108\left(\frac{\theta}{10}\right) + 0.004270\left(\frac{\theta}{10}\right)^2$$

For benzene

$$C_\pi = 1.7184 + 0.02016\left(\frac{\theta}{10}\right) + 0.0007386\left(\frac{\theta}{10}\right)^2$$

From specific volume and thermal expansion data it is possible to transform the values of changes in heat content under saturation conditions to values of the changes under a constant pressure of 1 atmosphere. Such transformations have been made and equations for $H]_1^2$ at $p=1$ atmosphere have been fitted.

From these it is possible to get derived equations for $C_p=\left(\frac{\partial H}{\partial \theta}\right)_{p=1\text{ atm.}}$ defined as the rate of change of heat content with temperature under a constant pressure of 1 atmosphere. Values of C_p were calculated for each of the three liquids at temperatures below the normal boiling points. A comparison of these values of C_p with the recorded values of C_π showed that the difference between the two was less than 1 part in 500 at every temperature. Since this difference is believed to be within the error involved in deriving values of specific heat from measured values of α, the recorded values of C_π are not sensibly different from the values of C_p as indicated by these experiments.

The specific volumes of the saturated vapors can be calculated from the relation $\gamma=\Theta u'\frac{d\pi}{d\Theta}$ to the degree of precision of our knowledge of $\frac{d\pi}{d\Theta}$. The values of u' thus computed are shown in Table 9. The values of $\frac{d\pi}{d\Theta}$ are calculated from Young's vapor pressure equations and the values of γ result from the present investigation.

TABLE 9.—*Computation of specific volumes*

$$u'=\frac{\gamma}{\Theta\frac{d\pi}{d\Theta}}$$

Temperature		Methyl alchohol			Ethyl alcohol			Benzene		
θ	Θ	γ	$\frac{d\pi}{d\Theta}$	u'	γ	$\frac{d\pi}{d\Theta}$	u'	γ	$\frac{d\pi}{d\Theta}$	u'
°C.	°K.	*L.-atm./g*	*Atm./deg*	*L./g*	*L.-atm./g*	*Atm./deg*	*L./g*	*L.-atm./g*	*Atm./deg.*	*L./g*
0	273.1	11.85	0.00245	17.71	9.340	0.00111	30.81	4.416	(0.0020)	8.085
10	283.1	11.74	.00416	9.97	9.243	.00200	16.32	4.356	.00309	4.980
20	293.1	11.61	.00677	5.851	9.137	.00344	9.062	4.298	.00469	3.127
25	298.1	11.54	.00852	4.544	9.081	.00443	6.877	4.266	.00586	2.442
30	303.1	11.47	.01061	3.567	9.020	.00570	5.221	4.235	.00688	2.031
40	313.1	11.31	.01606	2.249	8.894	.00907	3.132	4.171	.00978	1.362
50	323.1	11.14	.02353	1.465	8.757	.01394	1.944	4.106	.01350	.9413
60	333.1	10.97	.03355	.9816	8.611	.02073	1.247	4.039	.01814	.6684
70	343.1	10.78	.04651	.6755	8.454	.02989	.8244	3.971	.02383	.4857
80	353.1	10.58	.06302	.4755	8.287	.04192	.5599	3.902	.03064	.3607
90	363.1	10.36	.08359	.3413	8.110	.05729	.3899	3.831	.03865	.2730
100	373.1	10.13	.1088	.2495	7.922	.07648	.2776	3.759	.04794	.2102
110	383.1	9.89	.1391	.1856	7.727	.0999	.2019	3.684	.05857	.1642
120	393.1	9.64	.1751	.1401	7.517	.1280	.1494	3.608	.07059	.1300
130	403.1	9.37	.2174	.1069	7.299	.1612	.1123	3.542	.08407	.1045

Table 10 has been prepared to summarize the thermal properties of these three saturated fluids. The values of π are from the data of Young. The values of u at temperatures below the normal boiling points are from density determinations as recorded in the International Critical Tables, volume 3, pages 27 to 30. Values of u above the boiling points are those determined by Young. The values of u' are computed as shown in Table 9. The results of the present

investigation are extrapolated down to 0° C. and up to 130° C. The value of H has been arbitrarily chosen as 0° at 0° C. for each liquid. For the benzene which freezes at about 5° above this temperature the datum $H=0$ is for the undercooled liquid. The heat of fusion is therefore not included in the tabulated values.

It is hoped that this table may prove useful as a working table for those who are concerned with the thermal properties of any one of these saturated fluids.

TABLE 10.—*Thermal properties of methyl alcohol, ethyl alcohol, and benzene at saturation*

METHYL ALCOHOL

Temperature θ	Vapor pressure π	Specific volume		Heat content Liquid H	Latent heat L	Heat content Vapor H'
		Liquid $u\times10^3$	Vapor u'			
°C.	*Atmospheres*	*Liters/g*	*Liters/g*	*Int. J./g*	*Int. J./g*	*Int. J./g*
0	0.0389	1.234	17.71	0.0	1,200.1	1,200.1
10	.0713	1.249	9.97	23.80	1,188.5	1,212.3
20	.1251	1.264	5.851	48.17	1,175.4	1,223.6
25	.1632	1.271	4.544	60.59	1,168.4	1,229.0
30	.2109	1.279	3.567	73.18	1,161.0	1,234.2
40	.3427	1.295	2.249	98.89	1,145.3	1,244.2
50	.5388	1.311	1.465	125.4	1,128.2	1,253.6
60	.8255	1.324	.9816	152.6	1,109.7	1,262.3
70	1.219	1.340	.6755	180.8	1,089.8	1,270.6
80	1.764	1.360	.4755	209.9	1,068.3	1,278.2
90	2.493	1.379	.3413	240.0	1,045.2	1,285.2
100	3.451	1.401	.2495	271.2	1,020.5	1,291.7
110	4.686	1.424	.1856	303.4	994.1	1,297.5
120	6.252	1.449	.1401	336.9	965.9	1,302.8
130	8.209	1.477	.1069	371.6	935.7	1,307.3

ETHYL ALCOHOL

0	0.0162	1.240	30.81	0.0	946.0	946.0
10	.0312	1.253	16.32	22.97	936.2	959.2
20	.0579	1.267	9.062	46.63	925.4	972.0
25	.0771	1.274	6.877	58.75	919.6	978.4
30	.1028	1.281	5.221	71.08	913.5	984.6
40	.1756	1.295	3.132	96.39	900.5	996.9
50	.2892	1.310	1.944	122.7	886.5	1,009.2
60	.4608	1.326	1.247	150.0	871.3	1,021.3
70	.7117	1.343	.8244	178.4	854.9	1,033.3
80	1.068	1.361	.5599	208.0	837.3	1,045.3
90	1.561	1.379	.3899	239.9	818.5	1,058.4
100	2.227	1.397	.2776	271.2	798.4	1,069.6
110	3.105	1.417	.2019	305.0	777.0	1,082.0
120	4.241	1.444	.1494	340.3	754.0	1,094.3
130	5.682	1.473	.1123	377.3	729.6	1,106.9

BENZENE

0	0.0349	1.111	8.805	0.0	447.2	447.2
10	.0598	1.124	4.980	17.29	441.2	458.5
20	.0982	1.138	3.127	34.79	435.0	469.8
25	.1235	1.145	2.442	43.59	431.9	475.5
30	.1556	1.152	2.031	52.52	428.7	481.2
40	.2383	1.166	1.362	70.51	422.1	492.6
50	.3539	1.181	.9413	88.75	415.4	504.2
60	.5113	1.197	.6684	107.3	408.4	508.6
70	.7203	1.213	.4857	126.1	401.3	527.4
80	.9916	1.228	.3607	145.2	393.9	539.1
90	1.337	1.244	.2730	164.6	386.3	550.9
100	1.769	1.262	.2102	184.4	378.4	562.8
110	2.300	1.281	.1642	204.5	370.3	574.8
120	2.945	1.300	.1300	225.0	361.9	586.9
130	3.717	1.321	.1045	245.8	353.2	599.0

VI. DISCUSSION OF ACCURACY

An estimate of the accuracy of the tabulated values of H and L within the range of the experiments has been made on a basis similar to that outlined in the report on the properties of steam. The systematic errors in calorimetry are believed to be essentially the same in both sets of experiments.

By a study of the factors which enter into the measurements, a figure was assigned to each which represents an estimate of the outstanding systematic error, after all known corrections have been applied. In addition to these, corresponding figures were deduced which represent the error in both the α and the γ due to accidental errors in the measurements. An estimate was also made of the probable error in the calculated values of β. The density determinations furnish a basis for estimating the error which may be present on account of impurities in the liquids investigated.

These estimates were combined to obtain a value for the uncertainty in the final tabulated results. On this basis it is believed that more precise determinations on compounds of a higher degree of purity would yield values of H and L differing by less than 1 part per 1,000 from those of the present investigation in the range from 40° to 110° C.

VII. COMPARISON WITH PREVIOUS WORK

1. HEAT CAPACITY

The results of calorimetric determinations of heat capacity have usually been recorded in terms of specific heats. For comparison of the present results with those of other observers the calculated values of specific heats can be compared directly, or, where equations are available, the values of changes in heat content can be calculated from integrated specific heat equations. The latter method would have been followed if the termperature ranges of the various experiments had overlapped sufficiently. However, the earlier work is confined to the range well below the normal boiling points, and hence covers regions in general, below that of the present investigation.

The values of specific heat indicated by the present work have been extrapolated down to 20° C. for purposes of comparison. The extrapolated values of this derived quantity involve considerable uncertainties and should not be given a great deal of weight in the selection of the best values below 40° C. A graphical comparison of previously published values of specific heats with those of the present work is given in Figure 2. This summary includes the experimental results of Bose,[8] Kelley,[9] Williams, and Daniels,[10] Forch,[11] Mills and MacRae,[12] Dejardin,[13] Tréhin,[14] and Andrews, Lynn, and Johnston.[15]

[8] Z. phys. Chem., **58**, p. 585; 1907.
[9] J. Am. Chem. Soc., **51**, p. 180; 1929; and **51**, p. 779; 1929.
[10] J. Am. Chem. Soc., **46**, p. 903; 1924.
[11] Annalen der Physik, **317**, p. 202; 1903.
[12] J. phys. Chem., **14**, p. 797; 1910.
[13] Annales de Physique, **11**, p. 253; 1919.
[14] Annales de Physique, **15**, p. 246; 1921.
[15] J. Am. Chem. Soc., **48**, p. 1274; 1926.

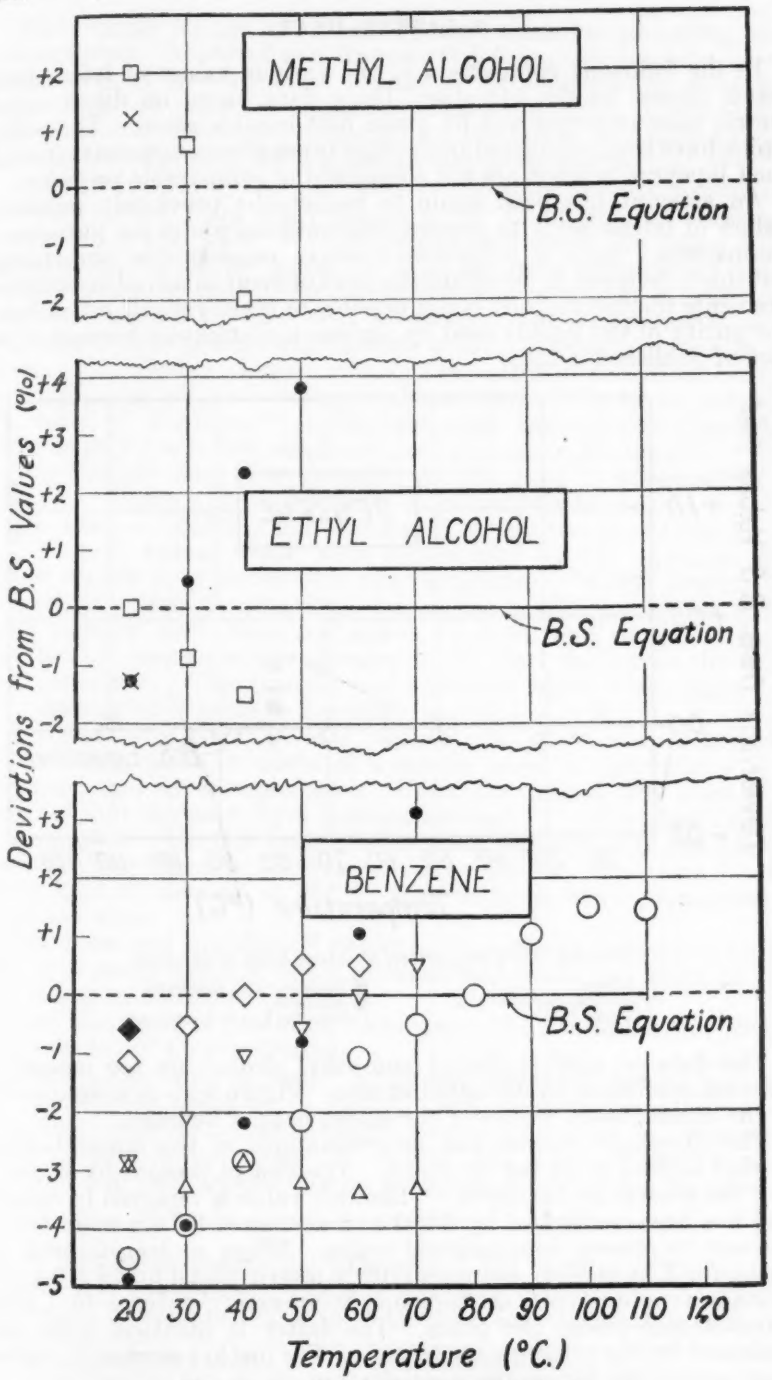

FIGURE 2.—*Comparison of specific heats*

□ Bose.
× Kelley.
● Williams and Daniels.
◆ Forch.
△ Mills and MacRea.
◇ Dejardin.
▽ Tréhin.
○ Andrews, Lynn, and Johnston.

2. LATENT HEAT

In the following comparison of the various values of latent heats which appear in the literature, those data based on direct calorimetric measurements will be given first consideration. The values which have been calculated from other types of measurements through the Clapeyron relation are not considered of comparable precision.

An attempt has been made to reduce the previously published values of latent heats to present international joules for purposes of comparison. Such a reduction involves considerable uncertainty, but this is believed to be within the limit of error involved in the measurements themselves. It is not possible to make reliable estimates of the purity of the liquids used by various investigators because of the lack of published details.

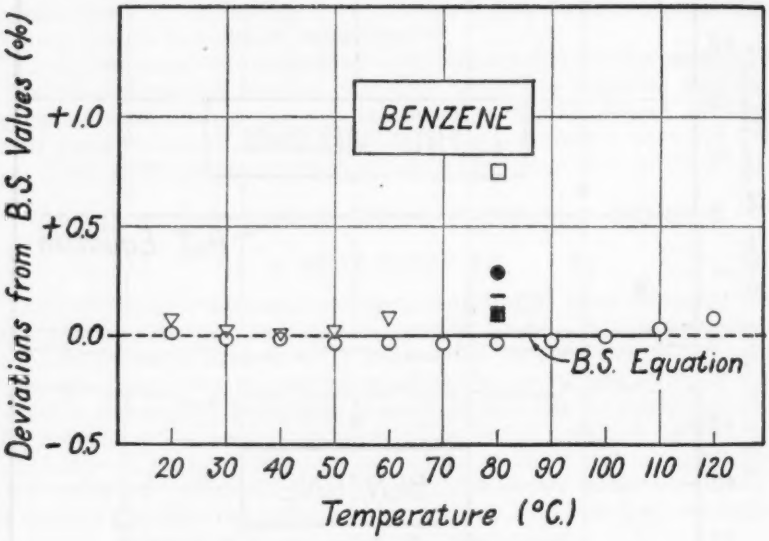

FIGURE 3.—*Comparison of latent heats of benzene*

□ Brown.
▽ Griffiths and Marshall.
– Tyrer.
■ Nagornow and Rotinjanz.
● Mathews.
○ Sutcliffe, Lay and Prichard.

The data on methyl alcohol and ethyl alcohol are too meager to warrant exhibition on deviation charts. Figure 3 gives a comparison of the experimental values of the latent heat of benzene.

The literature records two determinations of the latent heat of methyl alcohol at its boiling point. The first of these is by Brown [16] and the second by Mathews.[17] Brown's value is reported in calories and has been multiplied by 4.199 and decreased by 1 part in 512 to convert to present international joules. When so transformed, his value for L at 64.7° C. becomes 1,101.6 international joules per gram. Mathews' value for L at the same temperature reduces to 1,100.5 international joules per gram. The latter is identical with that indicated by the present experiments. For methyl alcohol the agreement among the few results is satisfactory.

[16] J. Chem. Soc., 83, p. 987; 1903.

[17] J. Am. Chem. Soc., 48, p. 562; 1926.

Three values for the latent heat of ethyl alcohol at its boiling point are recorded. Marshall and Ramsay [18] determined the ratio of the latent heat of absolute ethyl alcohol at its boiling point to that of benzene at the same temperature. This ratio, 2.293, together with the value of Griffiths and Marshall for the latter, indicates a latent heat for the alcohol of 902.7 international joules per gram at 80° C.

A determination by Brown,[19] when transformed as already described gives a value of L for ethyl alcohol at 80° C. of 903.5 international joules per gram. The work of Mathews [20] gives the value 840.3 international joules per gram for L at the same temperature. The density which he records for his sample indicates that it may have contained nearly 0.2 per cent of water. The comparative value indicated by the present experiments is 837.3 international joules per gram. The alcohol samples which gave values of the latent heat of over 900 joules per gram were probably not dry. The agreement with the value of Mathews is moderately good, the difference probably being largely due to the small amount of water in his sample.

Considerable data are available on the heat of vaporization of benzene. These will be discussed in chronological order.

The work of Griffiths and Marshall [21] at temperatures from 20° to 50° C. gave values which were represented by the equation $L = 107.05 - 0.158\ \theta$, in terms of a calorie defined as 4.199 joules. To convert to present international joules, the coefficients of the right-hand member have been multiplied by 4.199 and decreased by 1 part in 512, because of the changes in electrical units since the work was performed. The transformed equation which gives values of L in international joules is $L = 448.6 - 0.66\ \theta$.

The work of Tyrer [22] gives a value of the latent heat of benzene at its boiling point in terms of a calorie based on indications of a voltmeter and silver voltameter. From the date of this work it is assumed that the units were those established by international agreement in 1910. On this basis the electrical equivalent of the calorie used by Tyrer becomes 4.188 international joules. His value for the latent heat of benzene at 80° C. then becomes 394.8 international joules per gram.

Nagornow and Rotinjanz [23] report a group of determinations which yielded a mean value of 393.4 international joules per gram as the latent heat of benzene at 80° C.

From the work of Mathews [24] the value 395.1 international joules per gram at 80° C. is indicated.

Sutcliffe, Lay and Prichard [25] determined the latent heat of benzene from its boiling point up to 152° C., and by combining their data with those of Griffiths and Marshall, fitted an equation to the experimental values in the range 20° to 150° C. Transformed to yield values of L in international joules per gram, this equation becomes

$$L = 447.72 - 0.6163\theta - 6.141 \times 10^{-4}\theta^2 - 1.509 \times 10^{-6}\theta^3$$

The agreement among the values of L for benzene in the entire range is very gratifying. The equation of Sutcliffe, Lay, and Prichard, which represents the data of Griffiths and Marshall as well as

[18] Phil. Mag., **41**, p. 38; 1896.
[19] J. Chem. Soc., **87**, p. 265; 1905.
[20] See footnote 17, p. 898.
[21] Phil. Mag. **41**, p. 1; 1896.
[22] J. Chem. Soc., **99**, p. 1633; 1911.
[23] Z. phys. Chem., **77**, p. 700; 1911.
[24] See footnote 17, p. 898.
[25] Proc. Roy. Soc. London, **115**, p. 88; 1927.

their own, yields values which are everywhere in agreement with those calculated from our equation, within the limit of our own experimental error.

For all three of the fluids the values of L derived from the present measurements differ from those caluclated from the data of Young with the aid of the Clapeyron relation by approximately 1 part in 50 at the boiling points and 1 part in 100 at 110° C.

VIII. SUMMARY

Thermal properties of methyl alcohol, ethyl alcohol, and benzene were investigated in the temperature range 40° to 110° C. Determinations were made of the latent heats of vaporization and the changes in heat content of the saturated fluids in this range. The results have been assembled in the form of tables and empirical equations have been fitted to the experimental values to aid in the application of the data. A working table of the thermal properties of these three fluids at saturation conditions has been prepared from the present and previously published data.

IX. ACKNOWLEDGMENT

The authors wish to extend their thanks to N. S. Osborne and H. F. Stimson, of this laboratory, as well as to all others who have aided in the project.

WASHINGTON, March 10, 1931.

CHARACTERISTICS OF AIRPLANE ANTENNAS FOR RADIO RANGE-BEACON RECEPTION

By H. Diamond and G. L. Davies

ABSTRACT

This paper gives the results of an investigation on the characteristics of airplane receiving antennas to determine whether an antenna arrangement could be devised which would have all the desirable electrical properties of the vertical pole antenna and yet be free from the mechanical difficulties encountered in the use of the pole antenna. The antennas studied include the inclined antenna with both forward and backward inclination, the horizontal dipole antenna, the horizontal L antenna, the horizontal V antenna, the inclined V antenna, the symmetrical transverse T antenna, and the symmetrical longitudinal T antenna. A theoretical treatment is given which enables the voltage induced by a radio range beacon transmitting station to be calculated for any receiving antenna in space. This theoretical analysis is used to determine the received voltage, course error, and localizing effect for each of the antenna types studied. An experimental study was also made to check the theoretical analysis. The results obtained by experiment check very well with the theoretical predictions for each type of antenna. The symmetrical transverse T antenna and the symmetrical longitudinal T antenna, with vertical lead-in portions, are both found to fulfill the desired requirements. Neither of these antennas shows any course errors and give the same received voltage as the vertical pole antenna having much greater actual height, thus reducing the mechanical troubles caused by vibration and ice formation. An appendix gives the mathematical derivation of the equation used as a starting point for the theoretical analysis.

CONTENTS

	Page
I. Introduction	902
II. Theoretical analysis	903
III. Application of theory to specific antenna structures	906
1. Vertical antenna	906
(*a*) Localizing effect	906
(*b*) Course error	908
(*c*) Received voltage	908
2. Inclined antenna	908
(*a*) Localizing effect	908
(*b*) Course error	908
(*c*) Received voltage	909
3. Horizontal dipole antenna	909
4. Horizontal V antenna	909
5. Symmetrical T antenna	910
6. Other antenna systems	910
IV. Experimental results	910
1. Relative received voltages	911
2. Course error effects	911
(*a*) Inclined antenna ($\beta_2=20°$, inclination forward)	911
(*b*) Inclined antenna ($\beta_2=-20°$, inclination backward)	911
(*c*) Inclined V antenna	912
(*d*) Symmetrical T antenna	912
3. Localizing effects	912
V. Conclusions	912
VI. Appendix	912

I. INTRODUCTION

Since the advent of the radio range beacon, the vertical pole antenna has been widely used because of its nondirectional properties and consequent freedom from course errors in radio range-beacon reception. The vertical pole antenna, however, is subject to considerable mechanical trouble because of vibration and ice formation, and for this reason, an antenna free from these mechanical difficulties and yet having all the desirable electrical properties of the simple pole antenna would be preferable.

Accordingly, a study of various types of airplane antennas was begun, a theoretical analysis being checked by experimental observa-

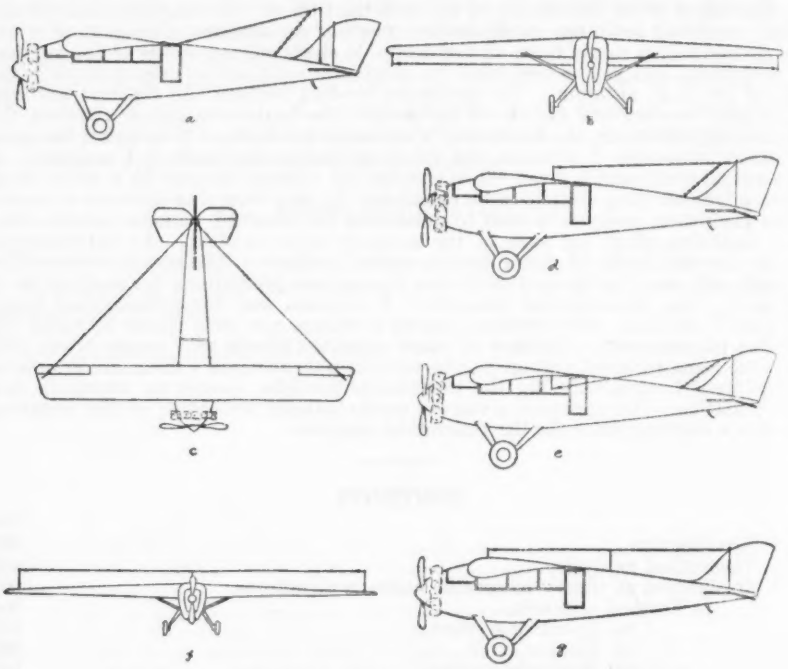

FIGURE 1.—*Experimental installations of antennas studied*

a, Inclined antenna; *b*, horizontal dipole antenna (half of this was used for a horizontal L antenna); *c*, top view, V antenna; *d*, side view, horizontal V antenna; *e*, side view, inclined V antenna; *f*, symmetrical transverse T antenna; *g*, symmetrical longitudinal T antenna

tions in the air and on the ground. A number of antenna arrangements were included in this study. For each type of antenna, the tests in the air included observation of the received voltage, the localizing effect or variation of the received voltage in the immediate vicinity of the beacon tower, and the course error as observed by circling the beacon. These were compared directly with the results obtained using the vertical pole antenna. The types studied included the inclined antenna, with both forward and backward inclination (one example of the latter being the trailing wire antenna), the horizontal dipole antenna, the horizontal L antenna, the horizontal V antenna, the inclined V antenna, the symmetrical transverse T antenna, and the symmetrical longitudinal T antenna. Figure 1 shows experimental installations of these antennas on an airplane. The

results of this experimental work check the theoretical analysis with sufficient accuracy for the desired purpose, although exact quantitative data are almost impossible to obtain in the air because of the difficulties incurred in any attempt to measure the geometrical quantities involved.

II. THEORETICAL ANALYSIS

It is found convenient to treat the subject by the use of vector analysis. A somewhat similar treatment, using a trigonometric method, has been given by Capt. William H. Murphy, of the Signal

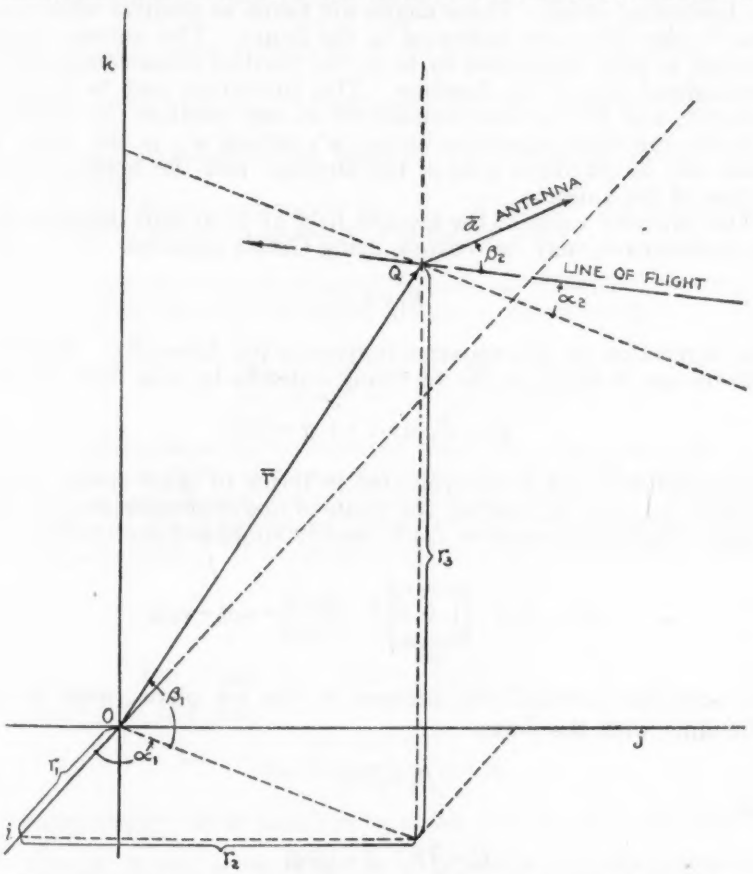

FIGURE 2.—*Diagram showing quantities used in the theoretical analysis*

Corps.[1] In this work, as in Captain Murphy's, relative rather than absolute field intensities and received voltages are desired. Consequently, all constants are considered equal to unity and omitted from the vector equations. The airplane is also considered to be at unit distance from the transmitter.

The transmitting loop antenna is taken in the $\bar{j}$-$\bar{k}$ plane, with its center at o (fig. 2), so that the $\bar{\imath}$-axis coincides with the axis of the

[1] W. H. Murphy, "Space Characteristics of Antennae," J. Frank. Inst., **201**, pp. 411–429; April, 1926; **203**, pp. 289–312; February, 1927.

loop antenna. The airplane is located at the point Q whose position vector is $\bar{r}$, and is flying in the direction indicated by the line marked "Line of flight." The line of flight is assumed to lie in a plane parallel to the $\bar{i}$-$\bar{j}$ plane. The vector $\bar{a}$ is a unit vector in the direction of the antenna, pointing away from Q. α_1 is the angle between the axis of the loop antenna ($\bar{i}$-axis) and the projection of the line of sight (or the vector $\bar{r}$) on the $\bar{i}$-$\bar{j}$ plane. α_2 is the angle between the line of flight and the projection of the line of sight on the horizontal plane containing the line of flight. β_1 is the angle of elevation of the airplane. β_2 is the angle of inclination of the antenna with respect to the horizontal plane. These angles are taken as positive when measured in the directions indicated in the figure. The antenna on the airplane is here considered to be in the vertical plane containing the longitudinal axis of the fuselage. This limitation may be removed, however, and the antenna considered in any position, by replacing α_2 in the following equations by $\alpha_2+\alpha'_2$, where α'_2 is the angle between the longitudinal axis of the airplane and the horizontal projection of the antenna.

The effective value of the electric field at Q, at unit distance from the transmitter, may be written, using Gibb's notation

$$\bar{E}_1=\bar{r}\times\bar{\imath} \tag{1}$$

The derivation of this equation is given in the Appendix. The effective voltage induced in the receiving antenna by this field vector is

$$E_1=\bar{E}_1\cdot\bar{a}=\bar{r}\times\bar{\imath}\cdot\bar{a}=[\bar{r}\bar{\imath}\bar{a}] \tag{2}$$

If the vectors $\bar{r}$ and $\bar{a}$ are evaluated in terms of their scalar components r_1, r_2, r_3, a_1, a_2, and a_3, the value of this expression may be computed. However, equation (2) is readily simplified still further:

$$E_1=[\bar{r}\bar{\imath}\bar{a}]=\begin{vmatrix} r_1 & r_2 & r_3 \\ 1 & 0 & 0 \\ a_1 & a_2 & a_3 \end{vmatrix}=-\begin{vmatrix} r_2 & r_3 \\ a_2 & a_3 \end{vmatrix}=a_2r_3-r_2a_3 \tag{3}$$

Similarly, for a second loop antenna in the $\bar{i}$-$\bar{k}$ plane, with its axis coinciding with the $\bar{j}$-axis

$$\bar{E}_2=\bar{j}\times\bar{r} \tag{4}$$

and

$$E_2=\bar{j}\times\bar{r}\cdot\bar{a}=[\bar{j}\bar{r}\bar{a}] \tag{5}$$

$$E_2=\begin{vmatrix} 0 & 1 & 0 \\ r_1 & r_2 & r_3 \\ a_1 & a_2 & a_3 \end{vmatrix}=-\begin{vmatrix} r_1 & r_3 \\ a_1 & a_3 \end{vmatrix}=a_1r_3-r_1a_3 \tag{6}$$

Now the components r_1, r_2, r_3, a_1, a_2, and a_3 of the unit vectors $\bar{r}$ and $\bar{a}$ may be expressed in any system of coordinates, but the most convenient form is that of the spherical coordinates shown in Figure

2. In this system, and since the vectors are unit vectors (that is, $|\bar{r}|=|\bar{a}|=1$)

$$\left.\begin{aligned} r_1&=\cos\alpha_1\cos\beta_1\\ r_2&=\sin\alpha_1\cos\beta_1\\ r_3&=\sin\beta_1 \end{aligned}\right\} \tag{7}$$

and

$$\left.\begin{aligned} a_1&=\cos(\alpha_1+\alpha_2)\cos\beta_2\\ a_2&=\sin(\alpha_1+\alpha_2)\cos\beta_2\\ a_3&=\sin\beta_2 \end{aligned}\right\} \tag{8}$$

On substitution of these values, equations (3) and (6) become

$$E_1=a_2r_3-r_2a_3=\sin(\alpha_1+\alpha_2)\sin\beta_1\cos\beta_2-\sin\alpha_1\cos\beta_1\sin\beta_2 \tag{9}$$

$$E_2=a_1r_3-r_1a_3=\cos(\alpha_1+\alpha_2)\sin\beta_1\cos\beta_2-\cos\alpha_1\cos\beta_1\sin\beta_2 \tag{10}$$

These two equations form the basis of the remainder of the theoretical analysis.

A course is obtained whenever $E_1=E_2$. Thus, for the general antenna shown in Figure 2, a course is obtained when

$$\begin{aligned}&\sin(\alpha_1+\alpha_2)\sin\beta_1\cos\beta_2-\sin\alpha_1\cos\beta_1\sin\beta_2\\ &=\cos(\alpha_1+\alpha_2)\sin\beta_1\cos\beta_2-\cos\alpha_1\cos\beta_1\sin\beta_2\end{aligned} \tag{11}$$

or when

$$\tan\alpha_1=\frac{\tan\beta_1(\cos\alpha_2-\sin\alpha_2)-\tan\beta_2}{\tan\beta_1(\sin\alpha_2+\cos\alpha_2)-\tan\beta_2} \tag{12}$$

where α_1 is the course angle measured from axis of loop antenna 1.

If the currents in the two loop antennas are equal, the true courses bisect the angles between the transmitting loop antennas. Assuming equal currents, then, the course error for any type of receiving antenna may be found. If the course error is here defined by e,[2] where

$$e=\alpha_1-\pi/4 \tag{13}$$

then

$$\tan e=\tan(\alpha_1-\pi/4)=\frac{\tan\alpha_1-1}{1+\tan\alpha_1} \tag{14}$$

Combining (12) and (14)

$$\tan e=\frac{\sin\alpha_2\tan\beta_1}{\tan\beta_2-\cos\alpha_2\tan\beta_1} \tag{15}$$

Mathematically, it is possible to make this course error zero in several ways: $\beta_1=0$, $\alpha_2=0$, or $\beta_2=\frac{\pi}{2}$. The last is the only practicable method (heretofore accomplished through the use of a vertical antenna). However, a consideration of the physical significance of equation (11) shows that the course error is introduced by the horizontal component of the field vector, for equation (11) can be true for $\alpha_1=45°$ (that is, $e=0$) only if $\alpha_2=0$. Since α_2 can be considered as a generalized direction angle of the vector sum of the horizontal projections of the antenna, it follows that α_2 can be zero for all directions of

[2] This is the usual way of defining course error in connection with flight on a radio range beacon.

flight only if the vector sum of the horizontal projections of the antenna is zero. Obviously, the horizontal projection of the antenna is affected only by the horizontal component of the field vector, so that it is evident that the course error is introduced by this horizontal component. The horizontal component of the field vector can not be eliminated (except by changes in the transmitting antenna, which are not convenient), so that it becomes necessary to construct the receiving antenna so that it will not respond to this horizontal component; that is, as noted above, the vector sum of the horizontal projections of the receiving antenna must be zero. Since the use of flat top portions is thus permissible so long as they fulfill these conditions, it becomes possible to design antennas having smaller actual height than that of the usual pole antenna, and yet having the same effective height. Such an antenna would give the same received voltage as the vertical pole antenna, and would likewise be immune to course errors.

III. APPLICATION OF THEORY TO SPECIFIC ANTENNA STRUCTURES

The theory is readily applied to indicate the results obtainable from several types of simple antennas. In each case, it is desirable to determine the localizing effect (the behavior of the signal in the immediate vicinity of the beacon), the course error, and the relative received voltage. The accompanying graphs (see fig. 3) show the localizing effect for the antennas considered.

1. VERTICAL ANTENNA

$$\beta_2=\frac{\pi}{2} \tag{16}$$

(a) LOCALIZING EFFECT

Substituting this condition in equations (9) and (10) and adding, the total received voltage is

$$E=E_1+E_2=-\sin\ \alpha_1\ \cos\ \beta_1-\cos\ \alpha_1\ \cos\ \beta_1 \tag{17}$$

This equation is strictly correct only when the two loop antennas are energized simultaneously and in the same time phase (for example, in the case of the two-course visual type beacon). However, the results secured in the following analysis are independent of this limitation, although the equations used in securing these results are somewhat different if the loop antenna currents are displaced from each other in time phase, or if the loop antennas are energized separately as in the case of the aural type beacon.

The value of E in equation (17) becomes zero when

$$\beta_1=\frac{\pi}{2} \tag{18}$$

Thus, this antenna gives a zero signal zone directly over the beacon. (Fig. 3(*A*).)

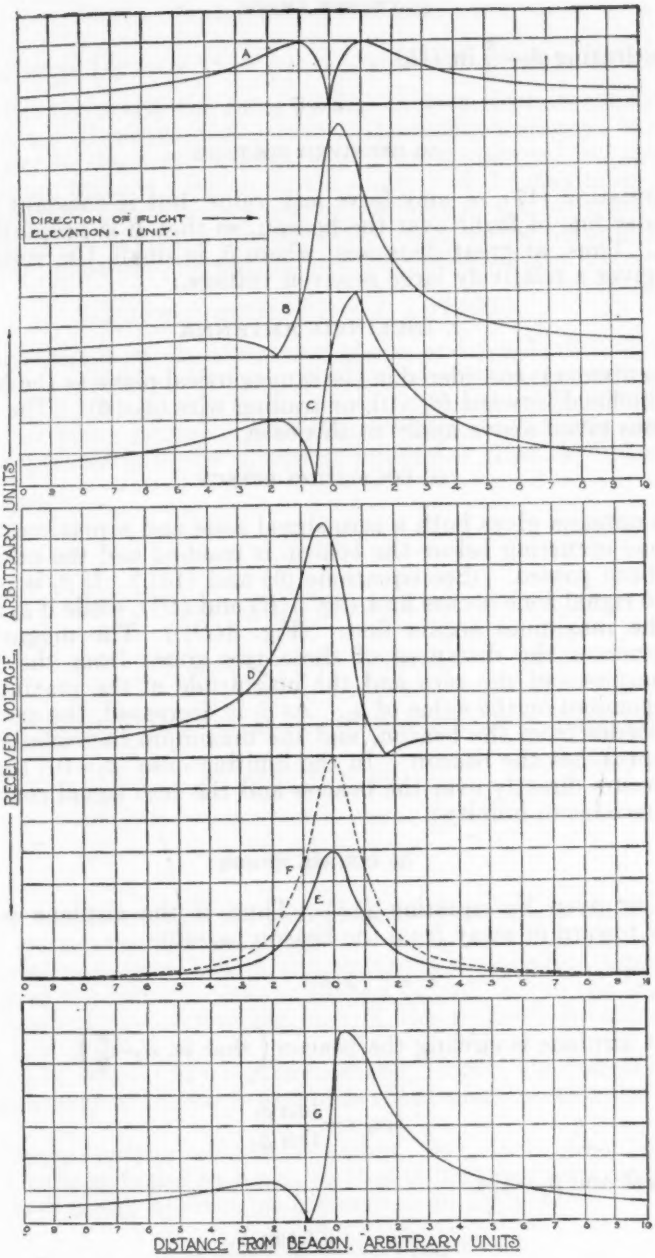

FIGURE 3.—*Graphs of localizing effects for antennas studied*

A, vertical antenna; *B*, inclined antenna ($\beta_2=30°$); *C*, inclined antenna ($\beta_2=60°$); *D*, trailing wire antenna ($\beta_2=-30°$); *E*, horizontal L antenna; *F*, horizontal V antenna (angle between each wire and fuselage center line=30°); *G*, inclined V antenna, angle between each wire and fuselage center line=30°, angle of inclination=45°.

(b) COURSE ERROR

Substituting $\beta_2=\frac{\pi}{2}$ in (15)

$$e=0 \tag{19}$$

(c) RECEIVED VOLTAGE

In equation (17), α_1 may have any value, but is constant for any particular line of flight over the beacon, so that E is proportional to $\cos \beta_1$. Thus, at great distances, where β_1 is small, the vertical antenna gives a relatively large received voltage.

2. INCLINED ANTENNA

The antenna is considered in the same vertical plane as the fuselage, either inclined forward ($\beta_2>0$), or trailing wire ($\beta_2<0$). The general equations given above apply to this case.

(a) LOCALIZING EFFECT

This antenna gives both a zero signal zone and a maximum signal zone, one occurring before the beacon is reached and the other after it has been passed. (See equations (9) and (10).) If β_2 is positive, the zero signal zone occurs first (fig. 3(*B*) and (*C*)), while if β_2 is negative, the maximum occurs first. (Fig. 3(*D*).) The magnitude of β_2 determines the distances of these two zones from the beacon. The sharpness of the zero and the magnitude of the maximum are also dependent on the value of β_2. As β_2 is decreased, the zero signal zone recedes from the beacon, and the maximum increases in value and approaches the beacon. In the limiting case ($\beta_2=0$), the maximum occurs directly over the beacon and the zero signal zone disappears (recedes to infinity).

(b) COURSE ERROR

This is given by equation (15). Thus, if the airplane is flying directly toward or away from the beacon ($\alpha_2=0$)

$$e=0 \tag{20}$$

If the airplane is circling the beacon $\left(\text{that is, } \alpha_2=\frac{\pi}{2}\right)$,

$$\tan e=\frac{\tan \beta_1}{\tan \beta_2} \tag{21}$$

If $\alpha_2=\pi/4$ and $\beta_2=\pi/4$

$$\tan e=\frac{\sqrt{2}\tan \beta_1}{2-\sqrt{2}\tan \beta_1} \tag{22}$$

In equation (15), when $\tan \beta_2-\cos \alpha_2 \tan \beta_1$ becomes very small, $\tan e$ becomes very large and e becomes nearly equal to $\frac{\pi}{2}$.

(c) RECEIVED VOLTAGE

If β_2 is large $\left(\text{greater than } \frac{\pi}{3}\right)$, the received voltage in an inclined antenna is very nearly the same as that in a vertical antenna of the same length. However, if β_2 is small, the inclined antenna is markedly inferior to the vertical antenna at great distances from the beacon, although there is a region, in the vicinity of the maximum signal zone mentioned above, where the inclined antenna is superior to the vertical antenna. This is a small region close to the beacon, and of little value practically, except for localizing effects.

3. HORIZONTAL DIPOLE ANTENNA

This antenna is in the horizontal plane, and perpendicular to the line of flight. The results apply also to an L-type antenna from the wing tip to the fuselage. In this case, the antenna does not lie in the vertical plane containing the longitudinal axis of the fuselage, and consequently α_2 in the preceding equations must be replaced by $\alpha_2+\frac{\pi}{2}$. Also

$$\beta_2=0$$

Now

$$\left.\begin{aligned}\sin\left(\alpha_2+\frac{\pi}{2}\right)&=\cos\alpha_2\\ \cos\left(\alpha_2+\frac{\pi}{2}\right)&=-\sin\alpha_2\end{aligned}\right\} \tag{23}$$

By substitution of these values in equation (15), it is found that

$$\tan e=\cot\alpha_2 \tag{24}$$

and

$$e=\frac{\pi}{2}-\alpha_2 \tag{25}$$

Thus the course error is the complement of the angle at which the airplane crosses the beacon course.

(1) *Localizing effect.*—With this antenna, a maximum signal zone occurs over the beacon. As mentioned before, this is the localizing effect obtained in the limiting case of the inclined antenna, when $\beta_2=0$. (Fig. 3(*E*).)

(2) *Course error.*—As noted immediately above, the course error is the complement of the angle at which the airplane crosses the beacon course.

(3) *Received voltage.*—From equation (24), it is seen that the received voltage varies as $\sin\beta_1$, so that it becomes very small when the airplane is any appreciable distance from the beacon.

4. HORIZONTAL V ANTENNA

One variation of the horizontal antenna is the V antenna from wing tips to vertical fin. The performance of this type of antenna is essentially the same as that of the horizontal dipole, except that the received voltage is somewhat greater, since both horizontal components of the transmitted signal are received. The localizing effect is shown in Figure 3(*F*).

5. SYMMETRICAL T ANTENNA

This can be either longitudinal or transverse. The received voltage of this type of antenna is due entirely to the vertical portion, the flat top merely increasing the charging current at the top of the vertical portion, thus increasing the effective height. Consequently, the antenna will have the characteristics of its vertical or lead-in portion. If this is truly vertical, the arrangement will act the same as the simple vertical antenna, while if the lead-in portion is inclined, the characteristics will be those of the inclined antenna. The T antenna gives greater effective height than either type simple antenna having the same actual height because of the more uniform current distribution resulting from the additional capacity at the top of the antenna.

6. OTHER ANTENNA SYSTEMS

The general theory outlined in Section II is also applicable to other and more complicated antennas. For example, consider the inclined V antenna from the wing tips to the vertical fin, with the lead-in running from the junction of the two wires at the vertical fin. This is essentially a form of T antenna, the effects of the horizontal components perpendicular to the axis of the fuselage cancelling. The antenna, therefore, performs as an inclined antenna having a vertical portion and also having a horizontal portion in the axis of the fuselage. The localizing effect for this type of antenna is shown in Figure 3(*G*).

Similarly, consider any antenna having a vertical lead-in and a flat-top arrangement symmetrically disposed about the vertical lead-in so that the vector sum of the horizontal projections of the individual elements of the flat top is equal to zero. This antenna will behave in every way as a vertical antenna, but giving greater received voltage than a vertical antenna of the same actual height. It is this type of antenna which offers advantages of reduced mechanical vibration over the conventional vertical pole antenna. When the flat-top portions lie along the longitudinal axis of the fuselage, for example, the longitudinal T antenna, the problems due to ice formation are also reduced.

IV. EXPERIMENTAL RESULTS

Antennas of each of the types analyzed above were installed on the National Bureau of Standards' airplane and compared (in flight on the visual radio range beacon) with the vertical pole antenna as a standard of comparison. Relative effective heights were determined by switching the antenna under test and the pole antenna alternately to the same receiving set and recording the receiving set output voltage. Course error effects were obtained by using two receiving sets, one connected to the antenna under test and the other to the pole antenna, and comparing the course indications (as obtained on two reed indicators connected in the output circuits of the two receiving sets), while circling the beacon at various altitudes and various distances from the beacon. The localizing effects were obtained by flying at a constant altitude on a beacon course directly over the beacon tower.

The results secured in the air were approximate only, exact quantitative measurements being very difficult because of the difficulty in measuring the geometric quantities involved. However, the results were sufficiently accurate to corroborate the theoretical analysis.

1. RELATIVE RECEIVED VOLTAGES

The data obtained showed that, of the antennas studied, the symmetrical T antenna of either type and the wing tip to vertical fin inclined V antenna both gave effective heights equivalent to that obtained with the vertical pole antenna without requiring nearly the same actual height as the pole antenna. For example, a symmetrical transverse T antenna having a 12-inch vertical lead-in and a flat top extending 15 feet on each side of the fuselage, parallel to and 12 inches above the wing surfaces, gave slightly better effective height than a 5-foot vertical pole.

2. COURSE ERROR EFFECTS

(a) INCLINED ANTENNA ($\beta_2=20°$, INCLINATION FORWARD)

When circling the beacon at constant distance from the beacon tower, the on-course indications of the reed indicator operated from the receiving set connected to the inclined antenna were in advance of the on-course indications of the reed indicator in the output circuit of the receiving set connected to the pole antenna. The angle of lead increased with decreasing distance from the beacon and also increased with the altitude of the airplane for a given distance from the beacon. This angle of lead is equal to the course error. The results are in accordance with equation (15), placing $\alpha_2=\frac{\pi}{2}$, since, when circling the beacon, the line of flight is perpendicular to the line of sight. Equation (15) then resolves into equation (21), namely

$$\tan e=\frac{\tan \beta_1}{\tan \beta_2}$$

where β_1 is the angle of elevation of the line connecting the airplane with the beacon (the line of sight) and β_2 the angle of inclination of the antenna (20° in this case). Some idea of the magnitude of the course errors involved may be obtained from one specific case. Flying at an elevation of 3,000 feet along a circle of three miles radius, the course error is 27.5°.

When flying along a beacon course directly to or from the beacon, no course error was obtained. This is also in accordance with equation (15), since, when $\alpha_2=0$, equation (15) resolves into equation (20), namely

$$\tan e=0$$

(b) INCLINED ANTENNA ($\beta_2=-20°$, INCLINATION BACKWARD)

The results obtained were exactly the same as for the antenna with forward inclination except that the on-course indications of the reed indicator operated from the receiving set connected to the inclined antenna lagged the on-course indications obtained on the reed indicator in the output circuit of the set connected to the pole antenna.

(c) INCLINED V ANTENNA

The results secured were the same as for the inclined antenna with forward inclination.

(d) SYMMETRICAL T ANTENNA (EITHER TYPE)

No course errors were obtained under any conditions. Both the transverse T and longitudinal T antennas were tested.

3. LOCALIZING EFFECTS

The localizing effect for each of the antennas studied was found to be very nearly the same as shown in the graphs of Figure 3. This was, perhaps, the most satisfactory test of all, checking, within the limits of error, the exact theoretical analysis. At 3,000 feet altitude, by changing the angle of inclination of the inclined antenna from 20° to 90°, the zero signal zone could be moved from approximately 1 mile from the beacon to directly over the beacon tower. When setting up the longitudinal T antenna, the zero signal effect directly over the beacon tower was employed as a check on the electrical symmetry of the flat-top arrangement.

V. CONCLUSIONS

For reception of signals from radio range beacons, an antenna arrangement of which the symmetrical T antenna is a typical example was found to give good electrical performance and to be free from trouble due to vibration. In addition, the performance of this type of antenna under conditions favoring ice formation should prove superior to that of the vertical pole antenna. To reduce the effects of mechanical vibration, this antenna employs vertical poles considerably shorter than the conventional pole antenna (10 to 18 inches instead of 5 to 6 feet). Equivalent effective height is secured through the addition of a flat top. In order to prevent directional effects, which introduce course errors, the flat top is made up of two, three, or more elements symmetrically disposed about the vertical lead-in, so that the vector sum of the horizontal projections of the individual elements is equal to zero. When but two flat-top elements are employed, the antenna takes the form of either a transverse or longitudinal T. The latter arrangement is preferable from the viewpoint of freedom from trouble due to ice formation. Furthermore, such a longitudinal T antenna has an aerodynamical resistance very much smaller than that of the transverse T antenna, and probably as small, if not smaller, than that of the vertical pole antenna.

VI. APPENDIX

This calculation of the field due to a loop antenna is based on the Lorentz solution of the electromagnetic field equations for a known distribution of currents and charges.

The notation used (Gibbs-"Vector analysis") is as follows:

$\overline{H}$ = magnetic field intensity.

$\overline{E}$ = electric field intensity.

ρ = density of charge.

v = velocity of motion of charge.

μ, c, K = constants depending upon system of units used

$\nabla\times$ = curl.

$\nabla\cdot$ = divergence.

$\text{Pot}\ \bar{w} = \int\int\int \frac{\bar{w}}{r}\, d\tau$ where the integration is extended over all space, $d\tau$ represents the element of volume, and r the distance from $d\tau$ to the point at which the potential is computed.

I_o = Maximum value of current in loop antenna.

ω = angular velocity of current in loop antenna.

t = time

V = velocity of electromagnetic waves in medium surrounding loop.

$[u]$ = value of u at time $t-\frac{r}{V}$, where r is the distance from source of disturbance to point at which $[u]$ is considered.

The loop is assumed to be square and the current to be the same throughout the loop.

In this notation, Maxwell's equations of the electromagnetic field are

$$\left.\begin{aligned} \nabla\times\bar{H} &= \frac{4\pi}{c}\left(\rho\bar{v}+\frac{K}{4\pi}\frac{\partial\bar{E}}{\partial t}\right) \\ \nabla\times\bar{E} &= -\frac{\mu}{c}\frac{\partial\bar{H}}{\partial t} \\ \nabla\cdot\bar{E} &= \frac{4\pi\rho}{K} \\ \nabla\cdot\bar{H} &= 0 \end{aligned}\right\} \tag{1}$$

A solution of this system sometimes used (neglecting a term in the value of $\bar{E}$ which is immaterial in this discussion) may be written

$$\left.\begin{aligned} \bar{H} &= \frac{1}{c}\nabla\times\text{Pot}\ [\rho\bar{v}] = \frac{1}{c}\,\text{Lap}\ [\rho\bar{v}] \\ \bar{E} &= -\frac{\mu}{c^2}\frac{\partial}{\partial t}\text{Pot}\ [\rho\bar{v}] = -\frac{\mu}{c^2}\text{Pot}\left[\frac{\partial}{\partial t}(\rho\bar{v})\right] \end{aligned}\right\} \tag{2}$$

Now

$$\rho\bar{v} = \bar{I} = I\bar{b} = I_o\bar{b}\sin\omega t \tag{3}$$

where $\bar{b}$ is the unit vector in the direction of the current.

$$\therefore \bar{E} = -\frac{\mu}{c^2}\text{Pot}\left[\frac{\partial\bar{I}}{\partial t}\right] \tag{4}$$

$$\frac{\partial\bar{I}}{\partial t} = \omega I_o\bar{b}\cos\omega t \tag{5}$$

$$\bar{E} = -\frac{\mu\omega I_o}{c^2}\,\text{Pot}\ [\bar{b}\cos\omega t] = -\frac{\mu\omega I_o}{c^2}\int_{(c)}\frac{\bar{b}\cos\omega\left(t-\frac{h}{V}\right)}{h}\,ds \tag{6}$$

where h represents the distance from current element to P of Figure 4, which shows the position of the loop antenna and the distances and vectors used in the following treatment:

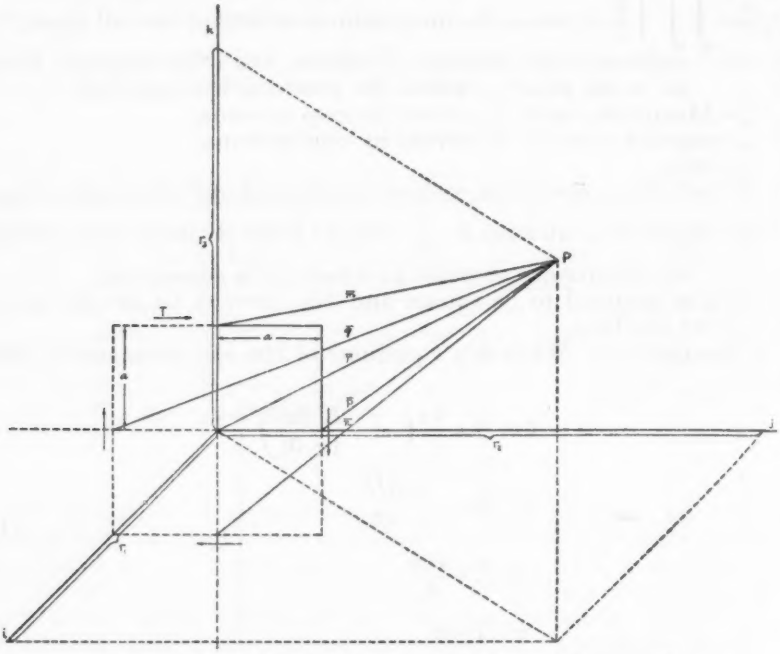

FIGURE 4.—*Diagram showing quantities used in appendix*

$$\bar{E}=-\frac{\mu\omega I_o}{c^2}\left[-\bar{k}\frac{\cos\omega\left(t-\frac{p}{V}\right)}{p}-\bar{j}\frac{\cos\omega\left(t-\frac{n}{V}\right)}{n}+\bar{k}\frac{\cos\omega\left(t-\frac{q}{V}\right)}{q}+\bar{j}\frac{\cos\omega\left(t-\frac{m}{V}\right)}{m}\right]\int_{-a}^{a}ds \tag{7}$$

But

$$\int_{-a}^{a}ds=2a \tag{8}$$

$$\bar{E}=\frac{2\mu\omega a I_o}{c^2}\left[\left\{\frac{\cos\omega\left(t-\frac{p}{V}\right)}{p}-\frac{\cos\omega\left(t-\frac{q}{V}\right)}{q}\right\}\bar{k}+\left\{\frac{\cos\omega\left(t-\frac{n}{V}\right)}{n}-\frac{\cos\omega\left(t-\frac{m}{V}\right)}{m}\right\}\bar{j}\right] \tag{9}$$

Now

$$\left.\begin{aligned}\bar{p}&=\bar{r}-a\bar{j}=r_1\bar{i}+(r_2-a)\bar{j}+r_3\bar{k}\\ \bar{q}&=\bar{r}+a\bar{j}=r_1\bar{i}+(r_2+a)\bar{j}+r_3\bar{k}\\ \bar{m}&=\bar{r}-a\bar{k}=r_1\bar{i}+r_2\bar{j}+(r_3-a)\bar{k}\\ \bar{n}&=\bar{r}+a\bar{k}=r_1\bar{i}+r_2\bar{j}+(r_3+a)\bar{k}\end{aligned}\right\} \tag{10}$$

r_1, r_2, and r_3 are the components of $\bar{r}$ along the $\bar{i}$, $\bar{j}$, and $\bar{k}$ axes, respectively.

$$p=[r_1^2+(r_2-a)^2+r_3^2]^{1/2}=(r^2-2r_2a+a^2)^{1/2}=r-\frac{ar_2}{r} \tag{11}$$

This is an approximation obtained by expanding the value of p by the binomial theorem and neglecting terms involving a in powers higher than the first. Thus

$$\left.\begin{aligned} p&=r-\frac{ar_2}{r}\\ q&=r+\frac{ar_2}{r}\\ m&=r-\frac{ar_3}{r}\\ n&=r+\frac{ar_3}{r}\end{aligned}\right\} \tag{12}$$

Also, by the same method

$$\left.\begin{aligned} \frac{1}{p}&=\frac{1}{r}+\frac{ar_2}{r^3}\\ \frac{1}{q}&=\frac{1}{r}-\frac{ar_2}{r^3}\\ \frac{1}{m}&=\frac{1}{r}+\frac{ar_3}{r^3}\\ \frac{1}{n}&=\frac{1}{r}-\frac{ar_3}{r^3}\end{aligned}\right\} \tag{13}$$

By the use of equations (12) and (13) and the trigonometrical formulas

$$\cos(x+y)-\cos(x-y)=-2\sin x\sin y$$

$$\cos(x+y)+\cos(x-y)=2\cos x\cos y$$

the coefficients of $\bar{j}$ and $\bar{k}$ in (9) may be simplified.

$$\begin{aligned}&\frac{\cos\omega\left(t-\frac{p}{V}\right)}{p}-\frac{\cos\omega\left(t-\frac{p}{V}\right)}{q}\\ &=\cos\omega\left(t-\frac{r}{V}+\frac{ar_2}{rV}\right)\left(\frac{1}{r}+\frac{ar_2}{r^3}\right)-\left(\frac{1}{r}-\frac{ar_2}{r^3}\right)\cos\omega\left(t-\frac{r}{V}-\frac{ar_2}{rV}\right)\\ &=\frac{1}{r}\left[\cos\omega\left(t-\frac{r}{V}+\frac{ar_2}{rV}\right)-\cos\omega\left(t-\frac{r}{V}-\frac{ar_2}{rV}\right)\right]\\ &\quad+\frac{ar_2}{r^3}\left[\cos\omega\left(t-\frac{r}{V}+\frac{ar_2}{rV}\right)+\cos\omega\left(t-\frac{r}{V}-\frac{ar_2}{rV}\right)\right]\\ &=-\frac{2}{r}\sin\omega\left(t-\frac{r}{V}\right)\sin\frac{\omega ar_2}{rV}+\frac{2ar_2}{r^3}\cos\omega\left(t-\frac{r}{V}\right)\cos\frac{\omega ar_2}{rV}\\ &=-\frac{4\pi ar_2}{\lambda r^2}\sin\omega\left(t-\frac{r}{V}\right)+\frac{2ar_2}{r^3}\cos\omega\left(t-\frac{r}{V}\right)\end{aligned} \tag{14}$$

Since $\frac{\omega a}{V}=\frac{2\pi a}{\lambda}$, and a is small in comparison with λ, $\sin \frac{\omega\, ar_2}{Vr}$ may be replaced by $\frac{2\pi ar_2}{\lambda r}$ and $\cos \frac{2\pi ar_2}{\lambda r}$ may be considered equal to one. Similarly

$$\frac{\cos \omega\left(t-\frac{n}{V}\right)}{n}-\frac{\cos \omega\left(t-\frac{m}{V}\right)}{m}$$

$$=\frac{4\pi\ \mathrm{ar}_3}{\lambda r^2} \sin \omega\left(t-\frac{r}{V}\right)-\frac{2ar_3}{r^3} \cos \omega\left(t-\frac{r}{V}\right) \tag{15}$$

Then

$$\bar{E}=\frac{2\mu\omega a I_o}{c^2}\left\{\bar{k}\left[-\frac{4\pi ar_2}{\lambda r^2} \sin \omega\left(t-\frac{r}{V}\right)+\frac{2ar_2}{r^3} \cos \omega\left(t-\frac{r}{V}\right)\right]\right.$$

$$\left.+\bar{j}\left[\frac{4\pi ar_3}{\lambda r^2} \sin \omega\left(t-\frac{r}{V}\right)-\frac{2ar_3}{r^3} \cos \omega\left(t-\frac{r}{V}\right)\right]\right\}$$

$$=\frac{2\mu\omega a I_o}{c^2}\left(r_3\bar{j}-r_2\bar{k}\right)\left[\frac{4\pi a}{\lambda r^2} \sin \omega\left(t-\frac{r}{V}\right)-\frac{2a}{r^3} \cos \omega\left(t-\frac{r}{V}\right)\right] \tag{16}$$

Now

$$r_3\bar{j}-r_2\bar{k}=\bar{r}\times\bar{i}$$

$$\therefore\ \bar{E}=\left[\frac{8\pi\mu\omega a^2 I_o}{\lambda c^2 r} \sin\ \omega\left(t-\frac{r}{V}\right)-\frac{4\mu\omega a^2 I_o}{c^2 r^2} \cos\ \omega\left(t-\frac{r}{V}\right)\right]\frac{\bar{r}\times\bar{i}}{r} \tag{17}$$

The first term represents the radiation field and the second term the induction field. If the radiation term alone is considered, no error is introduced except one of magnitude for small values of r. As interest in this treatment centers chiefly on relative rather than absolute field intensities, the quantity $\frac{8\pi\mu\omega a^2 I_o}{\lambda c^2}$ may be considered constant and equal to unity. Furthermore, the airplane is considered to be at unit distance from the transmitter, so that equation (17) may be written

$$\bar{E}_{eff.}=r\times\bar{i} \tag{18}$$

However, for the calculation of curves showing the localizing effect when an airplane flies at constant height over the beacon, it is necessary to take the variation of $\bar{r}$ into account and the equation then used is

$$\bar{E}=\frac{\bar{r}\times\bar{i}}{r^2} \tag{19}$$

WASHINGTON, January 24, 1931.

○